

AD\_\_\_\_\_

Award Number: DAMD17-01-1-0446

TITLE: PET Radiotracers for Imaging the Proliferation Status of Breast Tumors

PRINCIPAL INVESTIGATOR: Robert H. Mach, Ph.D.

CONTRACTING ORGANIZATION: Washington University  
St. Louis, Missouri 63110

REPORT DATE: December 2004

TYPE OF REPORT: Final

PREPARED FOR: U.S. Army Medical Research and Materiel Command  
Fort Detrick, Maryland 21702-5012

DISTRIBUTION STATEMENT: Approved for Public Release;  
Distribution Unlimited

The views, opinions and/or findings contained in this report are those of the author(s) and should not be construed as an official Department of the Army position, policy or decision unless so designated by other documentation.

# REPORT DOCUMENTATION PAGE

*Form Approved  
OMB No. 074-0188*

Public reporting burden for this collection of information is estimated to average 1 hour per response, including the time for reviewing instructions, searching existing data sources, gathering and maintaining the data needed, and completing and reviewing this collection of information. Send comments regarding this burden estimate or any other aspect of this collection of information, including suggestions for reducing this burden to Washington Headquarters Services, Directorate for Information Operations and Reports, 1215 Jefferson Davis Highway, Suite 1204, Arlington, VA 22202-4302, and to the Office of Management and Budget, Paperwork Reduction Project (0704-0188), Washington, DC 20503

<b>1. AGENCY USE ONLY (Leave blank)</b>			<b>2. REPORT DATE</b> December 2004			<b>3. REPORT TYPE AND DATES COVERED</b> Final (15 May 2001 - 30 Nov 2004)		
<b>4. TITLE AND SUBTITLE</b> PET Radiotracers for Imaging the Proliferation Status of Breast Tumors						<b>5. FUNDING NUMBERS</b> DAMD17-01-1-0446		
<b>6. AUTHOR(S)</b> Robert H. Mach, Ph.D.								
<b>7. PERFORMING ORGANIZATION NAME(S) AND ADDRESS(ES)</b> Washington University St. Louis, Missouri 63110						<b>8. PERFORMING ORGANIZATION REPORT NUMBER</b>		
<i>E-Mail:</i> rhmach@mir.wustl.edu								
<b>9. SPONSORING / MONITORING AGENCY NAME(S) AND ADDRESS(ES)</b> U.S. Army Medical Research and Materiel Command Fort Detrick, Maryland 21702-5012						<b>10. SPONSORING / MONITORING AGENCY REPORT NUMBER</b>		
<b>11. SUPPLEMENTARY NOTES</b> Original contains color plates: All DTIC reproductions will be in black and white.								
<b>12a. DISTRIBUTION / AVAILABILITY STATEMENT</b> Approved for Public Release; Distribution Unlimited						<b>12b. DISTRIBUTION CODE</b>		
<b>13. ABSTRACT (Maximum 200 Words)</b> <p>The goal of this research project is to develop radiotracers for imaging the proliferative status of breast tumors using the noninvasive imaging technique, Positron Emission Tomography (PET). The strategy taken involves developing radiotracers having a high affinity and selectivity for the <math>\sigma_2</math> receptor, which has been shown to be a useful receptor-based biomarker of proliferation in breast tumor cells growing both in vitro and in vivo. During the second year of the three-year IDEA project, we identified a new class of ligands displaying an outstanding affinity and selectivity for <math>\sigma_2</math> versus <math>\sigma_1</math> receptors. Preliminary in vivo biodistribution and microPET imaging studies with Br-76, C-11 and I-125-labeled analogs indicate that these agents may be useful for use in the diagnosis and determination of the proliferative status of breast tumors in breast cancer patients.</p>								
<b>14. SUBJECT TERMS</b> Positron emission tomography, nuclear medicine, breast cancer diagnosis, tumor proliferation, therapeutic monitoring						<b>15. NUMBER OF PAGES</b> 75		
						<b>16. PRICE CODE</b>		
<b>17. SECURITY CLASSIFICATION OF REPORT</b> Unclassified		<b>18. SECURITY CLASSIFICATION OF THIS PAGE</b> Unclassified		<b>19. SECURITY CLASSIFICATION OF ABSTRACT</b> Unclassified		<b>20. LIMITATION OF ABSTRACT</b> Unlimited		

## **Table of Contents**

Cover.....	1
SF 298.....	2
Table of Contents.....	3
Introduction.....	4
Body.....	4
Key Research Accomplishments.....	16
Reportable Outcomes.....	17
Conclusions.....	17
References.....	17
Appendices.....	18

## Introduction

The goal of this research is to develop radiotracers that can be used to determine the proliferative status of breast tumors using the noninvasive imaging technique, Positron emission Tomography (PET). Our strategy involves using the sigma-2 ( $\sigma_2$ ) receptor as a biomarker of the proliferative status of breast tumors [1-3]. This report describes the progress achieved during the three-year period of this Army Breast Cancer IDEA grant.

## Body

Synthesis and in vivo studies of Azabicyclo[3.3.1]nonane analogs. The initial step of this project was to conduct a structure-activity relationship (SAR) study of our lead compound, **1**, in order to identify a suitable radiotracer for imaging the  $\sigma_2$  receptor status of breast tumors. The results of this SAR study revealed that *N*-(9-(4-fluorobenzyl))-9-azabicyclo[3.3.1]nonan-3 $\alpha$ -yl-*N'*-(2-methoxy-4-methylphenyl)carbamate, **2** (Figure 1), has a modest affinity and moderate selectivity for  $\sigma_2$  versus  $\sigma_1$  receptors [4]. The higher affinity of **2** for  $\sigma_2$  versus  $\sigma_1$  receptors, and the observation that the fluorine-18 labeled analog of **2** could be prepared via alkylation of the des-benzyl precursor with [ $^{18}\text{F}$ ]4-fluorobenzyl iodide [5], led us to explore the use of [ $^{18}\text{F}$ ]**2** as a potential PET radiotracer for imaging the  $\sigma_2$  receptor status of breast tumors. Therefore, our initial goal was to synthesize [ $^{18}\text{F}$ ]**2** and conduct in vivo studies of this radiotracer in a murine model of breast cancer.

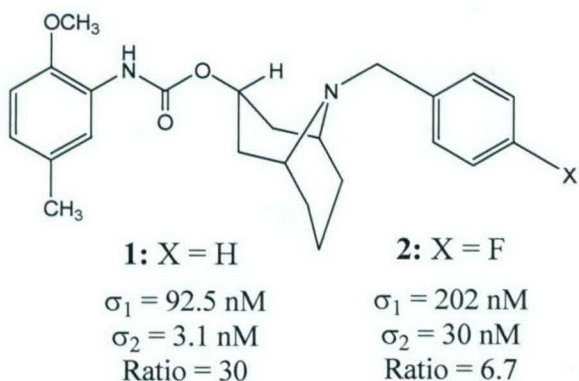
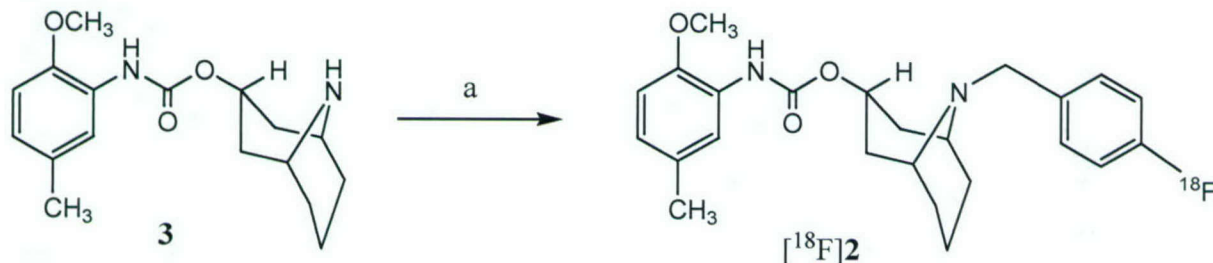


**Figure 1.** Structure and in vitro binding properties of compounds **1** and **2**.

The synthesis of [ $^{18}\text{F}$ ]**2** was accomplished via N-alkylation of the des-benzyl precursor, **3**, with [ $^{18}\text{F}$ ]4-fluorobenzyl iodide (Scheme I). The product was purified by reverse-phase semi-preparative HPLC and obtained in an overall yield of ~10% from solubilized [ $^{18}\text{F}$ ]CsF. The specific activity of the final product was  $2320 \pm 1384 \text{ mCi}/\mu\text{mol}$  ( $85.1 \pm 51.2 \text{ GBq}/\mu\text{mol}$ ). The radiotracer was of sufficient radiochemical purity (>95%) for the in vivo tumor uptake studies.

## Scheme I



**Reagents:** (a) [ $^{18}\text{F}$ ]4-fluorobenzyl iodide/triethylamine/DMF/90°C.

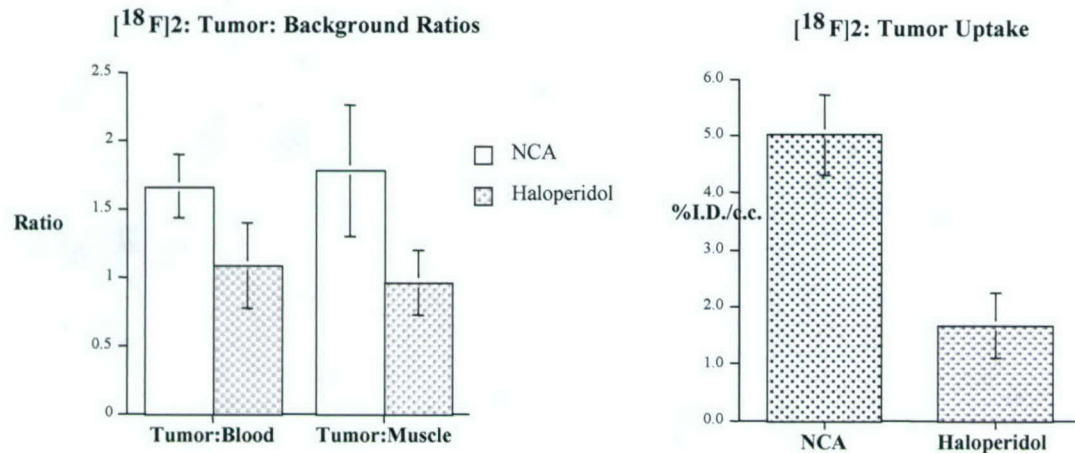
Preliminary *in vivo* biodistribution studies were conducted in nude mice bearing xenografts of the mouse mammary adenocarcinoma tumor cell line, 66. The results of this study are shown in Table I. There was a gradual increase in the uptake of [<sup>18</sup>F]2 in the tumor xenografts between 30-min and 60-min post-i.v. injection of the radiotracer. There was a slow rate of washout of radiotracer from the tumor (Table I) and a progressive increase in the tumor:blood and tumor:muscle ratios over time. The tumor:blood and tumor:muscle ratios were 2.5 and 4.0, respectively at 4 hr post-i.v. injection. Blocking studies with haloperidol (50 µg), a known sigma ligand, resulted in a reduction in tumor uptake of the radiotracer at 60 min post-i.v. injection (Figure 2), which represents the time of peak accumulation of the radiotracer in the tumor (Table I). These data are consistent with the labeling of σ<sub>2</sub> receptors *in vivo*.

**Table I.** Results of biodistribution studies of [<sup>18</sup>F]2 in tumor-bearing mice.

**%I.D./c.c. Tissue**

Tissue	30 min	60 min	120 min	240 min
Brain	1.18 ± 0.19	1.92 ± 0.24	1.18 ± 0.19	0.13 ± 0.01
Blood	1.47 ± 0.10	3.07 ± 0.45	1.90 ± 0.18	0.37 ± 0.06
Lung	6.81 ± 0.85	5.11 ± 1.36	3.77 ± 0.39	0.65 ± 0.11
Heart	2.10 ± 0.18	3.30 ± 0.54	1.80 ± 0.21	0.31 ± 0.05
Liver	7.92 ± 1.18	10.93 ± 1.00	7.36 ± 0.89	1.14 ± 0.18
Kidney	6.40 ± 0.25	14.71 ± 4.57	5.50 ± 0.76	1.08 ± 0.11
Intestine	6.49 ± 0.69	17.92 ± 3.19	9.40 ± 0.87	2.23 ± 0.21
Muscle	1.25 ± 0.23	3.43 ± 0.58	1.84 ± 0.24	0.23 ± 0.02
Spleen	4.55 ± 0.33	5.87 ± 0.71	3.45 ± 0.39	0.55 ± 0.11
Tumor	1.34 ± 0.21	5.02 ± 0.85	3.18 ± 0.12	0.89 ± 0.03
Tumor:Blood <sup>a</sup>	0.80 ± 0.08	1.66 ± 0.23	1.72 ± 0.17	2.48 ± 0.22
Tumor:Muscle <sup>b</sup>	1.13 ± 0.27	1.78 ± 0.48	1.78 ± 0.18	3.98 ± 0.30

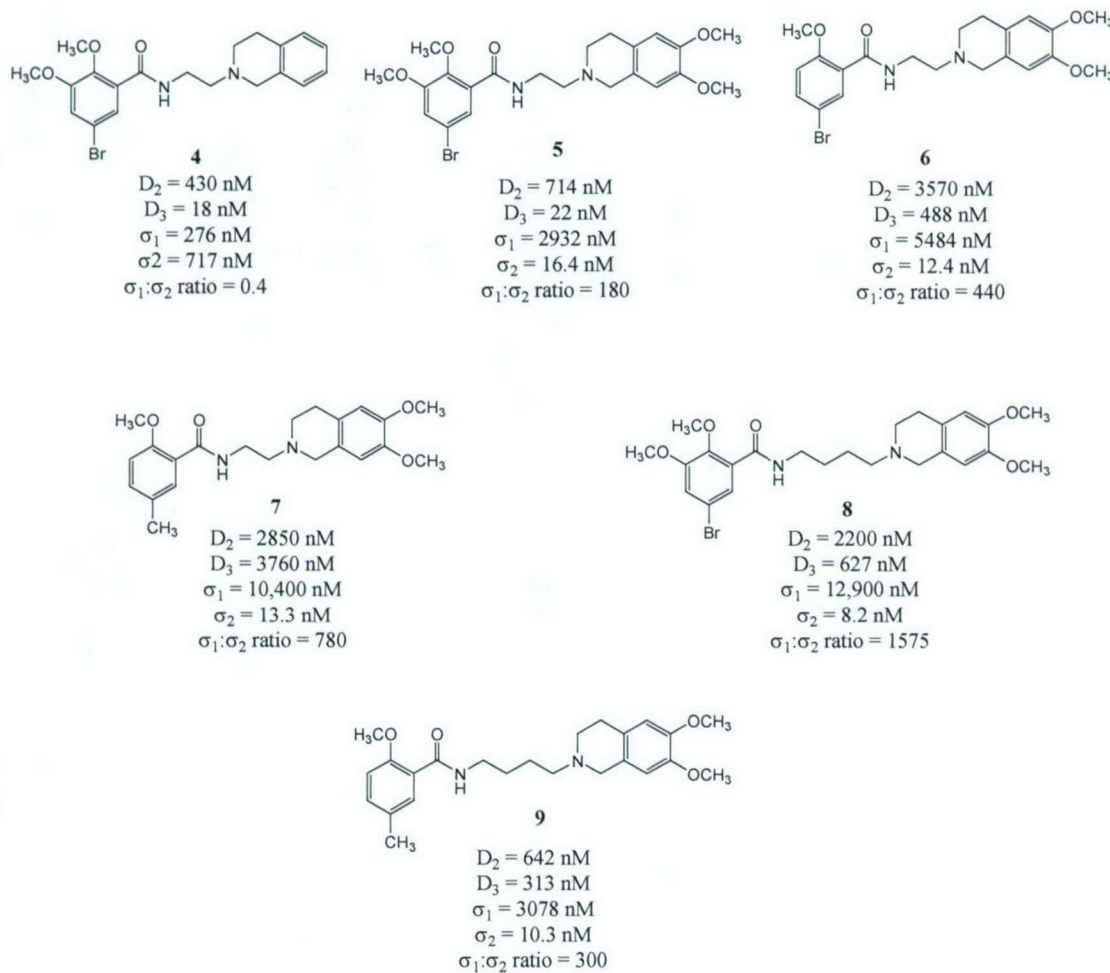
<sup>a</sup>%I.D. tumor/%I.D. blood; <sup>b</sup>%I.D. tumor/%I.D. muscle.



**Figure 2.** Blocking studies with haloperidol. Co-injection of 50 µg of haloperidol resulted in a reduction in tumor:background ratios and uptake of [<sup>18</sup>F]2 at 60 min post-i.v. injection of the radiotracer.

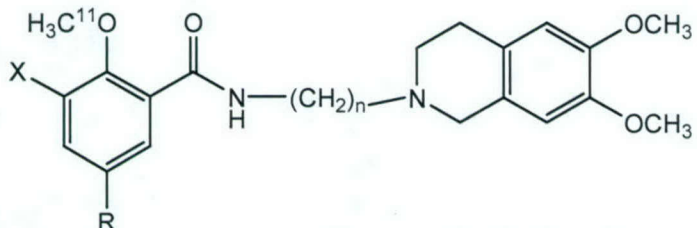
Conclusion. The results of this study indicate that [<sup>18</sup>F]1 labels σ<sub>2</sub> receptors in breast tumors. However, the relatively low tumor:background ratios of this radiotracer, which is likely due to the moderate affinity of 2 for σ<sub>2</sub> receptors, prompted us to investigate other ligands having a higher affinity for σ<sub>2</sub> receptors.

**2. Synthesis of  $\sigma_2$  selective conformational-flexible benzamide analogs.** During the year 2 of this research project, we turned our attention to the development of a new class of  $\sigma_2$ -selective compounds that were discovered as part of a parallel research program in the laboratory of the P.I.. Over the past 9 years, the P.I. of this Army Breast Cancer grant has had funding from the National Institute on Drug Abuse to develop dopamine receptor antagonists displaying a high affinity and selectivity for dopamine D<sub>3</sub> versus D<sub>2</sub> receptors. Since many D<sub>2</sub> antagonists have been found to have a high affinity for sigma receptors, we typically screen our dopamine antagonists for sigma receptor affinity. An interesting, and somewhat serendipitous, observation was made with the benzamide analogues **5** and **6** (Figure 3). The 2,3-dimethoxy-5-bromo benzamide analogue, **4**, displayed a high affinity for dopamine D<sub>3</sub> receptors and a relatively low affinity for D<sub>2</sub>,  $\sigma_1$  and  $\sigma_2$  receptors. Introduction of a dimethoxy substitution into the tetrahydroisoquinoline moiety (compound **5**) resulted in a dramatic increase in affinity for  $\sigma_2$  receptors, no change in D<sub>3</sub> affinity, and a reduction in affinity for D<sub>2</sub> and  $\sigma_1$  receptors. Since our previous structure-activity relationship studies had demonstrated that removal of the 3-methoxy group from the benzamide moiety results in a dramatic reduction in affinity for D<sub>2</sub> and D<sub>3</sub> receptors [6], compound **6** was prepared as a potential  $\sigma_2$  receptor. As expected, the results of in vitro binding studies revealed that **6** had a reduced affinity for dopamine D<sub>2</sub> and D<sub>3</sub> receptors, a lower affinity for  $\sigma_1$  receptors, and an increase in affinity for  $\sigma_2$  receptors (compare **6** versus **5**). Further structural modifications resulting in the identification of potent  $\sigma_2$  ligands involved the replacement of the 5-bromo substituent of **6** with a methyl group (compound **7**), and increasing the length of the methylene spacer from 2 carbons in **5** and **7** to four carbons (i.e., compounds **8** and **9**). Compounds **6**, **7**, **8**, and **9** are the most potent and selective  $\sigma_2$  receptor ligands identified to date.



**Figure 3.** Structures of the  $\sigma_2$ -selective compounds for PET radiotracer development.

2.1. Carbon-11 labeled analogs. The presence of a 2-methoxy group in the lead compounds **6**, **7**, **8**, and **9** indicates that it is possible to prepare a <sup>11</sup>C-labeled version of the  $\sigma_2$  ligands using standard radiochemistry procedures. This was accomplished via O-alkylation of the phenol precursor with [<sup>11</sup>C]methyl iodide. The overall yield (15-75% from [<sup>11</sup>C]methyl iodide) and specific activity (1000 – 4000 mCi/ $\mu$ mol) of each radiotracer was suitable for in vivo studies.

**Table II.**

#	X	R	n	$\sigma_1$	$\sigma_2$	$\sigma_1: \sigma_2$ Ratio	% Yield	Specific Activity (EOB)
7	H	CH <sub>3</sub>	2	10,412	13.3	783	60-75	~5,000 mCi/ $\mu$ mol
9	H	CH <sub>3</sub>	4	3,078	10.3	300	60-75	~4,000 mCi/ $\mu$ mol
6	H	Br	2	5,484	12.2	442	10-15	~1,000 mCi/ $\mu$ mol
8	OCH <sub>3</sub>	Br	4	12,900	8.2	1,573	30-40	~4,000 mCi/ $\mu$ mol

2.2. Biodistribution Studies of the <sup>11</sup>C-labeled radiotracers in Tumor-Bearing Mice. Biodistribution studies were conducted in mature Balb/c mice that were implanted with EMT-6 mammary tumors. The mice were implanted in the scapular region 7 days prior to the study. Animals were injected with 100-150  $\mu$ Ci of the <sup>11</sup>C-labeled radiotracer and the animals were sacrificed at 5, 30, and 60 min post-i.v. injection of the radiotracer. The results of the biodistribution studies are given in Tables III-VI.

**Table III.**

<sup>[11]C]7</sup> Biodistribution in EMT-6 BALB/C mice			
%ID per gram	5 min	30 min	1 hour
blood	5.89 ± 0.29	2.62 ± 0.22	1.98 ± 0.35
lung	5.69 ± 0.70	1.42 ± 0.15	1.39 ± 0.67
liver	18.49 ± 2.87	3.87 ± 0.67	1.70 ± 0.23
kidney	44.07 ± 1.67	2.77 ± 0.42	1.01 ± 0.12
muscle	1.75 ± 0.21	0.56 ± 0.19	0.41 ± 0.22
fat	3.07 ± 0.40	0.38 ± 0.12	0.26 ± 0.09
heart	2.89 ± 0.36	0.76 ± 0.06	0.76 ± 0.46
brain	1.63 ± 0.30	0.11 ± 0.01	0.10 ± 0.04
tumor	3.10 ± 0.25	1.08 ± 0.08	0.85 ± 0.14
<b>ratio</b>			
Tumor:blood	0.53 ± 0.04	0.41 ± 0.02	0.44 ± 0.06
Tumor:lung	0.55 ± 0.07	0.77 ± 0.14	0.68 ± 0.19
Tumor:muscle	1.79 ± 0.20	2.08 ± 0.59	2.40 ± 0.84
Tumor:fat	1.03 ± 0.21	3.10 ± 1.21	3.46 ± 0.91
Tumor:heart	1.08 ± 0.10	1.43 ± 0.14	1.32 ± 0.45

**Table IV.**

[ <sup>11</sup> C]9 Biodistribution in EMT-6 BALB/C mice			
%ID per gram	5 min	30 min	1 hour
blood	3.09 ± 0.33	1.31 ± 0.11	0.73 ± 0.05
lung	14.02 ± 1.40	2.27 ± 0.42	1.09 ± 0.26
liver	12.32 ± 1.73	9.65 ± 2.00	3.00 ± 0.21
kidney	20.50 ± 1.86	4.12 ± 0.51	2.26 ± 0.36
muscle	4.49 ± 0.45	0.75 ± 0.13	0.49 ± 0.11
fat	1.88 ± 0.50	0.68 ± 0.19	0.33 ± 0.24
heart	5.86 ± 0.47	0.95 ± 0.17	0.50 ± 0.11
brain	2.29 ± 0.28	0.28 ± 0.03	0.15 ± 0.01
tumor	4.22 ± 1.01	2.35 ± 0.27	1.32 ± 0.17
<b>ratio</b>			
Tumor:blood	1.37 ± 0.33	1.80 ± 0.26	1.81 ± 0.11
Tumor:lung	0.31 ± 0.11	1.06 ± 0.24	1.28 ± 0.41
Tumor:muscle	0.93 ± 0.13	3.18 ± 0.51	2.78 ± 0.62
Tumor:fat	2.28 ± 0.32	3.68 ± 1.14	5.36 ± 2.38
Tumor:heart	0.71 ± 0.12	2.53 ± 0.55	2.78 ± 0.79

**Table V.**

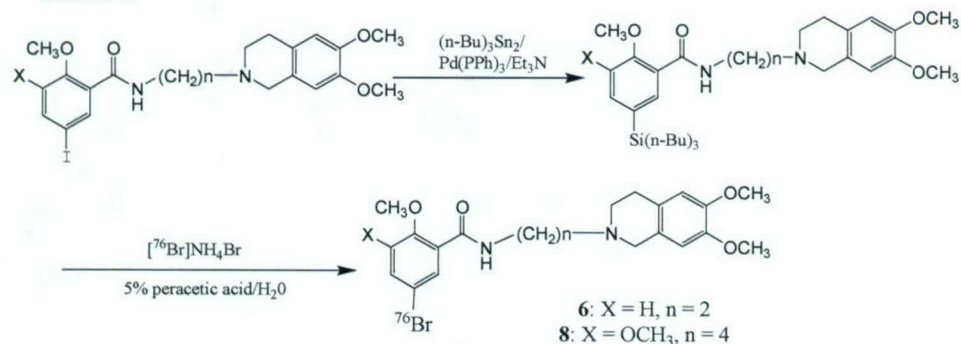
[ <sup>11</sup> C]6 Biodistribution in EMT-6 BALB/C mice			
%ID per gram	5 min	30 min	1 hour
blood	5.25 ± 0.39	2.35 ± 0.16	1.88 ± 0.16
lung	5.72 ± 0.40	1.83 ± 0.13	1.32 ± 0.11
liver	19.88 ± 3.10	5.89 ± 0.82	2.65 ± 0.29
kidney	51.03 ± 7.14	34.19 ± 1.74	19.78 ± 1.99
muscle	1.73 ± 0.11	0.52 ± 0.23	0.36 ± 0.08
fat	2.05 ± 0.49	0.63 ± 0.19	0.37 ± 0.13
heart	3.18 ± 0.26	0.77 ± 0.08	0.56 ± 0.05
brain	2.52 ± 0.15	0.26 ± 0.10	0.14 ± 0.02
tumor	1.82 ± 0.39	1.06 ± 0.09	0.87 ± 0.09
<b>ratio</b>			
Tumor:blood	0.35 ± 0.07	0.45 ± 0.05	0.46 ± 0.02
Tumor:lung	0.32 ± 0.06	0.58 ± 0.07	0.66 ± 0.03
Tumor:muscle	1.05 ± 0.21	2.24 ± 0.63	2.52 ± 0.66
Tumor:fat	0.93 ± 0.27	1.76 ± 0.40	2.64 ± 1.12
Tumor:heart	0.57 ± 0.09	1.39 ± 0.17	1.56 ± 0.16

**Table VI.**

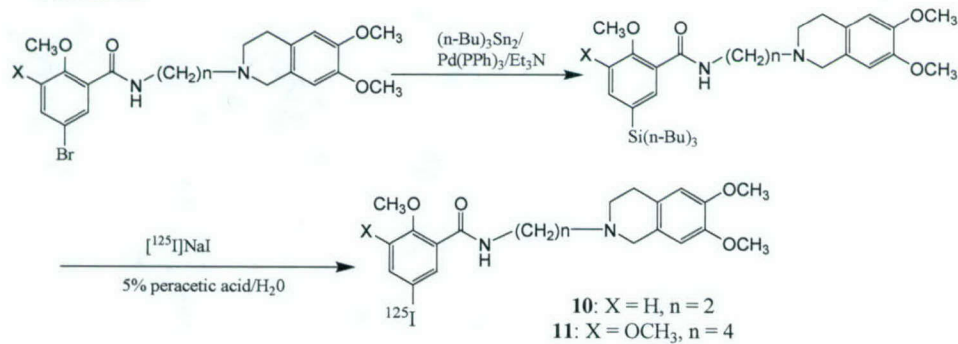
[ <sup>11</sup> C]8 Biodistribution in EMT-6 BALB/C mice			
%ID per gram	5 min	30 min	1 hour
blood	7.12 ± 1.01	0.99 ± 0.15	0.45 ± 0.04
lung	6.01 ± 0.77	1.34 ± 0.23	0.70 ± 0.26
liver(all)	25.02 ± 3.70	2.48 ± 0.52	1.19 ± 0.17
kidney	19.48 ± 1.46	2.57 ± 0.78	1.34 ± 0.19
muscle	1.94 ± 0.13	1.67 ± 0.14	0.26 ± 0.07
fat	1.66 ± 0.41	0.46 ± 0.19	0.20 ± 0.08
heart	3.54 ± 0.31	0.68 ± 0.12	0.29 ± 0.10
brain	0.33 ± 0.09	0.10 ± 0.00	0.03 ± 0.00
tumor	2.82 ± 0.36	0.92 ± 0.10	0.50 ± 0.09
<b>ratio</b>			
Tumor:blood	0.40 ± 0.01	0.94 ± 0.05	1.10 ± 0.11
Tumor:lung	0.47 ± 0.04	0.69 ± 0.08	0.79 ± 0.30
Tumor:muscle	1.46 ± 0.19	0.59 ± 0.05	1.84 ± 0.25
Tumor:fat	1.82 ± 0.45	2.05 ± 0.57	2.77 ± 0.82
Tumor:heart	0.80 ± 0.07	1.36 ± 0.12	1.86 ± 0.64

**2.3. Synthesis of Radiohalogenated  $\sigma_2$  Receptor Ligands.** The presence of a bromine atom in compounds **6** and **8** (Table I) indicates that it is possible to prepare radiohalogenated probes of the  $\sigma_2$  receptors by isotopic substitution with B-76, or by replacing the bromine atom with I-125. This was accomplished by preparing the corresponding tin precursor and conducting the oxidative radiohalogenation reactions outlined in Schemes II and III. The  $^{125}\text{I}$ -labeled analogs, **10** and **11**, were obtained in an overall yield of 50% and a specific activity of 2200 mCi/ $\mu\text{mol}$ . Similarly, the  $^{76}\text{Br}$ -labeled analogs of **5** and **7** were obtained in a yield of 50-60% and a specific activity >1,000 mCi/ $\mu\text{mol}$ . The  $\sigma_2$  receptor affinity of the radioiodinated probes was 0.5 nM for [ $^{125}\text{I}$ ]**10** and 0.25 nM for [ $^{125}\text{I}$ ]**11** from Scatchard studies using membranes isolated from either rat liver or EMT-6 breast tumor cells.

**Scheme II**



**Scheme III**



A series of biodistribution studies in tumor-bearing mice were also conducted with [<sup>76</sup>Br]6, [<sup>76</sup>Br]8, [<sup>125</sup>I]10, and [<sup>125</sup>I]11. The results of these studies are presented in Tables VII-X.

**Table VII.**

<sup>76</sup> Br]6 Biodistribution in EMT-6 BALB/C mice				
%ID per gram	5 min.	30 min.	1 hour	2 hour
blood	4.55 ± 0.59	2.55 ± 0.06	2.08 ± 0.69	3.46 ± 0.66
lung	5.52 ± 0.73	1.59 ± 0.10	1.20 ± 0.27	1.75 ± 0.20
liver(all)	17.85 ± 3.17	5.57 ± 1.31	3.09 ± 0.48	3.77 ± 0.80
spleen	3.22 ± 0.75	0.92 ± 0.26	0.59 ± 0.06	0.72 ± 0.05
kidney	50.08 ± 2.09	32.24 ± 4.64	15.60 ± 2.01	3.61 ± 0.52
muscle	1.42 ± 0.05	0.57 ± 0.07	0.56 ± 0.26	0.45 ± 0.02
fat	2.61 ± 0.45	0.80 ± 0.05	0.66 ± 0.11	0.69 ± 0.18
heart	2.44 ± 0.43	0.99 ± 0.13	0.78 ± 0.14	1.23 ± 0.18
brain	1.69 ± 0.18	0.24 ± 0.05	0.15 ± 0.01	0.21 ± 0.01
bone	1.55 ± 0.20	0.52 ± 0.02	0.50 ± 0.17	0.49 ± 0.17
tumor	2.28 ± 0.14	1.30 ± 0.08	1.12 ± 0.20	1.19 ± 0.13
<b>ratio</b>				
Tumor:blood	0.50 ± 0.04	0.51 ± 0.02	0.58 ± 0.22	0.35 ± 0.21
Tumor:lung	0.42 ± 0.05	0.82 ± 0.05	0.98 ± 0.34	0.68 ± 0.10
Tumor:muscle	1.61 ± 0.05	2.31 ± 0.40	2.47 ± 1.53	2.63 ± 2.47
Tumor:fat	0.90 ± 0.20	1.63 ± 0.02	1.71 ± 0.29	1.82 ± 2.22
Tumor:heart	0.95 ± 0.13	1.32 ± 0.19	1.50 ± 0.49	0.98 ± 0.13

**Table VIII.**

<sup>76</sup> Br]8 Biodistribution in EMT-6 BALB/C mice					
%ID per gram	5 min.	30 min.	1 hour	2 hour	4 hour
blood	2.12 ± 0.20	2.20 ± 0.24	1.60 ± 0.22	0.46 ± 0.07	0.21 ± 0.03
lung	24.64 ± 2.74	5.81 ± 1.12	2.45 ± 0.17	0.74 ± 0.04	0.29 ± 0.03
liver(all)	10.99 ± 0.29	8.85 ± 0.52	4.58 ± 0.36	1.67 ± 0.10	0.71 ± 0.08
spleen	12.50 ± 1.46	6.91 ± 1.22	2.61 ± 0.62	0.60 ± 0.03	0.20 ± 0.03
kidney	31.20 ± 2.92	18.51 ± 2.66	10.81 ± 1.72	1.85 ± 0.54	0.57 ± 0.12
muscle	3.62 ± 0.27	1.54 ± 0.49	0.61 ± 0.11	0.20 ± 0.03	0.07 ± 0.01
fat	3.78 ± 0.97	2.27 ± 0.16	0.81 ± 0.16	0.22 ± 0.05	0.04 ± 0.02
heart	7.31 ± 0.70	2.15 ± 0.30	1.08 ± 0.07	0.30 ± 0.03	0.11 ± 0.02
brain	1.60 ± 0.15	0.41 ± 0.06	0.17 ± 0.02	0.05 ± 0.00	0.03 ± 0.00
bone	3.10 ± 0.67	2.76 ± 0.58	1.38 ± 0.09	0.56 ± 0.20	0.12 ± 0.03
tumor	4.78 ± 0.78	5.31 ± 0.62	3.98 ± 0.58	1.71 ± 0.17	0.68 ± 0.15
<b>ratio</b>					
Tumor:blood	2.25 ± 0.28	2.41 ± 0.08	2.53 ± 0.54	3.79 ± 0.99	3.17 ± 0.58
Tumor:lung	0.19 ± 0.02	0.93 ± 0.09	1.64 ± 0.30	2.30 ± 0.13	2.36 ± 0.46
Tumor:muscle	1.32 ± 0.16	3.70 ± 1.06	6.76 ± 2.09	8.81 ± 0.91	9.48 ± 2.14
Tumor:fat	1.30 ± 0.24	2.35 ± 0.34	5.09 ± 1.39	7.97 ± 1.95	20.69 ± 10.77
Tumor:heart	0.65 ± 0.07	2.48 ± 0.17	3.72 ± 0.72	5.77 ± 0.60	6.24 ± 1.28

**Table IX.**

[ <sup>125</sup> I]10 Biodistribution in EMT-6 BALB/C mice				
%ID per gram	5 min.	30 min.	1 hour	2 hour
blood	6.90 ± 1.29	2.44 ± 0.65	1.17 ± 0.29	3.37 ± 1.23
lung	5.95 ± 1.30	1.39 ± 0.29	0.81 ± 0.20	1.27 ± 0.37
liver(all)	41.37 ± 7.23	8.20 ± 1.05	2.87 ± 0.34	3.47 ± 1.05
kidney	54.77 ± 8.42	38.59 ± 2.05	18.07 ± 2.07	8.46 ± 1.26
muscle	1.47 ± 0.20	0.70 ± 0.25	0.37 ± 0.23	0.38 ± 0.06
fat	3.46 ± 0.59	1.03 ± 0.44	0.77 ± 0.66	0.37 ± 0.13
heart	2.79 ± 0.35	0.94 ± 0.19	0.40 ± 0.02	0.86 ± 0.26
brain	1.42 ± 0.33	0.20 ± 0.06	0.06 ± 0.02	0.09 ± 0.03
tumor	2.91 ± 0.40	1.33 ± 0.13	0.71 ± 0.12	0.82 ± 0.09
<b>ratio</b>				
Tumor:blood	0.42 ± 0.03	0.57 ± 0.12	0.62 ± 0.09	0.26 ± 0.08
Tumor:lung	0.50 ± 0.07	0.98 ± 0.16	0.91 ± 0.24	0.67 ± 0.14
Tumor:muscle	2.00 ± 0.37	2.06 ± 0.69	2.14 ± 0.99	2.17 ± 0.23
Tumor:fat	0.84 ± 0.06	1.49 ± 0.65	1.93 ± 1.87	2.44 ± 0.77
Tumor:heart	1.04 ± 0.08	1.44 ± 0.18	1.81 ± 0.32	1.00 ± 0.27

**Table X.**

[ <sup>125</sup> I]11 Biodistribution in EMT-6 BALB/C mice					
%ID per gram	5 min.	30 min.	1 hour	2 hour	4 hour
blood	2.37 ± 0.26	2.19 ± 0.16	1.52 ± 0.49	0.65 ± 0.07	0.29 ± 0.11
lung	27.13 ± 1.61	5.50 ± 0.62	2.12 ± 0.19	1.01 ± 0.18	0.29 ± 0.05
liver(all)	13.20 ± 2.04	8.77 ± 0.88	4.24 ± 0.60	1.91 ± 0.20	0.90 ± 0.21
kidney	29.51 ± 2.23	13.69 ± 0.35	5.94 ± 1.22	2.45 ± 0.25	0.63 ± 0.11
muscle	4.10 ± 0.33	1.21 ± 0.17	0.87 ± 0.22	0.31 ± 0.10	0.10 ± 0.04
fat	4.15 ± 0.91	1.73 ± 0.20	0.74 ± 0.17	0.33 ± 0.08	0.10 ± 0.05
heart	6.55 ± 0.54	1.94 ± 0.09	0.91 ± 0.10	0.40 ± 0.05	0.15 ± 0.04
brain	1.53 ± 0.14	0.39 ± 0.03	0.15 ± 0.03	0.06 ± 0.01	0.02 ± 0.01
tumor	4.02 ± 0.55	4.50 ± 0.43	3.53 ± 0.42	1.88 ± 0.76	0.82 ± 0.09
<b>ratio</b>					
Tumor:blood	1.73 ± 0.46	2.07 ± 0.32	2.44 ± 0.53	2.83 ± 1.62	3.11 ± 0.85
Tumor:lung	0.15 ± 0.02	0.82 ± 0.09	1.66 ± 0.17	1.99 ± 1.04	2.83 ± 0.19
Tumor:muscle	0.98 ± 0.13	3.94 ± 0.55	4.26 ± 0.74	6.99 ± 4.44	8.98 ± 3.01
Tumor:fat	1.00 ± 0.20	2.62 ± 0.27	4.85 ± 0.67	5.86 ± 2.93	9.59 ± 4.55
Tumor:heart	0.61 ± 0.07	2.32 ± 0.18	3.89 ± 0.08	4.85 ± 2.31	5.91 ± 1.65

**2.4. Blocking studies.** The results of the above biodistribution studies in tumor bearing rodents indicate that [<sup>11</sup>C]9, [<sup>76</sup>Br]8, and [<sup>125</sup>I]11 are potential candidates for further evaluation. The next step in the project was to conduct blocking studies in order to confirm that the radiotracer labeled  $\sigma_2$  receptors in the breast tumors. These studies were conducted using the nonselective sigma ligand, YUN 143 (1 mg/kg, i.v.), which has a high affinity for both  $\sigma_1$  and  $\sigma_2$  receptors. We have previously reported that [<sup>18</sup>F]YUN 143 labels  $\sigma_1$  and  $\sigma_2$  receptors in breast tumor xenografts [7]. The results of the blocking study are shown in Figure 4 and are consistent with the labeling of  $\sigma_2$  receptors in vivo.

## Tumor uptake of sigma-2 receptor compounds in control vs. block EMT-6 BALB/C mice

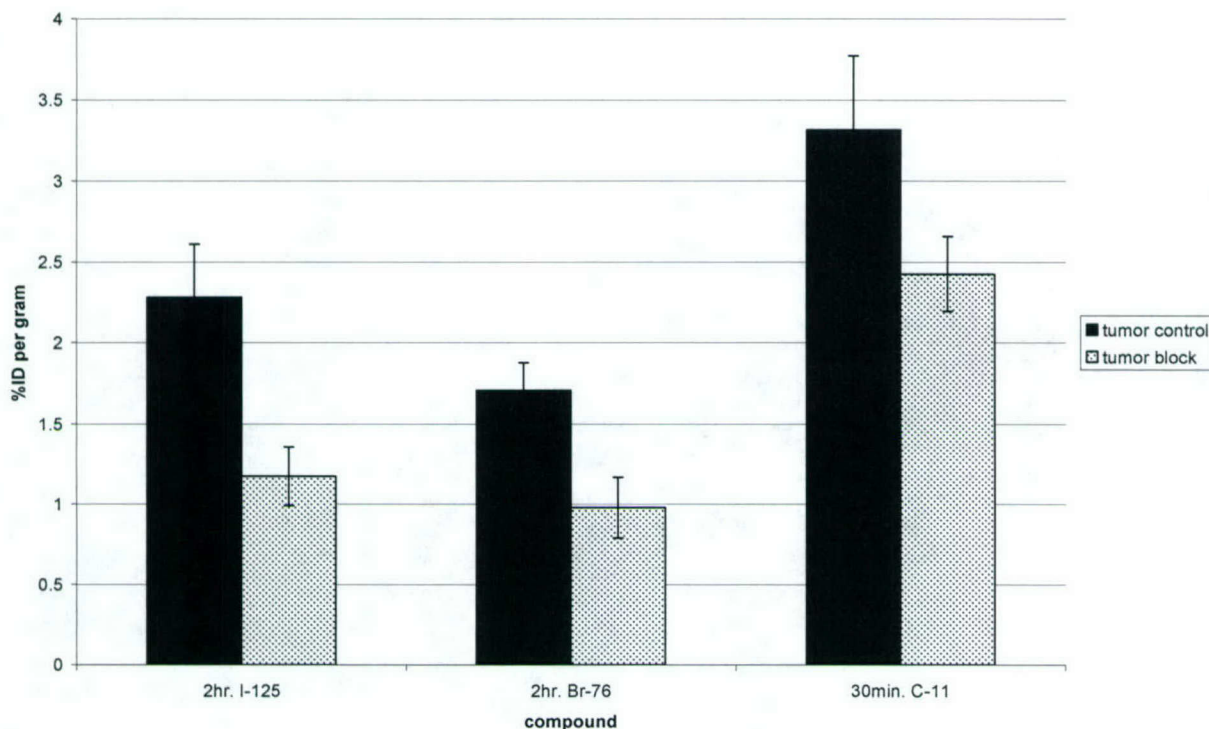
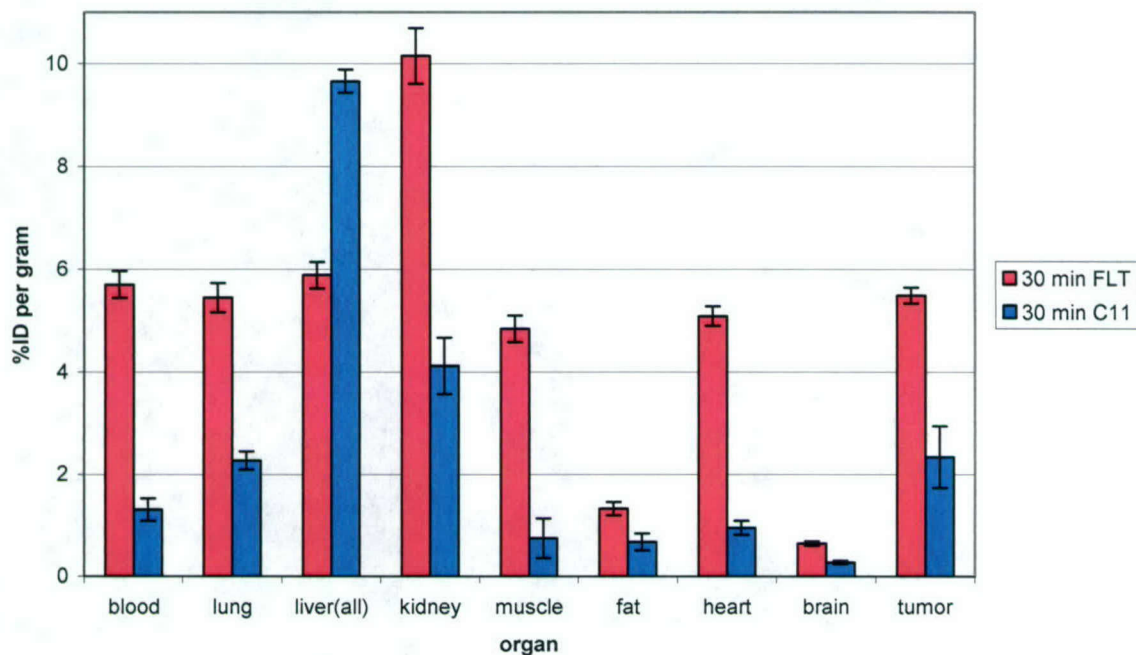


**Figure 4.** In vivo blocking studies of  $[^{125}\text{I}]11$  (left),  $[^{76}\text{Br}]8$  (center), and  $[^{11}\text{C}]9$  (right) in tumor-bearing mice. The blocking agent was YUN 143, which has a high affinity for  $\sigma_1$  and  $\sigma_2$  receptors. Animals were sacrificed at the time point displaying the highest %I.D./gram tumor. The data are consistent with the labeling of  $\sigma_2$  receptors in vivo by each radiotracer.

**2.5. Comparison with  $[^{18}\text{F}]FLT$ .** Although not a part of this IDEA grant award, we have also conducted a series of studies comparing the  $\sigma_2$  receptor imaging approach with  $[^{18}\text{F}]FLT$ .  $[^{18}\text{F}]FLT$  is a nucleoside-based approach that has been hypothesized to measure the proliferation in solid tumors. These studies were funded in part through the NIH grant CA102869 and the results are summarized in Figures 5-7. In this study, the uptake of  $[^{18}\text{F}]FLT$  at 1 hr was compared with the 1 hr data for  $[^{11}\text{C}]9$ . For studies comparing  $[^{18}\text{F}]FLT$  with  $[^{76}\text{Br}]8$  and  $[^{125}\text{I}]11$ , the 2 hr post-i.v. injection time point was used. The results of these studies can be summarized as follows:

1.  $[^{11}\text{C}]9$ , has tumor:lung and tumor:fat ratios equal to  $[^{18}\text{F}]FLT$  and tumor:blood, tumor:muscle and tumor:heart ratios that are greater than that of  $[^{18}\text{F}]FLT$ ;
2.  $[^{76}\text{Br}]8$ , has higher tumor:background ratios greater than that observed with  $[^{18}\text{F}]FLT$ ;
3.  $[^{125}\text{I}]11$ , has a similar tumor:fat ratio as  $[^{18}\text{F}]FLT$  and exceeds  $[^{18}\text{F}]FLT$  in all other tumor:background ratios.

## Uptake comparison for FLT vs. [C-11]9 in EMT-6 BALB/C mice



## Tumor to background for FLT vs. [C-11]9 in EMT-6 BALB/C mice

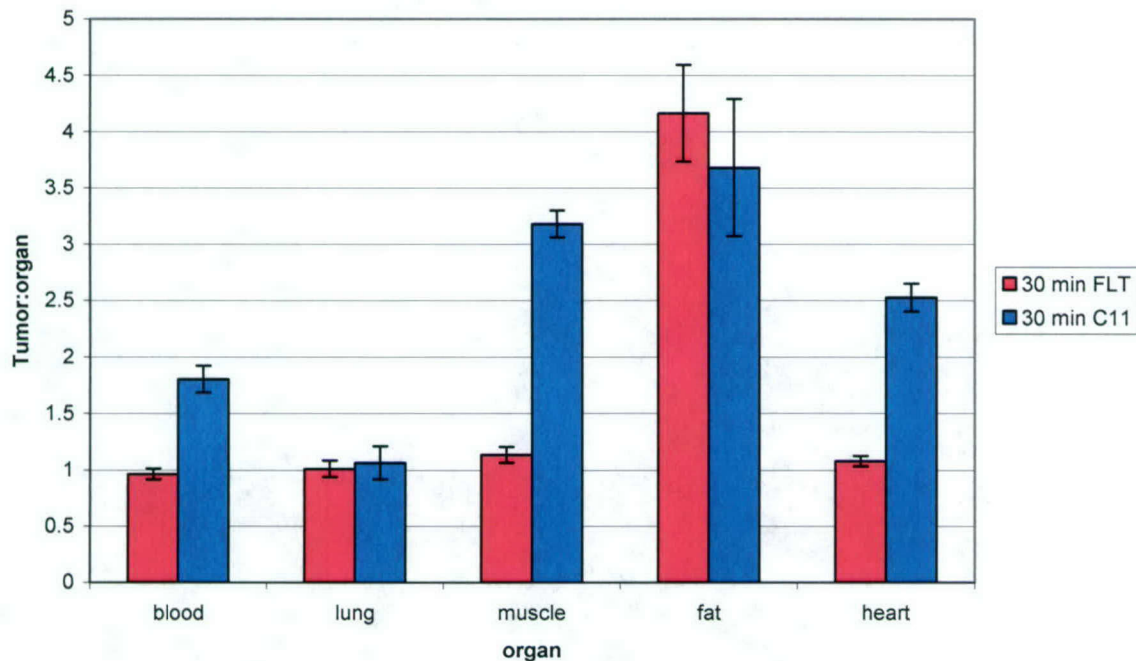
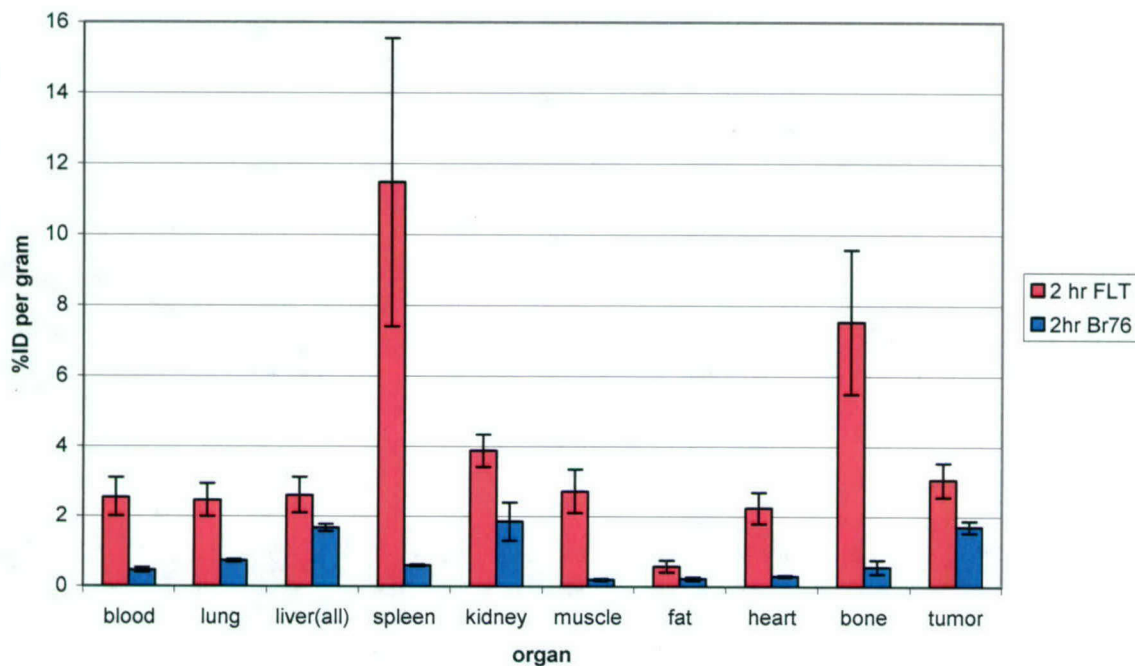
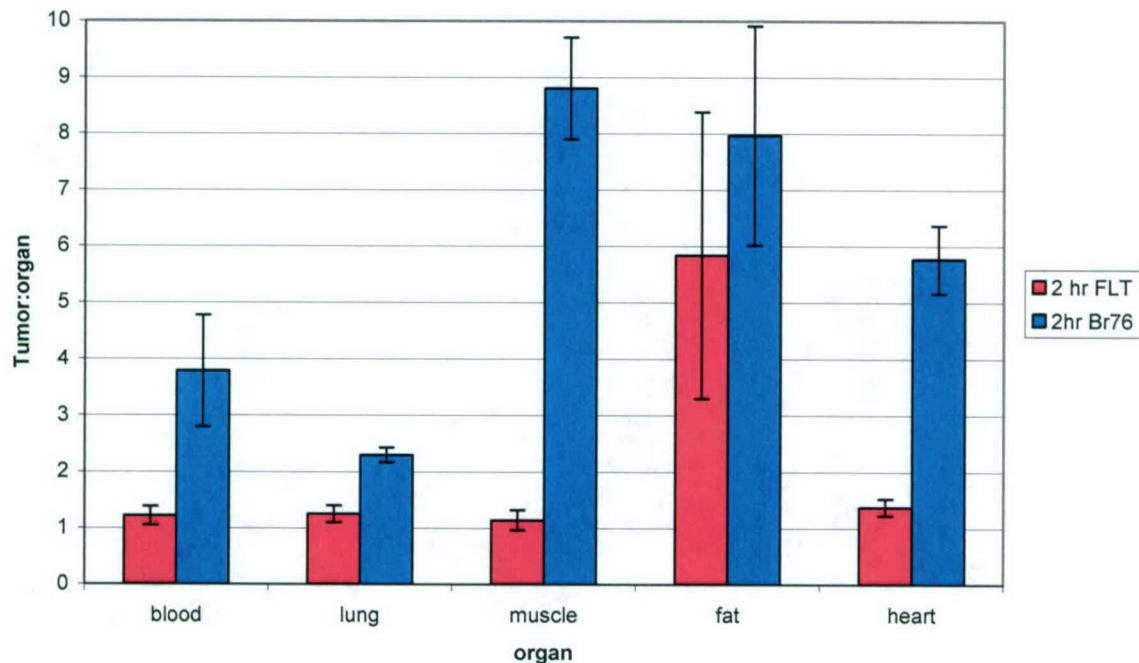


**Figure 5.** Comparison of  $[^{18}\text{F}]\text{FLT}$  and  $[^{11}\text{C}]9$ . Although  $[^{18}\text{F}]\text{FLT}$  has a high uptake in tumors (top graph), the high uptake of radioactivity in normal tissues results in a lower tumor:background ratio of  $[^{18}\text{F}]\text{FLT}$  relative to  $[^{11}\text{C}]9$ , particularly the tumor:muscle, tumor:blood, and tumor:heart ratios (bottom graph).

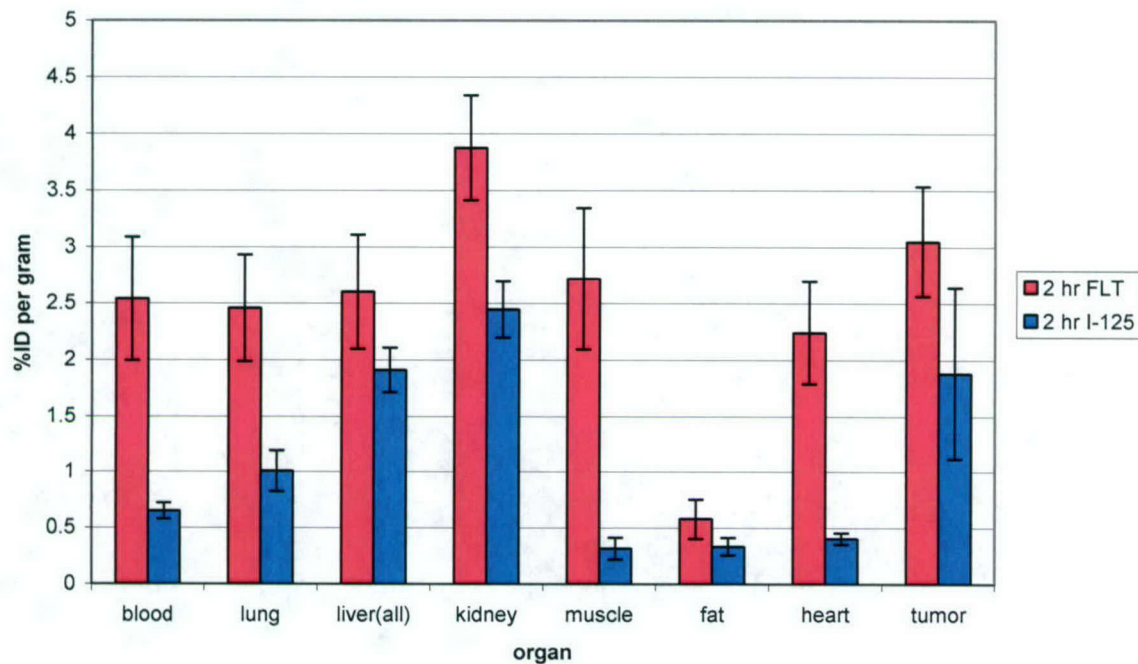
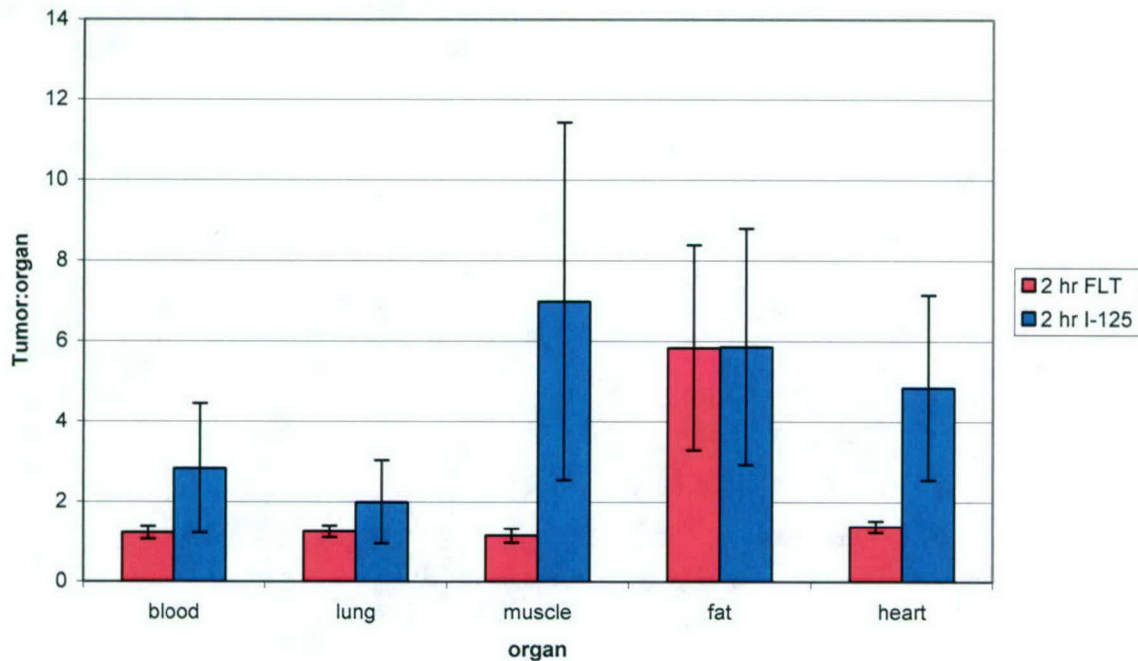
## Uptake comparison for FLT vs. [Br-76]8 in EMT-6 BALB/C mice



## Tumor to background for FLT vs. [Br-76]8 in EMT-6 BALB/C mice



**Figure 6.** Comparison of  $[^{18}\text{F}]\text{FLT}$  with  $[^{76}\text{Br}]8$  at 2 hrs post-i.v. injection. Notice the higher tumor:background ratios of  $[^{76}\text{Br}]7$  versus that of  $[^{18}\text{F}]\text{FLT}$ .

Uptake comparison for FLT vs. [ $\text{I-125}$ ]11 in EMT-6 BALB/C miceTumor to background for FLT vs. [ $\text{I-125}$ ]11 in EMT-6 BALB/C mice

**Figure 7.** Comparison of  $[^{18}\text{F}]\text{FLT}$  with  $[^{125}\text{I}]11$  at 2 hrs post-i.v. injection. Notice the higher tumor:blood, tumor:muscle, and tumor:heart ratios of  $[^{125}\text{I}]11$  versus that of  $[^{18}\text{F}]\text{FLT}$ .

2.6. MicroPET Imaging Studies. We have also conducted microPET imaging studies with [<sup>76</sup>Br]8 in Balb-c mice bearing EMT-6 breast tumor xenografts. The results of the imaging studies are shown in Figure 8. Note the high uptake of the radiotracer in the NCA study (left image), which can be blocked with a known sigma receptor ligand (right image). These data indicate that [<sup>76</sup>Br]8 is a potential radiotracer for imaging the  $\sigma_2$  receptor status of breast tumors.

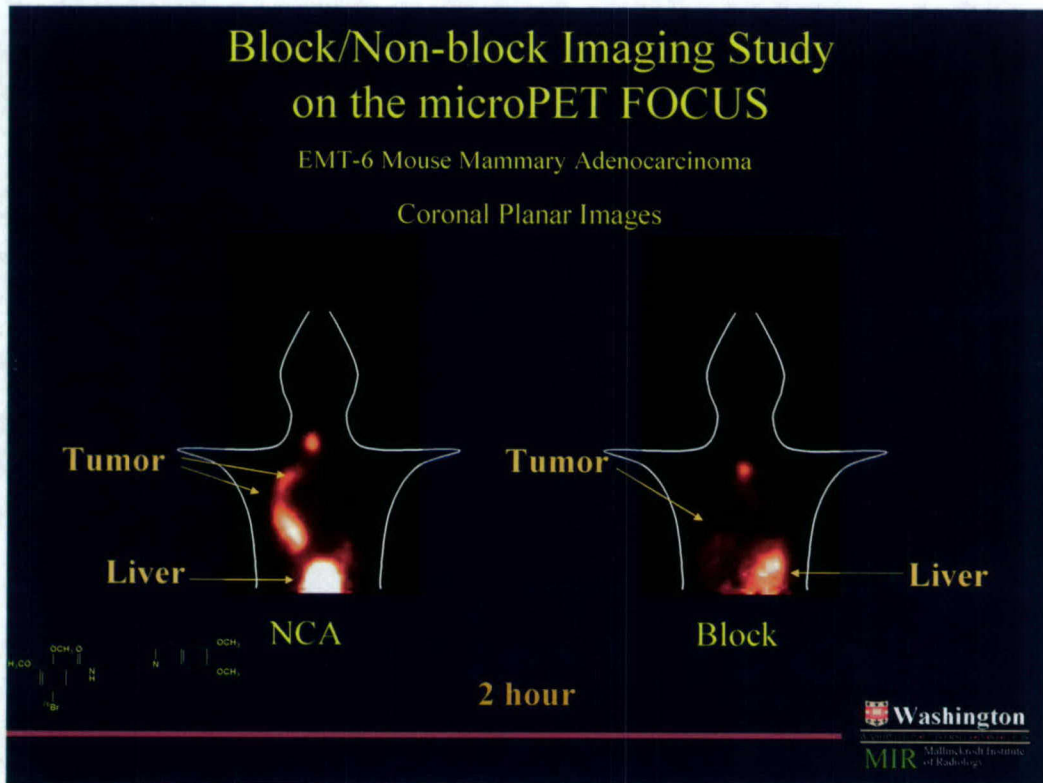


**Figure 8.** MicroPET imaging studies of [<sup>76</sup>Br]8 in Balb-c mice bearing an EMT-6 breast tumor xenograft. The no-carrier-added (NCA) study is on the left and the sigma receptor blocking study (1 mg/kg, i.v. YUN-143) is shown on the right.

### **Key Research Accomplishments**

- Identification of a new lead compound for PET radiotracer development and completion of a structure-activity relationship study aimed at improving the affinity and selectivity of the lead compound for  $\sigma_2$  versus  $\sigma_1$ , D<sub>2</sub> and D<sub>3</sub> receptors.
- Preparation of a <sup>11</sup>C-, <sup>125</sup>I, and <sup>76</sup>Br-labeled  $\sigma_2$  receptor ligands and completion of in vivo biodistribution and microPET imaging studies.
- Comparison of the  $\sigma_2$  receptor imaging approach with that of the nucleoside-based imaging agent, [<sup>18</sup>F]FLT, and demonstration that the  $\sigma_2$  receptor approach yields signal:noise ratios equal or greater than that of [<sup>18</sup>F]FLT.

## **Reportable Outcomes**

Mach R.H., Vangveravong S., Huang Y., Yang B., Blair J.B., Wu L. Synthesis of N-substituted 9-azabicyclo[3.3.1]nonan-3 $\alpha$ -yl phenylcarbamate analogs as sigma-2 receptor ligands. *Medicinal Chemistry Research* 2003; 11: 380-398.

Mach R.H., Huang Y., Freeman R.A., Wu L., Vangveravong S., Luedtke R.R. Conformationally-flexible benzamide analogs as dopamine D<sub>3</sub> and  $\sigma_2$  receptor ligands. *Bioorg Med. Chem. Lett* 2004; 14: 195-202.

Mach R.H., Brown-Proctor C., Vangveravong S., Blair J.B., Buchheimer N., Bottoms J., Wheeler K.T. Receptor-based radiotracers for imaging the proliferative status of breast tumors. *Synthesis and Applications of Isotopically Labelled Compounds, Volume 8*; 2004: 157-160.

Tu Z., Dence C.S., Ponde D.E., Jones L., Wheeler K.T., Welch M.J., Mach R.H. Carbon-11 labeled  $\sigma_2$  receptor ligands for imaging breast cancer. *Nucl. Med. Biol.*, accepted for publication.

Rowland D.J., Tu Z., Mach R.H., Welch M.J. Investigation of a new sigma-2 receptor ligand for detecting breast cancer. *J. Label. Compd. Radiopharm.* 2003; 46: S6.

Tu Z., Dence C.S., Wheeler K.T., Welch M.J., Mach R.H. Carbon-11 labeled sigma-2 receptor ligands for imaging breast cancer. *J. Nucl. Med.* 2004; 45: 168P.

Mach R.H., Kung M.-P., Tu Z., Vangveravong S., Wheeler K.T., Kung H.F., Welch M.J. Radioiodinated probes for imaging the  $\sigma_2$  receptor status of breast tumors. *J. Nucl. Med.* 2004; 45: 170P.

## **Conclusions**

We have made outstanding progress over the course of this research project. For example, we have identified a new class of  $\sigma_2$ -selective radiotracers that can be readily radiolabeled with C-11, I-125/I-123, and Br-76. Preliminary biodistribution studies indicate that [<sup>11</sup>C]8, [<sup>76</sup>Br]7, and [<sup>125</sup>I]11 display a high tumor uptake and reasonable target:background ratios. Comparison studies with [<sup>18</sup>F]FLT indicate that the  $\sigma_2$  receptor imaging approach may give a higher signal:noise background ratio versus the labeled nucleoside approach. The results of this IDEA grant have been used as the preliminary data to obtain funding from the National Cancer Institute (CA102869) to continue this avenue of research. We hope to initiate a clinical trial in breast cancer patients with one of the radiotracers described in this progress report.

## **References**

- [1] Mach RH, Smith CR, Al-Nabulsi I, Whirrett BR, Childers SR, Wheeler KT. Sigma-2 receptors as potential biomarkers of proliferation in breast cancer. *Cancer Res* 1997; 57:156-161.
- [2] Al-Nabulsi I, Mach RH, Wang L-M, Wallen CA, Keng PC, Sten K, Childers SR, Wheeler KT. Effect of ploidy, recruitment, environmental factors, and tamoxifen treatment on the expression of sigma-2 receptors in proliferating and quiescent tumor cells. *Br J Cancer* 1999; 81:925-933.

- [3] Wheeler KT, Wang L-M, Wallen CA, Childers SR, Cline JM, Keng PC, Mach RH. Sigma-2 receptors as a biomarker of proliferation in solid tumors. *Br J Cancer* 2000; 86:1223-1232.
- [4] Mach RH, Yang B, Wu L, Kuhner RJ, Whirrett BR, West T. Synthesis and sigma receptor binding affinities of 8-azabicyclo[3.2.1]octan-3 $\alpha$ -yl and 9 azabicyclo[3.3.1]nonan-3 $\alpha$ -yl phenyl carbamates. *Med Chem Res* 2001; 10(6):399-355.
- [5] Mach RH, Elder ST, Morton TE, Nowak PA, Evora PH, Scripko JG, Luedtke RR, Unsworth CD, Filtz T, Rao AV, Molinoff PB, Ehrenkaufer RL. The use of [ $^{18}$ F]4-fluorobenzyl iodide (FBI) in PET radiotracer synthesis: model alkylation studies and its application in the design of dopamine D<sub>1</sub> and D<sub>2</sub> receptor-based imaging agents. *Nucl Med Biol* 1993; 20:777-794.
- [6] Mach RH, Hammond PS, Huang Y, Yang B, Xu Y, Cheney JT, Freeman R, Luedtke RR. Structure-activity relationship studies of N-(9-benzyl)-9-azabicyclo-[3.3.1]nonan-3 $\beta$ -yl benzamide analogues for dopamine D<sub>2</sub> and D<sub>3</sub> receptors. *Med Chem Res* 1999; 9:355-373.
- [7] Mach RH, Huang Y, Buchheimer N, Kuhner R, Wu L, Morton TE, Wang L-M, Ehrenkaufer RL, Wallen CA, Wheeler KT. [ $^{18}$ F]N-4'-fluorobenzyl-4-(3-bromophenyl)acetamide for imaging the sigma receptor status of tumors: comparison with [ $^{18}$ F]FDG and [ $^{125}$ I]IUDR. *Nucl Med Biol* 2001; 28:451-458.

## Appendices

Mach R.H., Vangveravong S., Huang Y., Yang B., Blair J.B., Wu L. Synthesis of N-substituted 9-azabicyclo[3.3.1]nonan-3 $\alpha$ -yl phenylcarbamate analogs as sigma-2 receptor ligands. *Medicinal Chemistry Research* 2003; 11: 380-398.

Mach R.H., Huang Y., Freeman R.A., Wu L., Vangveravong S., Luedtke R.R. Conformationally-flexible benzamide analogs as dopamine D<sub>3</sub> and  $\sigma_2$  receptor ligands. *Bioorg Med. Chem. Lett* 2004; 14: 195-202.

Mach R.H., Brown-Proctor C., Vangveravong S., Blair J.B., Buchheimer N., Bottoms J., Wheeler K.T. Receptor-based radiotracers for imaging the proliferative status of breast tumors. *Synthesis and Applications of Isotopically Labelled Compounds, Volume 8*; 2004: 157-160.

Tu Z., Dence C.S., Ponde D.E., Jones L., Wheeler K.T., Welch M.J., Mach R.H. Carbon-11 labeled  $\sigma_2$  receptor ligands for imaging breast cancer. *Nucl. Med. Biol.*, accepted for publication.

## **APPENDICES**

**SYNTHESIS OF N-SUBSTITUTED 9-AZABICYCLO[3.3.1]NONAN-3 $\alpha$ -YL  
PHENYLCARBAMATE ANALOGS AS SIGMA-2 RECEPTOR LIGANDS**

Robert H. Mach,<sup>†,‡\*</sup> Suwanna Vangveravong,<sup>†,‡</sup> Yunsheng Huang,<sup>†,‡</sup>  
Biao Yang,<sup>†,‡</sup> Joseph B. Blair<sup>†</sup> and Li Wu,<sup>†</sup>

Departments of Radiology<sup>†</sup> and Physiology & Pharmacology,<sup>‡</sup>  
Wake Forest University School of Medicine, Winston-Salem, North Carolina 27157

\* Anasazi Biomedical Research, Inc., Winston-Salem, NC 27101

**Abstract.** A series of N-substituted-9-azabicyclo[3.3.1]nonan-3 $\alpha$ -yl)carbamate analogs was prepared and their affinities for sigma ( $\sigma_1$  and  $\sigma_2$ ) receptors was measured in vitro. The results of this structure-activity relationship study identified a novel compound, *N*-(9-(4-aminophenethyl))-9-azabicyclo[3.3.1]nonan-3 $\alpha$ -yl)-*N'*-(2-methoxy-5-methylphenyl)carbamate (**2f**), having a high affinity and excellent selectivity for  $\sigma_2$  versus  $\sigma_1$  receptors. This compound should be a useful ligand for characterizing the functional role of  $\sigma_2$  receptors *in vivo*.

Sigma ( $\sigma$ ) receptors represent a class of proteins that were initially thought to be a subtype of the opiate receptors. Subsequent studies revealed that sigma binding sites are a separate class of receptors located in the central nervous system and in a variety of tissues and organs.<sup>1,2</sup> It is widely accepted that there are two subtypes of the sigma receptor, termed  $\sigma_1$  and  $\sigma_2$ . Sigma-1 receptors have a molecular weight of ~25 kDa, whereas  $\sigma_2$  receptors have a molecular weight of ~21.5 kDa.

Address correspondence to: Robert H. Mach, Ph.D. Division of Radiological Sciences, Washington University School of Medicine, 510 S. Kingshighway Blvd., Campus Box 8225, St. Louis, MO 63110

The radioligand [<sup>3</sup>H](+)-pentazocine has a high affinity (3.2 nM) for the  $\sigma_1$  receptor and a low (>1,000 nM) affinity for the  $\sigma_2$  receptor, whereas [<sup>3</sup>H]DTG is equipotent at both  $\sigma_1$  and  $\sigma_2$  receptors.<sup>1</sup> An understanding of the functional significance of sigma binding sites has been limited by the failure to identify an endogenous ligand for these receptors. However, the  $\sigma_1$  receptor has been cloned and displays a 30% sequence homology with the enzyme yeast sterol isomerase.<sup>3</sup> Progesterone possesses a modest affinity for  $\sigma_1$  receptors,<sup>4</sup> which suggests that the  $\sigma_1$  receptor may play a role in steroid biochemistry. The  $\sigma_2$  receptor has not been cloned, but evidence suggests that it is linked to potassium channels in NCB-20 cells.<sup>1,2</sup> Attempts to clone the  $\sigma_2$  receptor have been hampered by the shortage of ligands displaying a high affinity and selectivity for this subtype.

A number of structurally-diverse compounds have been shown to possess a high affinity for sigma receptors.<sup>1</sup> Most of these compounds display either a high selectivity for the  $\sigma_1$  receptor or bind with equal affinity to both  $\sigma_1$  and  $\sigma_2$  receptors. Until recently, only a few  $\sigma_2$  selective ligands have been identified. For example, the phenyl morphan CD-184,<sup>5</sup> the trishomocubane analog ANSTO-20,<sup>6</sup> and the natural product ibogaine<sup>7,8</sup> have been shown to possess a moderate affinity and selectivity for  $\sigma_2$  versus  $\sigma_1$  receptors. Other reports have shown that spiro-joined piperidines,<sup>9</sup> and the corresponding 3-( $\alpha$ -aminoalkyl)-1H-indole derivatives of the spiro-joined piperidines and tropanes,<sup>10</sup> exhibit varying degrees of preference for  $\sigma_2$  versus  $\sigma_1$  receptors. In addition, the potent 5-HT<sub>3</sub> and 5-HT<sub>4</sub> ligand, BIMU-1,<sup>11</sup> was also found to have a moderate affinity and high selectivity for  $\sigma_2$  versus  $\sigma_1$  receptors.

Using BIMU-1 as a lead compound, we recently reported the synthesis and *in vitro* binding of a number of [3.2.1]azabicyclooctane (i.e., tropane) and [3.3.1]azabicyclononane (i.e., granatane) analogs having a modest affinity and selectivity for  $\sigma_2$  versus  $\sigma_1$  receptors.<sup>12</sup> The most active compound in this series was **1a**, which had a  $\sigma_2$  affinity of 3 nM and a  $\sigma_2$  versus  $\sigma_1$  selectivity ratio of 30 (Figure 1). The goal of the current study was to extend the structure-activity relationship study of this class of compounds by: 1) determining the effect of increasing the alkyl spacer group between the benzyl aromatic ring and the bridgehead nitrogen atom; and 2) the nature of the substituent effect in the aromatic ring attached to the bridgehead nitrogen atom. The results of this study led to the identification of **2f** as a highly selective  $\sigma_2$  ligand.

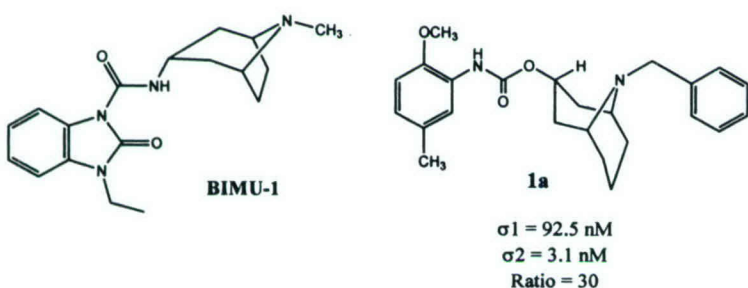


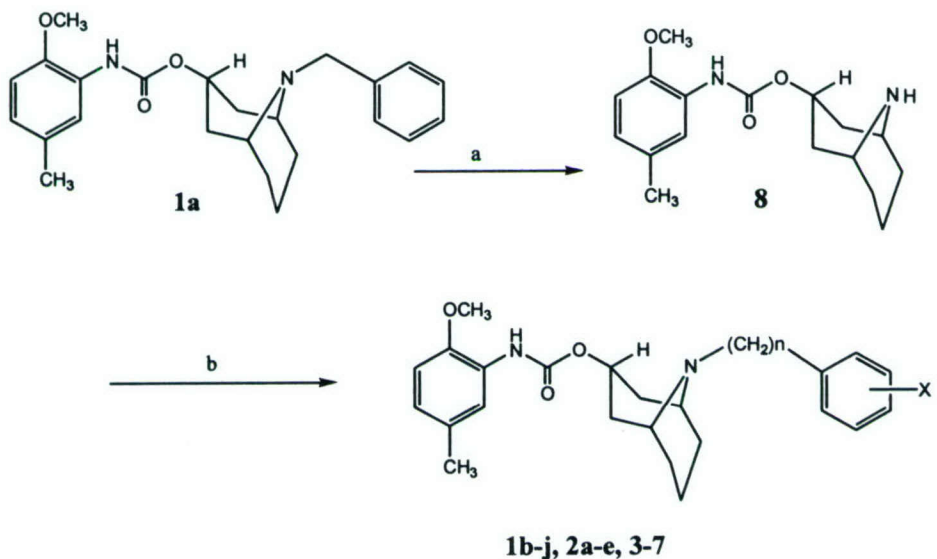
**Figure 1.** Structures of BIMU-1 and compound 1a.

## Methods

**Chemistry.** The synthesis of the target compounds is outlined in Schemes I and II. The first step in the synthesis involved the removal of benzyl group from **1a** via catalytic hydrogenation (Scheme I). N-alkylation of the secondary amine, **8**, with the corresponding alkyl halide or tosylate gave compounds **1b-j**, **2a-e**, and **3-7** in moderate yield. The synthesis of compound **1k** was achieved using the sequence of reactions outlined in Scheme II.

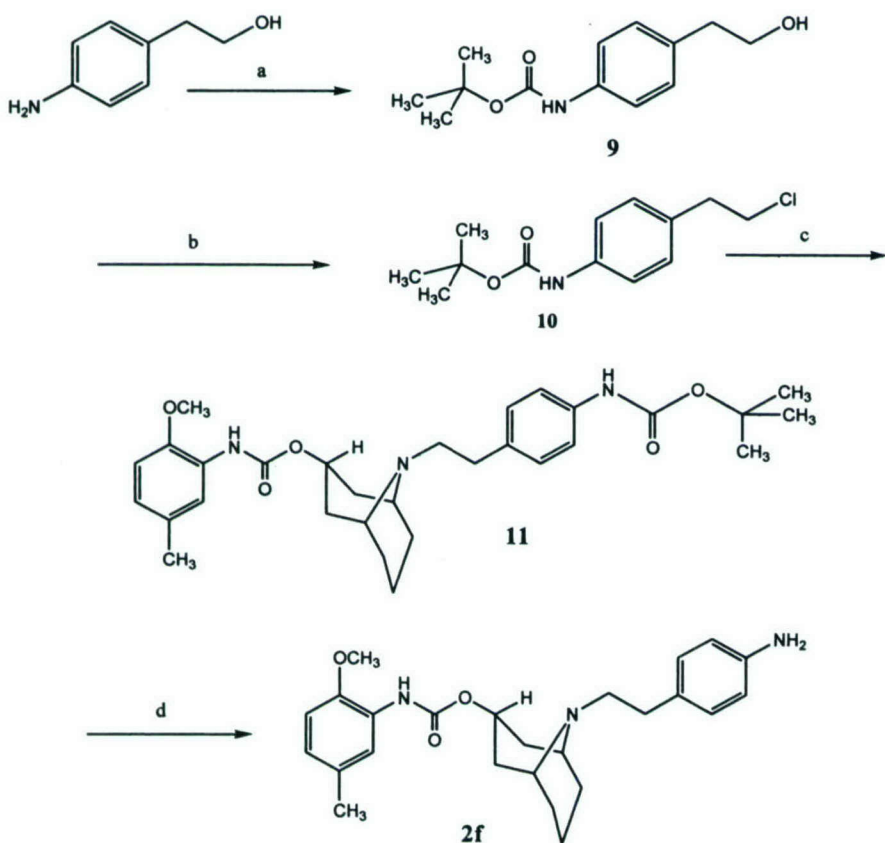
**Pharmacology.**  $\sigma_1$  binding studies were conducted using the  $\sigma_1$ -selective radioligand, [ $^3\text{H}$ ](-)-pentazocine in guinea pig brain membranes according to published procedures.<sup>1,2</sup>  $\sigma_2$  sites were assayed in rat liver membranes with [ $^3\text{H}$ ]DTG in the presence of (+)-pentazocine (100 nM) to mask  $\sigma_1$  sites.<sup>1,2</sup>

**Scheme I**



**Reagents:** a: H<sub>2</sub>/Pd/c/ethanol; Ar-(CH<sub>2</sub>)<sub>n</sub>Br, or Ar-(CH<sub>2</sub>)<sub>n</sub>Cl/, or Ar-(CH<sub>2</sub>)<sub>n</sub>OTs/KI/ethanol/reflux.

**Scheme II**



**Reagents:** **a:** di-*tert*-butyl dicarbonate/ethyl acetate; **b:**  $(\text{Ph})_3\text{P}/\text{CCl}_4$ /reflux;  
**c:**  $\text{K}_2\text{CO}_3/\text{KI}/\text{CH}_3\text{CN}$ /reflux; **d:**  $\text{CF}_3\text{COOH}/\text{CH}_2\text{Cl}_2$ .

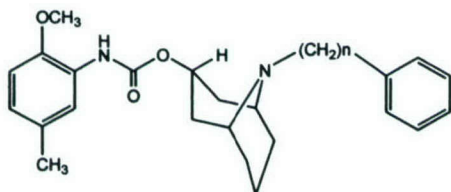
## Results

The results of the *in vitro* binding studies are shown in Tables I - III. Sequential extension of the methylene linker group separating the benzene ring and the bridgehead nitrogen atom from  $n = 1$  to  $n = 7$  had little effect on the binding affinity for sigma receptors. All compounds in this series (**1a**, **2a** and **3 – 7**) had a higher affinity for  $\sigma_2$  versus  $\sigma_1$  receptors. The  $\sigma_1/\sigma_2$  selectivity ratio, which is the ratio of the  $K_i$  values for the  $\sigma_1$  and  $\sigma_2$  receptors, ranged from 10 to 50 for this class of

compounds. In order to explore the nature of the substituent effect in the aromatic ring of compound **1a**, a number of substituted N-benzyl analogs were prepared and their affinities for  $\sigma_1$  and  $\sigma_2$  receptors were measured *in vitro* (Table II). Substitution of either the 2-, 3-, or 4-position of **1a** with any substituent resulted in either a modest or dramatic reduction in affinity for  $\sigma_2$  receptors. For example, there was a 10-fold reduction in affinity for  $\sigma_2$  receptors when the 4-position of the benzyl aromatic ring was substituted with a fluorine substituent. However, substitution of either the 2- or 3-position with a fluorine substituent resulted in a 70-100-fold reduction in  $\sigma_2$  receptor affinity. A similar trend was observed with the iodine-substituted analogs (**1e-g**) and the 2- and 4-nitro analogs, **1i** and **1j**. An interesting observation was the effect of substitution of the benzyl aromatic ring on the  $\sigma_1:\sigma_2$  selectivity ratio, which represents the relative selectivity of a compound for  $\sigma_2$  versus  $\sigma_1$  receptors. The  $\sigma_1:\sigma_2$  selectivity ratio of **1a** was 30, whereas the  $\sigma_1:\sigma_2$  selectivity ratio was lower for the substituted benzyl analogs possessing an appreciable affinity for  $\sigma_1$  and  $\sigma_2$  receptors (i.e., <1,000 nM). These data suggest that the effect of substitution of the aromatic ring on  $\sigma_1$  receptor affinity was not as dramatic as that of the  $\sigma_2$  receptor.

In order to further explore the nature of the substituent effects in this class of compounds, a number of 4-substituted N-phenethyl derivatives were prepared and their affinities for  $\sigma_1$  and  $\sigma_2$  receptors were measured (Table III). An unexpected finding was the difference in the substituent effect in the 4-position of the N-phenethyl series versus the N-benzyl series. For example, substitution of the 4-position of the N-benzyl analog with a fluorine atom resulted in a 10-fold reduction in  $\sigma_2$  receptor affinity, whereas the same substitution resulted in a lower reduction in  $\sigma_2$  affinity for the N-phenethyl analog, **2b**. In addition, there was no difference in  $\sigma_2$  receptor affinity for the 4-F and 4-I analogs in the N-benzyl series (compare **1b** and **1e**), but the 4-I analog, **2c**, had a much lower affinity for  $\sigma_2$  receptors than the corresponding 4-F analog, **2b**. A similar statement can be made for the 4-methyl analogs, **1h** versus **2d**. However, substitution of the 4-position with a nitro substituent resulted in about a 10-fold reduction in  $\sigma_2$  receptor affinity for both the N-benzyl and N-phenethyl analogs. An unexpected observation was the relatively high  $\sigma_2$  receptor affinity, and outstanding  $\sigma_1:\sigma_2$  selectivity ratio of the 4-amino analog, **2f**. This high  $\sigma_1:\sigma_2$  selectivity ratio was caused, in part, by the dramatic reduction in  $\sigma_1$  receptor affinity on introducing this substituent into the 4-position of the N-phenethyl aromatic ring. It is of interest to note that the N-BOC analog, **11**, was devoid of activity at both  $\sigma_1$  and  $\sigma_2$  receptors (Table III).

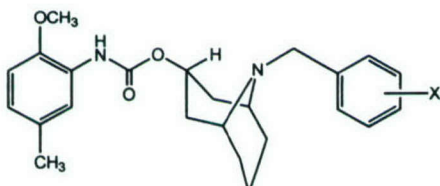
**Table I.** In vitro binding data for compounds 1 - 7.



#	n	$\sigma_1^a$	$\sigma_2^b$	$\sigma_1:\sigma_2$ Ratio <sup>c</sup>
1a	1	92.5 ± 11.0	3.1 ± 0.8	30
2a	2	59.9 ± 4.6	1.2 ± 0.1	50
3	3	73.0 ± 1.6	2.0 ± 0.1	37
4	4	65.5 ± 4.3	2.9 ± 0.2	23
5	5	17.3 ± 1.2	1.8 ± 0.2	9.6
6	6	214 ± 24	7.6 ± 0.4	28
7	7	230 ± 29	7.6 ± 0.2	30

<sup>a</sup>Ki for inhibiting the binding of [<sup>3</sup>H](+)-pentazocine to guinea pig brain homogenates (mean ± S.E.M.; n = 3); <sup>b</sup>Ki for inhibiting the binding of [<sup>3</sup>H]DTG to rat liver homogenates (mean ± S.E.M.; n = 3); <sup>c</sup>Ki for  $\sigma_1$ /Ki for  $\sigma_2$ .

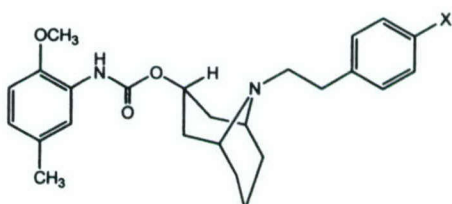
**Table II.** In vitro binding data for the substituted benzyl analogs.



#	X	$\sigma_1^a$	$\sigma_2^b$	$\sigma_1:\sigma_2$ Ratio <sup>c</sup>
1a	H	92.5 ± 11.0	3.1 ± 0.8	30
1b	4-F	202 ± 22	30.0 ± 2.0	6.7
1c	2-F	>1,000	206 ± 13	>5
1d	3-F	322 ± 37	318 ± 44	1
1e	4-I	454 ± 78	30.6 ± 3.9	14.8
1f	2-I	>1,000	>1,000	-
1g	3-I	1354 ± 213	50.9 ± 3.9	26.6
1h	4-CH <sub>3</sub>	273 ± 23	15.5 ± 1.8	17.7
1i	4-NO <sub>2</sub>	539 ± 42	25.2 ± 3.8	21.4
1j	2-NO <sub>2</sub>	>1,000	>1,000	-

<sup>a,b,c</sup>Refer to Table I.

**Table III.** In vitro binding data for the 4-substituted phenethyl analogs.



#	X	Ki [nM]		
		$\sigma_1^a$	$\sigma_2^b$	$\sigma_1:\sigma_2$ Ratio <sup>c</sup>
2a	H	59.9 ± 4.6	1.2 ± 0.1	30
2b	F	262 ± 37	5.9 ± 1.5	44
2c	I	175 ± 7	141 ± 9	1.2
2d	CH <sub>3</sub>	>1,000	83 ± 6	>12
2e	NO <sub>2</sub>	215 ± 39	11.5 ± 2.4	19
2f	NH <sub>2</sub>	2,250 ± 73	5.0 ± 0.2	510
11	NHBoc	>1,000	>1,000	-

<sup>a,b,c</sup>Refer to Table I.

## Discussion

The goal of the current study was to develop ligand having a high affinity and selectivity for  $\sigma_2$  versus  $\sigma_1$  receptors. In an earlier study, we prepared a number of structural analogs of the mixed serotonin 5-HT<sub>3</sub>/5-HT<sub>4</sub> ligand, BIMU-1, having a high affinity for  $\sigma_2$  versus  $\sigma_1$  receptors and a low (or negligible) affinity at serotonin 5-HT<sub>3</sub> and 5-HT<sub>4</sub> receptors. The structural modification of BIMU-1 in the previous study included: 1) replacing the urea linkage of BIMU-1 with a conformationally-flexible carbamate moiety; 2) replacing the N-methyl group with an N-benzyl group, which had an adverse effect on serotonin receptor affinity while causing little effect on binding to  $\sigma_1$  and  $\sigma_2$  receptors; and, 3) comparison of both the tropane and granatane ring systems. The results of this study revealed that the N-benzylgranatane analog, 1a, as a potential  $\sigma_2$  selective ligand having no affinity for either 5-HT<sub>3</sub> or 5-HT<sub>4</sub> receptors. The goal of the present study we to explore the N-benzyl region of 1a in order to determine if it is possible to further improve the affinity and selectivity of this compound for  $\sigma_2$  versus  $\sigma_1$  receptors.

The first strategy involved extending the length of the methylene spacer group between the bridgehead nitrogen and the benzene ring of the N-benzyl moiety. The result of this study (Table I)

revealed that this change had little effect on the binding to  $\sigma_2$  receptors, and a relatively minor effect on binding to the  $\sigma_1$  receptor. These data suggested that the substituent may not play a key role in binding to the  $\sigma_2$  receptor. If this was indeed the case, then the addition of a substituent in the aromatic ring of **1a** is expected to have little effect on  $\sigma_2$  receptor affinity. This turned out to be contrary to what was expected, and substitution of the benzyl aromatic ring of **1a** with any substituent resulted in a reduction in affinity to the  $\sigma_2$  receptor (Table II). Substitution of the 4-position of the benzyl ring had a lower reduction in  $\sigma_2$  receptor affinity when compared with the corresponding 2- and 3-substituted analogs. There was no clear trend with respect to the nature of the substituent effect since compounds **1b** – **1j** had a lower affinity for  $\sigma_2$  receptors relative to the unsubstituted analog, **1a**. However, substitution of the benzyl aromatic ring had a lesser effect on  $\sigma_1$  receptor affinity since the  $\sigma_1:\sigma_2$  selectivity ratio of compounds having an appreciable affinity for sigma receptors (<1,000 nM) was less than the ratio of that for **1a**.

As a means of further exploring the nature of the substituent effects for this class of compounds, we prepared a series of 4-substituted N-phenethyl analogs and measured their affinities for sigma receptors *in vitro*. Substitution of the 4-position was chosen since the substitution of this position resulted in a lower reduction in  $\sigma_2$  receptor affinity in the N-benzyl series of compounds. The results of this study revealed a different structure-activity relationship with respect to  $\sigma_2$  receptor affinity relative to that of the N-benzyl analogs. In the N-phenethyl series, substitution of the 4-position with a polar substituent such as a fluoro, nitro, or amino group retained a high affinity for  $\sigma_2$  receptors, whereas the nonpolar substituents, iodo and methyl groups, resulted in a 70 – 100-fold reduction in affinity for the  $\sigma_2$  receptor. This difference in substituent effect between the N-benzyl and N-phenethyl series is also apparent when one compares the binding properties of the 4-F and 4-I analogs. In the N-benzyl series, the 4-F and 4-I analogs had an identical  $\sigma_2$  receptor affinity, whereas the 4-F had a 25-fold higher  $\sigma_2$  receptor affinity versus the 4-I analog. Furthermore, the 4-methyl analog was more potent than the 4-F analog in the N-benzyl series, whereas the reverse is true for the N-phenethyl analogs. An unexpected observation was the outstanding  $\sigma_1:\sigma_2$  selectivity ratio of compound **2f**. This high ratio can be attributed to both the retention in  $\sigma_2$  affinity and the dramatic reduction in  $\sigma_1$  receptor affinity on introducing an amino group in the 4-position of **2a**. Compound **2f** is one of the most potent and selective  $\sigma_2$  receptor ligands reported to date.

In conclusion, we have extended our sigma receptor structure activity relationship study of the granatane analog, **1a**, to include an investigation of the N-benzyl region of this molecule. The results of this study revealed a high degree of steric tolerance in this region of the molecule with respect to  $\sigma_2$  receptor affinity since a methylene spacer group from  $n = 1$  to  $n = 7$  was well tolerated. Substitution of the N-benzyl aromatic ring resulted in a moderate to dramatic reduction in  $\sigma_2$  receptor affinity, depending on the position of the aromatic ring where the substitution occurred. Substitution of the 4-position of the N-phenethyl analog, **2a**, resulted in compounds having a high  $\sigma_2$  receptor affinity and good to excellent  $\sigma_1$ : $\sigma_2$  selectivity ratio, provided that the substituent was polar (i.e., F, NO<sub>2</sub> or NH<sub>2</sub>). Substitution with a nonpolar substituent (i.e., CH<sub>3</sub> or I) resulted in compounds having a low  $\sigma_2$  receptor affinity. The 4-amino phenethyl analog, **2f**, was found to have a high affinity and an outstanding  $\sigma_1$ : $\sigma_2$  selectivity ratio. This compound is likely to be a useful ligand for studying the functional role of  $\sigma_2$  receptors both *in vivo* and *in vitro*.

## Experimental

<sup>1</sup>H NMR spectra were recorded on a Bruker 300 MHz NMR spectrometer. Chemical shifts are reported in  $\delta$  values (parts per million, ppm) relative to an internal standard of tetramethylsilane (TMS). The following abbreviations are used for multiplicity of NMR signals: br s = broad singlet, d = doublet, dd = doublet of doublets, m = multiplet, q = quintet, s = singlet, t = triplet. Melting points were determined on a Fischer-Johns melting point apparatus and are uncorrected. Elemental analyses were performed by Atlantic Microlab, Inc., Norcross, GA and were within  $\pm$  0.4% of the calculated values. Mass spectrometry was provided by the Washington University Mass Spectrometry Resource (St. Louis, MO) with support from the NIH National Center for Research Resources (Grant No. P41RR0954). All reactions were carried out under an inert atmosphere of nitrogen.

### General procedure for the synthesis of *N*-substituted-9-azabicyclo[3.3.1]nonan-3 $\alpha$ -yl)-*N*-(2-methoxy-5-methylphenyl)carbamates (Scheme I).

A mixture of *N*-(9-azabicyclo[3.3.1]nonan-3 $\alpha$ -yl)-*N*-(2-methoxy-5-methylphenyl) carbamate (**8**)<sup>13</sup> (200 mg, 0.66 mmol), appropriate phenalkyl halides (2.64 mmol), potassium iodide (438 mg, 2.64

mmol), and potassium carbonate (729 mg, 5.28 mmol) in acetonitrile (10 mL) was stirred at reflux overnight. The volatile components were evaporated and water (10 mL) was added, and the product extracted into dichloromethane (3 x 10 mL). The organic layers were combined, dried (magnesium sulfate) and concentrated under reduced pressure. The residue was purified by silica gel column chromatography (5% methanol in dichloromethane) to afford the target compounds.

**N-(9-(4-Fluorobenzyl)-9-azabicyclo[3.3.1]nonan-3 $\alpha$ -yl)-N-(2-methoxy-5-methylphenyl)-carbamate hydrochloride (1b).** Yield 37% from 4-fluorobenzyl bromide, mp 157-160 °C (HCl salt).  $^1\text{H}$  NMR (300 MHz,  $\text{CDCl}_3$ )  $\delta$  7.96 (s, 1H), 7.29-7.36 (m, 2H), 7.16 (s, 1H), 6.96-7.03 (m, 2H), 6.73-6.80 (m, 2H), 5.24 (q,  $J = 7.3$  Hz, 1 H), 3.84 (s, 3H), 3.76 (s, 2H), 3.02-3.05 (m, 2 H), 2.41-2.51 (m, 2H), 2.30 (s, 3H), 2.10-2.22 (m, 1H), 1.87-1.99 (m, 2H), 1.48-1.54 (m, 3H), 1.16-1.20 (m, 2H). Anal. ( $\text{C}_{24}\text{H}_{29}\text{N}_2\text{O}_3\text{F}\text{HCl} \cdot 0.4\text{H}_2\text{O}$ ) C, H, N.

**N-(9-(2-Fluorobenzyl)-9-azabicyclo[3.3.1]nonan-3 $\alpha$ -yl)-N-(2-methoxy-5-methylphenyl)-carbamate (1c).** Yield 83% from 2-fluorobenzyl bromide.  $^1\text{H}$  NMR (300 MHz,  $\text{CDCl}_3$ )  $\delta$  7.33-7.46 (m, 2H), 6.93-7.20 (m, 5H), 6.71-6.75 (m, 2H), 5.18-5.28 (m, 1H), 3.76 (s, 3H), 3.70 (s, 2H), 2.80-2.99 (m, 2 H), 2.25-2.40 (m, 2H), 2.18 (s, 3H), 1.75-1.98 (m, 3H), 1.25-1.47 (m, 2H), 0.95-1.14 (m, 3H). HRFAB calculated for  $\text{C}_{24}\text{H}_{29}\text{N}_2\text{O}_3\text{F}$  [M+Li] 419.2322, found 419.2330.

**N-(9-(3-Fluorobenzyl)-9-azabicyclo[3.3.1]nonan-3 $\alpha$ -yl)-N-(2-methoxy-5-methylphenyl)-carbamate (1d).** Yield 60% from 3-fluorobenzyl bromide.  $^1\text{H}$  NMR (300 MHz,  $\text{CDCl}_3$ )  $\delta$  6.74-7.23 (m, 8H), 6.72-6.75 (m, 1H), 5.14-5.22 (m, 1H), 3.71 (s, 3H), 3.70 (s, 2H), 2.80-2.98 (m, 2 H), 2.25-2.35 (m, 2H), 2.19 (s, 3H), 1.60-1.89 (m, 3H), 1.26-1.35 (m, 2H), 0.86-1.00 (m, 3H). HRFAB calculated for  $\text{C}_{24}\text{H}_{29}\text{N}_2\text{O}_3\text{F}$  [M+Li] 419.2322, found 419.2336.

**N-(9-(4-Iodobenzyl)-9-azabicyclo[3.3.1]nonan-3 $\alpha$ -yl)-N-(2-methoxy-5-methylphenyl)-carbamate (1e).** Yield 44% from 4-iodobenzyl bromide, mp 97.5-100 °C.  $^1\text{H}$  NMR (300 MHz,  $\text{CDCl}_3$ )  $\delta$  7.96 (s, 1H), 7.68 (d,  $J = 8.7$  Hz, 1H), 7.62 (d,  $J = 8.7$  Hz, 2H), 7.12 (d,  $J = 8.4$  Hz, 2H), 6.73-6.80 (m, 2H), 5.22 (q,  $J = 7.3$  Hz, 1H), 3.84 (s, 3H), 3.74 (s, 2H), 3.01-3.04 (m, 2H), 2.41-2.51 (m, 2H), 2.30 (s, 3H), 2.10-2.21 (m, 1H), 1.86-1.97 (m, 2H), 1.48-1.54 (m, 2H), 1.16-1.26 (m, 3H). HRFAB calculated for  $\text{C}_{24}\text{H}_{30}\text{N}_2\text{O}_3\text{I}$  [M+H] $^+$  521.1301, found 521.1283.

**N-(9-(2-Iodobenzyl)-9-azabicyclo[3.3.1]nonan-3 $\alpha$ -yl)-N-(2-methoxy-5-methylphenyl)-carbamate (1f).** Yield 40% from 2-iodobenzyl chloride, mp 53-55 °C (free base).  $^1\text{H}$  NMR (300 MHz,  $\text{CDCl}_3$ )  $\delta$  7.74-7.79 (m, 2H), 7.37-7.49 (m, 2H), 6.88-7.00 (m, 3H), 6.72-6.75 (m, 1H), 5.19-5.30 (m, 1H), 3.76 (s, 3H), 3.69 (s, 2H), 2.86-3.05 (m, 2H), 2.30-2.40 (m, 2H), 2.17 (s, 3H), 1.75-1.90 (m, 3H), 1.30-1.40 (m, 2H), 0.95-1.10 (m, 3H). HRFAB calculated for  $\text{C}_{24}\text{H}_{29}\text{N}_2\text{O}_3\text{F}$  [M+Li] 527.1383, found 527.1386.

**N-(9-(3-Iodobenzyl)-9-azabicyclo[3.3.1]nonan-3 $\alpha$ -yl)-N-(2-methoxy-5-methylphenyl)-carbamate hydrochloride (1g).** Yield 44% from 3-iodobenzyl bromide, mp 167-168 °C (HCl salt).  $^1\text{H}$  NMR (300 MHz,  $\text{CDCl}_3$ )  $\delta$  7.96 (s, 1H), 7.68 (s, 1H), 7.56 (d,  $J = 7.7$  Hz, 1H), 7.35 (d,  $J = 7.7$  Hz, 1H), 7.15 (s, 1H), 7.05 (t,  $J = 7.7$  Hz, 1H), 6.73-6.80 (m, 2H), 5.22 (q,  $J = 7.1$  Hz, 1H), 3.85 (s, 3H), 3.74 (s, 2H), 3.00-3.04 (m, 2H), 2.41-2.51 (m, 2H), 2.30 (s, 3H), 2.11-2.21 (m, 1H), 1.87-1.98 (m, 2H), 1.49-1.55 (m, 3H), 1.18-1.22 (m, 2H). Anal. ( $\text{C}_{24}\text{H}_{29}\text{N}_2\text{O}_3\text{J}\cdot\text{HCl}$ ) C, H, N.

**N-(9-(4-Methylbenzyl)-9-azabicyclo[3.3.1]nonan-3 $\alpha$ -yl)-N-(2-methoxy-5-methylphenyl)-carbamate hydrochloride (1h).** Yield 85% from 4-methylbenzyl bromide, mp 146-148 °C (HCl salt).  $^1\text{H}$  NMR (300 MHz,  $\text{CDCl}_3$ )  $\delta$  8.00 (s, 1H), 7.15-7.29 (m, 5H), 6.77-6.82 (m, 2H), 5.26-5.30 (m, 1H), 3.88 (s, 3H), 3.80 (s, 2H), 3.08 (s, 2H), 2.49 (s, 2H), 2.37 (s, 3H), 2.34 (s, 3H), 2.15-2.20 (m, 1H), 1.92-2.00 (m, 2H), 1.50-1.61 (m, 3H), 1.12-1.20 (m, 2H). Anal. ( $\text{C}_{25}\text{H}_{32}\text{N}_2\text{O}_3\text{HCl}\cdot 0.5\text{H}_2\text{O}$ ) C, H, N.

**N-(9-(4-Nitrobenzyl)-9-azabicyclo[3.3.1]nonan-3 $\alpha$ -yl)-N-(2-methoxy-5-methylphenyl)-carbamate hydrochloride (1i).** Yield 84% from 4-nitrobenzyl bromide, mp 157-159 °C (HCl salt).  $^1\text{H}$  NMR (300 MHz,  $\text{CDCl}_3$ )  $\delta$  8.17 (d,  $J = 8.7$  Hz, 1H), 7.96 (s, 1H), 7.53 (d,  $J = 8.7$  Hz, 2H), 7.16 (s, 1H), 6.73-6.81 (m, 2H), 5.25 (q,  $J = 7.4$  Hz, 1H), 3.90 (s, 2H), 3.85 (s, 3H), 3.01-3.04 (m, 2H), 2.44-2.54 (m, 2H), 2.30 (s, 3H), 2.10-2.24 (m, 1H), 1.88-2.00 (m, 2H), 1.52-1.60 (m, 3H), 1.20-1.25 (m, 2H). Anal. ( $\text{C}_{24}\text{H}_{29}\text{N}_3\text{O}_5\text{HCl}$ ) C, H, N.

**N-(9-(2-Nitrobenzyl)-9-azabicyclo[3.3.1]nonan-3 $\alpha$ -yl)-N-(2-methoxy-5-methylphenyl)-carbamate (1j).** Yield 45 % from 2-nitrobenzyl bromide, mp 45-47 °C (free base).  $^1\text{H}$  NMR (300

MHz, CDCl<sub>3</sub>) δ 7.97 (s, 1H), 7.77-7.80 (m, 1H), 7.50-7.62 (m, 2H), 7.34-7.39 (m, 1H), 7.14 (s, 1H), 6.72-6.80 (m, 2H), 5.16 (q, *J* = 7.1 Hz, 1H), 4.06 (s, 2H), 3.84 (s, 3H), 2.95-2.98 (m, 2H), 2.40-2.50 (m, 2H), 2.30 (s, 3H), 2.09-2.18 (m, 1H), 1.83-1.93 (m, 2H), 1.48-1.56 (m, 3H), 1.18-1.23 (m, 2H). HRFAB calculated for C<sub>24</sub>H<sub>29</sub>N<sub>3</sub>O<sub>5</sub> [M+Li] 446.2267, found 446.2265.

***N-(9-Phenethyl-9-azabicyclo[3.3.1]nonan-3α-yl)-N-(2-methoxy-5-methylphenyl)carbamate***

**(2a).** Yield 45% from phenethyl bromide, mp 183.5-186 °C (free amine). <sup>1</sup>H NMR (300 MHz, CDCl<sub>3</sub>) δ 7.92 (s, 1H), 7.14 (s, 1H), 7.01 (d, *J* = 8.2 Hz, 2H), 6.74-6.82 (m, 2H), 6.64 (d, *J* = 8.2 Hz, 2H), 5.10-5.17 (m, 1H), 3.85 (s, 3H), 3.38-3.61 (m, 4H), 3.00-3.13 (m, 2H), 2.50-2.75 (m, 4H), 2.30 (s, 3H), 2.00-2.11 (m, 2H), 1.43-1.77 (m, 6H). Anal. (C<sub>25</sub>H<sub>32</sub>N<sub>2</sub>O<sub>3</sub>·HCl·0.25H<sub>2</sub>O) C, H, N.

***N-(9-(4-Fluorophenethyl)-9-azabicyclo[3.3.1]nonan-3α-yl)-N-(2-methoxy-5-methylphenyl)carbamate hydrochloride (2b).*** Yield 94% from 4-fluorophenethyl chloride, mp 172-174 °C (HCl salt). <sup>1</sup>H NMR (300 MHz, CDCl<sub>3</sub>) δ 7.96 (s, 1H), 7.15-7.20 (m, 3H), 6.95-7.01 (m, 2H), 6.74-6.81 (m, 2H), 5.13 (q, *J* = 6.8 Hz, 1H), 3.86 (s, 3H), 3.08-3.15 (m, 2H), 2.80-2.84 (m, 2H), 2.67-2.72 (m, 2H), 2.42-2.52 (m, 2H), 2.31 (s, 3H), 2.10-2.25 (m, 1H), 1.84-1.94 (m, 2H), 1.51-1.58 (m, 3H), 1.24-1.28 (m, 2H). Anal. (C<sub>25</sub>H<sub>31</sub>N<sub>2</sub>O<sub>3</sub>F·HCl) C, H, N.

***N-(9-(4-Iodophenethyl)-9-azabicyclo[3.3.1]nonan-3α-yl)-N-(2-methoxy-5-methylphenyl)carbamate (2c).*** Yield 50% from 4-iodophenethyl chloride, mp 239-242 °C. <sup>1</sup>H NMR (300 MHz, CDCl<sub>3</sub>) δ 7.91 (s, 1H), 7.68 (d, *J* = 6.0 Hz, 2H), 7.29-7.30 (m, 3H), 6.79-6.87 (m, 2H), 5.17-5.24 (m, 1H), 3.88 (s, 3H), 3.71 (s, 2H), 3.27-3.40 (m, 4H), 2.59-2.62 (m, 2H), 2.33 (s, 3H), 2.07-2.20 (m, 4H), 1.61-1.89 (m, 4H). HRFAB calculated for C<sub>25</sub>H<sub>32</sub>N<sub>2</sub>O<sub>3</sub>I [M+H]<sup>+</sup> 535.1458, found 535.1460.

***N-(9-(4-Nitrophenethyl)-9-azabicyclo[3.3.1]nonan-3α-yl)-N-(2-methoxy-5-methylphenyl)carbamate hydrochloride (2e).*** Yield 35% from 4-nitrophenethyl bromide, mp 164-165 °C (HCl salt). <sup>1</sup>H NMR (300 MHz, CDCl<sub>3</sub>) δ 8.15 (d, *J* = 8.6 Hz, 2H), 7.94 (s, 1H), 7.37 (d, *J* = 8.6 Hz, 2H), 7.14 (s, 1H), 6.73-6.81 (m, 2H), 5.09 (q, *J* = 7.0 Hz, 1H), 3.84 (s, 3H), 3.06-3.09 (m, 2H), 2.78-2.88 (m, 4H), 2.39-2.49 (m, 2H), 2.30 (s, 3H), 2.11-2.17 (m, 1H), 1.77-1.89 (m, 2H), 1.43-1.56 (m, 3H), 1.23-1.26 (m, 2H). Anal. (C<sub>25</sub>H<sub>31</sub>N<sub>3</sub>O<sub>5</sub>·HCl·0.5H<sub>2</sub>O) C, H, N.

*N*-(9-Phenpropyl-9-azabicyclo[3.3.1]nonan-3 $\alpha$ -yl)-*N*-(2-methoxy-5-methylphenyl)carbamate hydrochloride (**3**). Yield 58% from 1-bromo-3-phenylpropane, mp 174-176.5 °C (HCl salt).  $^1\text{H}$  NMR (300 MHz, CDCl<sub>3</sub>)  $\delta$  7.95 (s, 1H), 7.14-7.30 (m, 6H), 6.64-6.79 (m, 2H), 5.11-5.17 (m, 1H), 3.84 (s, 3H), 2.85-3.04 (m, 2H), 2.42-2.67 (m, 8H), 2.29 (s, 3H), 1.15-1.88 (m, 8H). Anal. (C<sub>26</sub>H<sub>34</sub>N<sub>2</sub>O<sub>3</sub>·HCl·0.6H<sub>2</sub>O) C, H, N.

*N*-(9-Phenbutyl-9-azabicyclo[3.3.1]nonan-3 $\alpha$ -yl)-*N*-(2-methoxy-5-methylphenyl)carbamate hydrochloride (**4**). Yield 90% from 1-chloro-4-phenylbutane, mp 179-182 °C (HCl salt).  $^1\text{H}$  NMR (300 MHz, CDCl<sub>3</sub>)  $\delta$  7.95 (s, 1H), 7.12-7.29 (m, 6H), 6.72-6.76 (m, 2H), 5.08-5.15 (m, 1H), 3.84 (s, 3H), 2.90-3.04 (m, 2H), 2.41-2.62 (m, 6H), 2.29 (s, 3H), 1.18-1.89 (m, 12H). Anal. (C<sub>27</sub>H<sub>36</sub>N<sub>2</sub>O<sub>3</sub>·HCl·0.5H<sub>2</sub>O) C, H, N.

*N*-(9-Phenpentyl-9-azabicyclo[3.3.1]nonan-3 $\alpha$ -yl)-*N*-(2-methoxy-5-methylphenyl)carbamate hydrochloride (**5**). Yield 63% from 1-chloro-5-phenylpentane, mp 192-195 °C (HCl salt).  $^1\text{H}$  NMR (300 MHz, CDCl<sub>3</sub>)  $\delta$  7.95 (s, 1H), 7.25-7.30 (m, 6H), 6.72-6.79 (m, 2H), 5.10-5.15 (m, 1H), 3.84 (s, 3H), 3.03 (s, 2H), 2.40-2.64 (m, 6H), 2.28 (s, 3H), 1.17-2.20 (m, 14H). Anal. (C<sub>28</sub>H<sub>38</sub>N<sub>2</sub>O<sub>3</sub>·HCl·0.5H<sub>2</sub>O) C, H, N.

*N*-(9-Phenhexyl-9-azabicyclo[3.3.1]nonan-3 $\alpha$ -yl)-*N*-(2-methoxy-5-methylphenyl)carbamate hydrochloride (**6**). Yield 37% from 1-chloro-6-phenylhexane, mp 180.5-185 °C (HCl salt).  $^1\text{H}$  NMR (300 MHz, CDCl<sub>3</sub>)  $\delta$  7.95 (s, 1H), 7.13-7.34 (m, 6H), 6.72-6.79 (m, 2H), 5.19-5.15 (m, 1H), 3.84 (s, 3H), 3.03 (s, 2H), 2.41-2.63 (m, 6H), 2.29 (s, 3H), 1.18-1.88 (m, 16H). Anal. (C<sub>29</sub>H<sub>40</sub>N<sub>2</sub>O<sub>3</sub>·HCl) C, H, N.

*N*-(9-Phenheptyl-9-azabicyclo[3.3.1]nonan-3 $\alpha$ -yl)-*N*-(2-methoxy-5-methylphenyl)carbamate hydrochloride (**7**). Yield 83% from 1-chloro-7-phenylheptane, mp 142-143.5 °C (HCl salt).  $^1\text{H}$  NMR (300 MHz, CDCl<sub>3</sub>)  $\delta$  7.95 (s, 1H), 7.13-7.27 (m, 6H), 6.72-6.76 (m, 2H), 5.11-5.15 (m, 1H), 3.84 (s, 3H), 3.03 (s, 2H), 2.38-2.60 (m, 8H), 2.29 (s, 3H), 1.83-1.90 (m, 2H), 1.19-1.59 (m, 14H). Anal. (C<sub>30</sub>H<sub>42</sub>N<sub>2</sub>O<sub>3</sub>·HCl·0.75H<sub>2</sub>O) C, H, N.

**N-(9-(4-Methylphenethyl)-9-azabicyclo[3.3.1]nonan-3 $\alpha$ -yl)-N-(2-methoxy-5-methylphenyl)-carbamate (2d).** A mixture of 4-methylphenethyl alcohol (1.00 g, 7.34 mmol) and p-toluenesulfonyl chloride (1.78 g, 9.34 mmol) in triethylamine (20 mL) was stirred at room temperature overnight. The resulting solid was filtered, dissolved in dichloromethane, washed with water, dried (magnesium sulfate) and concentrated *in vacuo* to give 4-methylphenethyl tosylate as a solid (52%), which was used crude for the next reaction.  $^1\text{H}$  NMR (300 MHz,  $\text{CDCl}_3$ )  $\delta$  7.68-7.78 (m, 2H), 7.19-7.29 (m, 2H), 6.98-7.04 (m, 4H), 4.16-4.20 (m, 2H), 2.89-2.93 (m, 2H), 2.43 (s, 3H), 2.31 (s, 3H).

A mixture of *N*-(9-azabicyclo[3.3.1]nonan-3 $\alpha$ -yl)-*N*-(2-methoxy-5-methylphenyl) carbamate (8) (400 mg, 1.31 mmol), 4-methylphenethyl tosylate (400 mg, 1.38 mmol) and 1,8-diazabicyclo[5.4.0]undec-7-ene (400 mg, 2.62 mmol) in dry toluene (8 mL) was refluxed overnight. The resulting residue after concentrating in *vacuo* was purified by silica gel column chromatography (5% methanol in dichloromethane) to give **2d** as a white solid (40%), mp 148-150 °C.  $^1\text{H}$  NMR (300 MHz,  $\text{CDCl}_3$ )  $\delta$  8.01 (s, 1H), 7.14 (s, 1H), 7.07-7.13 (m, 5H), 6.73-6.77 (m, 2H), 5.14 (d,  $J$  = 6.7 Hz, 1H), 4.43-4.48 (m, 2H), 3.85 (s, 3H), 3.08-3.13 (m, 2H), 2.65-2.82 (m, 4H), 2.37-2.48 (m, 4H), 2.32 (s, 3H), 2.29 (s, 3H), 1.68-1.93 (m, 4H). HRFAB calculated for  $\text{C}_{26}\text{H}_{35}\text{N}_2\text{O}_3$  [M+H] $^+$  423.2648, found 423.2624.

**N-(9-(4-Aminophenethyl)-9-azabicyclo[3.3.1]nonan-3 $\alpha$ -yl)-N-(2-methoxy-5-methylphenyl)-carbamate (2f). Scheme II**

**4-(*tert*-Butoxyformamido)phenethyl alcohol (9).** To a solution of 4-aminophenethyl alcohol (5.00 g, 36.4 mmol) in ethyl acetate (50 mL) was added di-*tert*-butyl dicarbonate (7.95 g, 36.4 mmol). The reaction mixture was stirred at room temperature for 48 h. Volatile components were removed *in vacuo* to give a pale brown solid (99%), which was used crude for the next reaction.  $^1\text{H}$  NMR (300 MHz,  $\text{CDCl}_3$ )  $\delta$  7.29 (d,  $J$  = 8.4 Hz, 2H), 7.14 (d,  $J$  = 8.4 Hz, 2H), 6.48 (br s, 1H), 3.82 (t,  $J$  = 6.5 Hz, 2H), 2.82 (t,  $J$  = 6.5 Hz, 2H), 1.51 (s, 9H).

**4-(*tert*-Butoxyformamido)phenethyl chloride (10).** To a solution of **9** (2.40 g, 10.0 mmol) in carbon tetrachloride (40 mL) was added triphenyl phosphine (2.65 g, 10.0 mmol). The reaction

mixture was reflux for 24 h. Volatile components were removed *in vacuo* to give an oil that was purified by silica gel column chromatography to afford **10** as a white solid (95 %): mp 79-81°C. <sup>1</sup>H NMR (300 MHz, CDCl<sub>3</sub>) δ 7.30 (d, *J* = 8.4 Hz, 2H), 7.14 (d, *J* = 8.4 Hz, 2H), 6.45 (br s, 1H), 3.67 (t, *J* = 7.5 Hz, 2H), 3.01 (t, *J* = 7.5 Hz, 2H), 1.51 (s, 9H).

**N-(9-(4-*tert*-Butoxyformamido)phenethyl)-9-azabicyclo[3.3.1]nonan-3 α-yl-*N'*-(2-methoxy-5-methylphenyl)carbamate (11).** Solid Potassium carbonate (1.35 g, 9.7 mmol), potassium iodide (325 mg, 1.9 mmol) and compound **10** (545 mg, 2.13 mmol) were added to a solution of *N*-(9-azabicyclo[3.3.1]nonan-3 α-yl)-*N'*(2-methoxy-5-methylphenyl)carbamate (**8**) (620 mg, 2.03 mmol) in acetonitrile (10 mL). The reaction mixture was refluxed for 48 h. Volatile components were removed *in vacuo* to give an oil that was purified by silica gel column chromatography to afford **11** as a yellow oil (38 %). <sup>1</sup>H NMR (300 MHz, CDCl<sub>3</sub>) δ 7.95 (s, 1H), 7.25-7.33 (m, 2H), 7.12-7.14 (m, 3H), 6.73-6.80 (m, 2H), 6.42 (s, 1H), 5.08-5.17 (m, 1H), 3.84 (s, 3H), 3.09-3.12 (m, 2H), 2.77-2.81 (m, 2H), 2.63-2.68 (m, 2H), 2.40-2.51 (m, 2H), 2.30 (s, 3H), 2.09-2.24 (m, 1H), 1.84-1.93 (m, 2H), 1.61-1.72 (m, 2H), 1.51 (s, 9H), 1.21-1.30 (m, 3H); HRFAB calculated for C<sub>30</sub>H<sub>42</sub>N<sub>3</sub>O<sub>5</sub> [M+H]<sup>+</sup> 524.3124, found 524.3108.

**N-(9-(4-Aminophenethyl))-9-azabicyclo[3.3.1]nonan-3 α-yl)-*N*-(2-methoxy-5-methylphenyl)carbamate (2f).** Trifluoroacetic acid (2 mL) was added to a solution of compound **11** (300 mg, 0.57 mmol) in dichloromethane (1 mL), and the reaction mixture was stirred at room temperature for 3 h. Volatile components were removed *in vacuo*. The resulting residue was dissolved in saturated aqueous bicarbonate (10 mL), and adjusted to pH 10 with an aqueous solution of 10 % sodium hydroxide. The mixture was extracted with dichloromethane (4 x 5 mL). The combined organic extracts were dried (magnesium sulfate), filtered, and concentrated to give **2f** as a yellow oil (97%). <sup>1</sup>H NMR (300 MHz, CDCl<sub>3</sub>) δ 7.92 (s, 1H), 7.14 (s, 1H), 7.01 (d, *J* = 8.2 Hz, 2H), 6.74-6.82 (m, 2H), 6.64 (d, *J* = 8.2 Hz, 2H), 5.10-5.17 (m, 1H), 3.85 (s, 3H), 3.38-3.61 (m, 4H), 3.00-3.13 (m, 2H), 2.50-2.75 (m, 4H), 2.30 (s, 3H), 2.00-2.11 (m, 2H), 1.43-1.77 (m, 6H); HRFAB calculated for C<sub>25</sub>H<sub>34</sub>N<sub>3</sub>O<sub>3</sub> [M+H]<sup>+</sup> 424.2600, found 424.2589.

## **Receptor Binding Studies**

$\sigma$  receptor assays.  $\sigma_1$  binding sites were labeled with the  $\sigma_1$ -selective radioligand, [ $^3\text{H}$ ](-)-pentazocine (DuPont-NEN, Billerica, MA) in guinea pig brain membranes (Rockland Biological, Gilbertsville, PA) according to published procedures.<sup>1,2</sup>  $\sigma_2$  sites were assayed in rat liver membranes with [ $^3\text{H}$ ]DTG (DuPont-NEN, Boston, MA) in the presence of (+)-pentazocine (100 nM) to mask  $\sigma_1$  sites.<sup>1,2</sup>

Membrane Preparation. Crude synaptosomal ( $P_2$ ) membrane homogenates were prepared from frozen guinea pig brains without cerebellum.<sup>1,2</sup> Brains were allowed to thaw slowly on ice before homogenization. Crude  $P_2$  membranes were also prepared from the livers of male Sprague-Dawley rats (300-350 g). Animals were sacrificed by decapitation and the livers were removed and minced before homogenization. Tissue homogenization was carried out at 4 °C in 10 ml/g tissue weight of 10 mM Tris-HCl/0.32 M sucrose, pH 7.4 using a Potter-Elvehjem tissue grinder. The crude homogenate was centrifuged for 10 min at 1000 g and the supernatant saved on ice. The pellet was resuspended in 2 ml/g tissue weight of ice-cold 10 mM Tris-HCl/0.32 M sucrose, pH 7.4 by vortexing. After centrifuging at 1000 g for 10 min, the pellet was discarded and the supernatants were combined and centrifuged at 31,000 g for 15 min. The pellet was resuspended in 3 ml/g 10 mM Tris-HCl, pH 7.4 by vortexing, and the suspension was allowed to incubate at 25 °C for 15 min. Following centrifugation at 31,000 g for 15 min, the aliquots were stored at -80 °C until used. The protein concentration of the suspension was determined by the method of Bradford<sup>14</sup> and generally ranged from 6-11 mg protein/ml.

$\sigma_1$  Binding Assay. Guinea pig brain membrane homogenates (100  $\mu\text{g}$  protein) were incubated with 3 nM [ $^3\text{H}$ ](-)-pentazocine (31.6 Ci/mmol) in 50 mM Tris-HCl (pH 8.0) at 25 °C for either 120 or 240 min. Test compounds were dissolved in ethanol then diluted in buffer for a total incubation volume of 0.5 ml. Test compounds were added in concentrations ranging from 0.005 to 1000 nM. Assays were terminated by the addition of ice-cold 10 mM Tris-HCl (pH 8.0) followed by rapid filtration through Whatman GF/B glass fiber filters (presoaked in 0.5 % polyethylenimine) using a Brandel cell harvester (Gaithersburg, MD). Filters were washed twice with 5 ml of ice cold buffer. Nonspecific binding was determined in the presence of 10  $\mu\text{M}$  (+)-pentazocine. Liquid scintillation

counting was carried out in EcoLite(+) (ICN Radiochemicals; Costa Mesa, CA) using a Beckman LS 6000IC spectrometer with a counting efficiency of 50%.

$\sigma_2$  Binding Assay. Rat liver membrane homogenates (35  $\mu$ g of protein) were incubated with 3 nM [ $^3$ H]DTG (38.3 Ci/mmol) in the presence of 100 nM (+)-pentazocine to block  $\sigma_1$  sites. Incubations were carried out in 50 mM Tris-HCl (pH 8.0) for 120 min at 25 °C in a total incubation volume of 0.5 ml. Test compounds were added in concentrations ranging from 0.005 to 1000 nM. Assays were terminated by the addition of ice-cold 10 mM Tris-HCl (pH 8.0) followed by rapid filtration through Whatman GF/B glass fiber filters (presoaked in 0.5% polyethylenimine) using a Brandel cell harvester (Gaithersburg, MD). Filters were washed twice with 5 ml of ice cold buffer. Nonspecific binding was determined in the presence of 5  $\mu$ M DTG. Liquid scintillation counting was carried out in EcoLite(+) (ICN Radiochemicals; Costa Mesa, CA) using a Beckman LS 6000IC spectrometer with a counting efficiency of 50%.

#### Data Analysis.

The IC<sub>50</sub> values at sigma sites were generally determined in triplicate from non-linear regression of binding data as analyzed by JMP (SAS Institute; Cary, NC), using 8 concentrations of each compound. K<sub>i</sub> values were calculated using the method of Cheng-Prusoff<sup>15</sup> and represent mean values  $\pm$  SEM. All curves were best fit to a one site fit and gave Hill coefficients of 0.8 – 1.0. The K<sub>d</sub> value used for [ $^3$ H]DTG in rat liver was 17.9 nM and was 4.8 nM for [ $^3$ H](+)-pentazocine in guinea pig brain.<sup>1,2</sup>

#### **Acknowledgments**

This research was funded by grants CA 80452 awarded by the National Cancer Institute, DE-FG02-00ER82945 awarded by the Department of Energy, and DAMD17-01-1-0446 awarded by the Department of Defense Breast Cancer Research Program of the US Army Medical Research and Materiel Command Office.

## References

1. Walker J.M., Bowen W.D., Walker F.O., Matsumoto R.E., De Costa B. and Rice K.R. *Pharmacol. Rev.* **1990**, *42*, 355-402.
2. Hellewell S.B., Bruce A., Feinstein G., Orringer J., Williams W. and Bowen, W.D. *Eur. J. Pharmacol. Mol. Pharmacol. Sec.* **1994**, *268*, 9-18.
3. Hanner M., Moebius F.F., Flandorfer A., Knaus H.-G., Striessnig J., Kempner E. and Glossmann H. *Proc. Natl. Acad. Sci. USA* **1996**, *93*, 8072-8077.
4. Su T.-P., London E. and Jaffe J. *Science* **1988**, *240*, 219-221.
5. Bowen W.D., Bertha C.M., Vilner B.J. and Rice K. *Eur. J. Pharmacol.* **1995**, *278*, 257-260.
6. Nguyen V.H., Kassiou M., Johnston G.A.R. and Christie M.J. *Eur. J. Pharmacol.* **1996**, *311*, 233-240.
7. Bowen W.D., Vilner B.J., Bertha C.M., Kuehne M.E. and Jocabson A.E. *Eur. J. Pharmacol.* **1995**, *279*, R1-3.
8. Mach R.H., Smith C.R. and Childers S.R. *Life Sci.* **1995**, *57*, PL 57-62.
9. Perredgaard J., Moltzen E.K., Meier E. and Sanchez C. *J. Med. Chem.* **1995**, *38*, 1998-2008.
10. Moltzen, E.K., Perregaaard J. and Meier E. *J. Med. Chem.* **1995**, *38*, 2009-2017.
11. Bonhaus D.W., Loury D.N., Jakeman L.B., To Z., DeSouza A., Eglen R.M. and Wong E.H.F. *J. Pharmacol. Exp. Ther.* **1993**, *267*, 961-970.
12. Mach R.H., Yang B., Kuhner R.J., Whirrett B.R. and West T. *Med. Chem. Res.* **2001**, *10*, 339-355.
13. Mach R.H., Wheeler K.T., Blair S., Yang B., Day C.S., Blair J.B., Choi S.-R. and Kung H.F. *J. Labelled Cmpds. Radiopharm.* **2001**, *44*, 899-908.
14. Bradford M.M. *Anal. Biochem.* **1976**, *72*, 248-254.
15. Cheng Y.C. and Prusoff W.H. *Biochem. Pharmacol.* **1973**, *22*, 3099-4022.

Received: 12-27-02 Accepted: 3-21-03



ELSEVIER

Available online at [www.sciencedirect.com](http://www.sciencedirect.com)SCIENCE @ DIRECT<sup>®</sup>

Bioorganic &amp; Medicinal Chemistry Letters 14 (2004) 195–202

Bioorganic &  
Medicinal  
Chemistry  
Letters

## Conformationally-flexible benzamide analogues as dopamine D<sub>3</sub> and σ<sub>2</sub> receptor ligands

Robert H. Mach,<sup>a,b,\*</sup> Yunsheng Huang,<sup>a</sup> Rebekah A. Freeman,<sup>c</sup> Li Wu,<sup>a</sup> Suwanna Vangveravong<sup>a</sup> and Robert R. Luedtke<sup>c</sup>

<sup>a</sup>Department of Radiology, PET Center, Wake Forest University School of Medicine, Winston-Salem, NC 27157, USA

<sup>b</sup>Department of Physiology & Pharmacology, Wake Forest University School of Medicine, Winston-Salem, NC 27157, USA

<sup>c</sup>Department of Pharmacology and Neuroscience, University of North Texas Health Science Center, Fort Worth, TX 76107, USA

Received 14 July 2003; accepted 25 September 2003

**Abstract**—A series of conformationally-flexible analogues was prepared and their affinities for D<sub>2</sub>-like dopamine (D<sub>2</sub>, D<sub>3</sub> and D<sub>4</sub>) were determined using in vitro radioligand binding assays. The results of this structure–activity relationship study identified one compound, **15**, that bound with high affinity ( $K_i$  value = 2 nM) and moderate selectivity (30-fold) for D<sub>3</sub> compared to D<sub>2</sub> receptors. In addition, this series of compounds were also tested for affinity at σ<sub>1</sub> and σ<sub>2</sub> receptors. We evaluated the affinity of these dopaminergic compounds at sigma receptors because (a) several antipsychotic drugs, which are high affinity antagonists at dopamine D<sub>2</sub>-like receptors, also bind to sigma receptors and (b) sigma receptors are expressed ubiquitously and at high levels (picomoles per mg proteins). It was observed that a number of analogues displayed high affinity and excellent selectivity for σ<sub>2</sub> versus σ<sub>1</sub> receptors. Consequently, these novel compounds may be useful for characterizing the functional role of σ<sub>2</sub> receptors and for imaging the σ<sub>2</sub> receptor status of tumors *in vivo* with PET.

© 2003 Elsevier Ltd. All rights reserved.

The dopamine receptor subtypes are members of the G protein coupled receptor protein superfamily. Based upon genetic and cDNA cloning studies it is currently thought that there are five functionally active dopamine receptor subtypes expressed in mammalian brain. These five subtypes have been classified into two major classes, the D<sub>1</sub>-like and D<sub>2</sub>-like receptors. Stimulation of the D<sub>1</sub>-like receptor subtypes, which include the D<sub>1</sub> (D<sub>1a</sub>) and the D<sub>5</sub> (D<sub>1b</sub>) receptors, results in an activation of adenylyl cyclase and an increase in the production of cAMP. Agonist stimulation of the D<sub>2</sub>-like receptors, which consist of the D<sub>2</sub>, D<sub>3</sub> and D<sub>4</sub> receptors, results in an inhibition of adenylyl cyclase activity, an increase in the release of arachadonic acid, and an increase in phosphatidylinositol hydrolysis.

Over the past 5 years, there has been interest in developing

agents that are antagonists of the dopamine D<sub>3</sub> receptor.<sup>1,2</sup> This interest was largely generated by the hypothesis that dopamine D<sub>3</sub> receptors may play a pivotal role in the development of a number of neurological and neuropsychiatric disorders. Receptor autoradiography studies have shown that both D<sub>2</sub> and D<sub>3</sub> receptors are widely distributed in striatal regions of human<sup>3</sup> and monkey<sup>4</sup> brain. However, the higher ratio of D<sub>3</sub> versus D<sub>2</sub> receptors in limbic structures indicates that the D<sub>3</sub> receptor may play an integral role in the pathological abnormalities that occur in neuropsychiatric disorders. Autoradiography studies have also revealed a decrease of D<sub>3</sub> receptors in the frontal cortex and an increase in expression in the ventral striatum of schizophrenics compared to normal individuals.<sup>5,6</sup> Dopamine D<sub>3</sub> receptors are also believed to play a role in the dyskinesias associated with l-dopa treatment of patients with Parkinson's Disease. For example, chronic treatment of squirrel monkeys with the neurotoxin, 1-methyl-4-phenyl-1,2,3,4-tetrahydropyridine (MPTP), which causes a selective destruction of the nigrostriatal dopaminergic system, results in a decline of D<sub>3</sub> receptors in the caudate (motor region) but not the putamen or globus pallidus (limbic regions). However, treatment

**Keywords:** dopamine D<sub>3</sub> receptors; atypical antipsychotics; σ<sub>2</sub> receptors.

\* Corresponding author at present address: Division of Radiological Sciences, Washington University School of Medicine, Campus Box 8225, 510 S. Kingshighway Blvd., St. Louis, MO 63110, USA. Fax: +1-314-362-0039; e-mail: rhmach@mir.wustl.edu

with the drug levodopa led to a restoration of D<sub>3</sub> receptor levels and a reversal of Parkinsonian symptoms in MPTP-treated animals. Finally, the activation of dopamine D<sub>3</sub> receptors in the nucleus accumbens is believed to be involved in the sensitization/rewarding properties of psychostimulants, such as cocaine. Therefore, agents that can block the interaction of psychostimulant-induced increases in synaptic dopamine levels with the D<sub>3</sub> receptor have potential for the pharmacological treatment of cocaine abuse.<sup>1</sup>

A number of conformationally-flexible benzamide analogues displaying a high affinity and selectivity for D<sub>3</sub> versus D<sub>2</sub> receptors have been reported in recent years. Examples of this include NGB 2849, NGB 2904, and the structural congeners **1–3** (Fig. 1). A common structural feature in the conformationally-flexible benzamide analogues is the *N*-2,3-dichlorophenylpiperazine ring and the four carbon spacer group separating the benzamide and the basic amino moieties.<sup>7–10</sup>

We have recently reported two different classes of compounds, naphthamide analogues and pyrrole derivatives, displaying a modest affinity and selectivity for D<sub>3</sub> versus D<sub>2</sub> receptors.<sup>11,12</sup> For example, the naphthamide analogues **4** and **5** have a moderate selectivity for D<sub>3</sub> versus D<sub>2</sub> receptors. Unfortunately, these compounds were found to have a relatively high affinity for sigma receptors (Fig. 2). Because sigma receptors are expressed ubiquitously and at high levels (picomoles per mg proteins), the high affinity of these compounds for sigma receptors limits their utility for in vitro and in vivo studies of dopamine D<sub>3</sub> receptors.<sup>11</sup> The pyrrole analogues **6** and **7** have a high affinity and 10-fold

selectivity for D<sub>3</sub> versus D<sub>2</sub> receptors. However, unlike the naphthamide analogues, the pyrrole analogues bound with low affinity at sigma receptors.<sup>12</sup> As part of a continuing effort to develop potent and selective D<sub>3</sub> receptor ligands as potential radiotracers for studies of the dopaminergic system with the noninvasive imaging procedure, Positron Emission Tomography (PET), we explored the possibility of preparing hybrid ligand structures of the conformationally-flexible benzamide analogues (Fig. 1) and the naphthamide and pyrrole analogues (Fig. 2). The results of this study led to the identification of a number of compounds possessing a high affinity and moderate selectivity for dopamine D<sub>3</sub> versus D<sub>2</sub> receptors.

In addition, the results of this structure–activity relationship study led to the identification of a number of conformationally-flexible benzamide analogues that had a high affinity and excellent selectivity for σ<sub>2</sub> versus σ<sub>1</sub> receptors. Sigma-2 receptors have been shown to be a potential biomarker for determining the proliferative status of breast tumors.<sup>13–15</sup> Therefore, the results of this study have led to the identification of lead compounds for radiotracer development with two completely different functions: (1) D<sub>3</sub> receptor imaging agents for studying the change in dopamine receptor function in a variety of neurological and neuropsychiatric disorders and, (2) σ<sub>2</sub> selective imaging agents for measuring the proliferative status of breast tumors in vivo with PET.

The strategy chosen for the current study involved the combination of the following structural moieties of the lead compounds: (a) the 2,3-dichlorophenylpiperazine

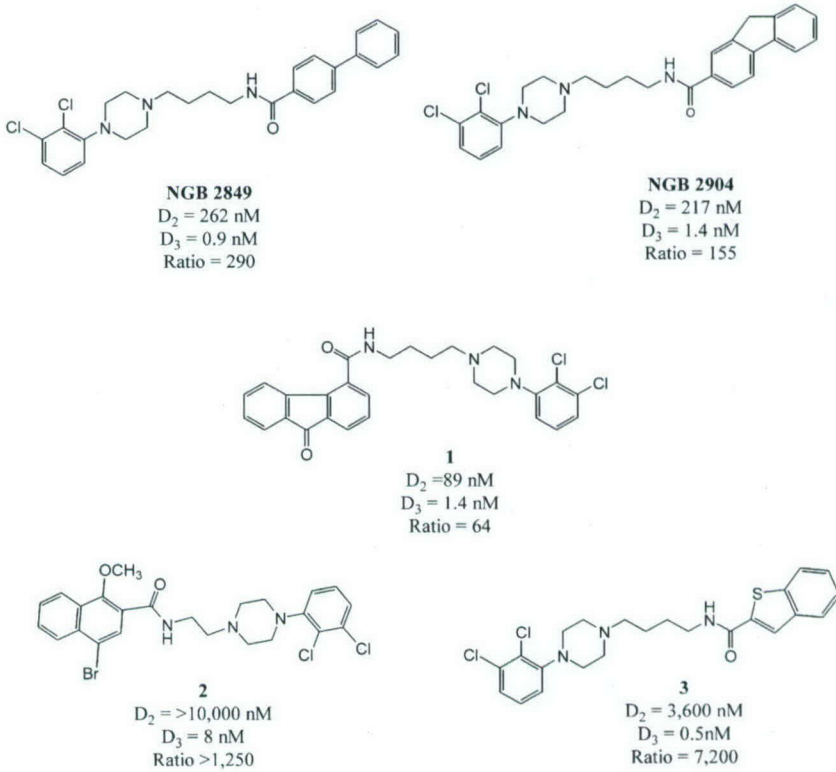


Figure 1.

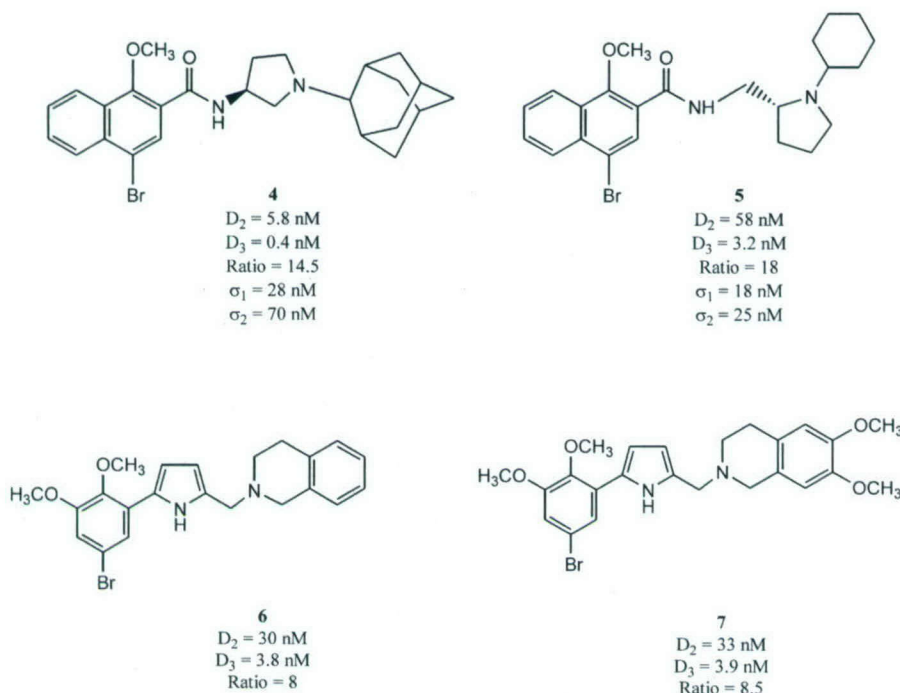


Figure 2.

and the two- and four-carbon spacer groups of the conformationally-flexible benzamide analogues shown in Figure 1; (b) the naphthyl group of naphthamide compounds shown in Figure 2; and, (c) the 2,3-dimethoxyphenyl and tetrahydroisoquinoline moieties of the pyrrole analogues shown in Figure 2.

The synthesis of the target tetrahydroisoquinoline analogues is shown in Scheme 1.<sup>16</sup> Reaction of the secondary amine of **8a** and **8b** with either bromoacetonitrile or bromobutyronitrile gave *N*-alkylated products, **9a–d**, in 75–85% yield. Reduction with either lithium aluminum hydride in THF or hydrogenation over palladium on charcoal gave the corresponding amines, **10a–d**, in quantitative yields. Condensation of amines **10a–d** with either 2-methoxy-5-bromonaphthoyl chloride<sup>12</sup> or 5-bromo-2,3-dimethoxybenzoic acid<sup>13</sup> gave the corresponding amide analogues, **11–14**, in excess of 90% yield. Synthesis of the 2,3-dichlorophenylpiperazine benzamide and naphthamide analogues, **15** and **16**, was accomplished using a similar reaction sequence as outlined in Scheme 2.<sup>16</sup>

The naphthamide analogue **11a**, which contains a two-carbon spacer group between the amide nitrogen and the basic amino group had a relatively low affinity for dopamine D<sub>3</sub> and D<sub>2</sub> receptors (Table 1). Compound **11a** also had an appreciable affinity for both σ<sub>1</sub> and σ<sub>2</sub> receptors. Introduction of a methoxy groups into the 4- and 5-positions of the tetrahydroisoquinoline ring resulted in a reduction in affinity for D<sub>2</sub>, D<sub>3</sub> and σ<sub>1</sub> receptors, and an increase in affinity for σ<sub>2</sub> receptors. Increasing the length of the spacer group from two carbon units in **11b** to four carbon units (i.e., **12**) resulted

**Table 1.** Binding affinities for dopamine D<sub>2</sub>/D<sub>3</sub> and sigma σ<sub>1</sub>/σ<sub>2</sub> receptors

Compnd	K <sub>i</sub> (nM) <sup>a</sup>			
	D <sub>2</sub> <sup>b</sup>	D <sub>3</sub> <sup>c</sup>	σ <sub>1</sub> <sup>d</sup>	σ <sub>2</sub> <sup>e</sup>
<b>11a</b>	131.6 ± 24.6	81.6 ± 21.28	15.1 ± 1.7	47.7 ± 2.5
<b>11b</b>	240.5 ± 19.4	126.5 ± 42.4	189.1 ± 2.6	21.2 ± 0.1
<b>12</b>	741.0 ± 287.3	106.5 ± 24.3	1,159 ± 7	17.6 ± 0.7
<b>13a</b>	429.7 ± 76.1	17.8 ± 0.5	276.5 ± 35.7	716.5 ± 9.8
<b>13b</b>	714.0 ± 133.7	21.4 ± 2.3	2932 ± 28	16.4 ± 2.0
<b>14</b>	2200 ± 390	627 ± 244	12,900 ± 111	8.2 ± 1.4
<b>15</b>	58.8 ± 13.7	2.1 ± 0.4	809 ± 66	75.0 ± 4.1
<b>16</b>	107.0 ± 19.0	10.2 ± 5.3	751 ± 6	26.4 ± 1.4

<sup>a</sup> Mean ± SEM, K<sub>i</sub> values were determined by at least three experiments.

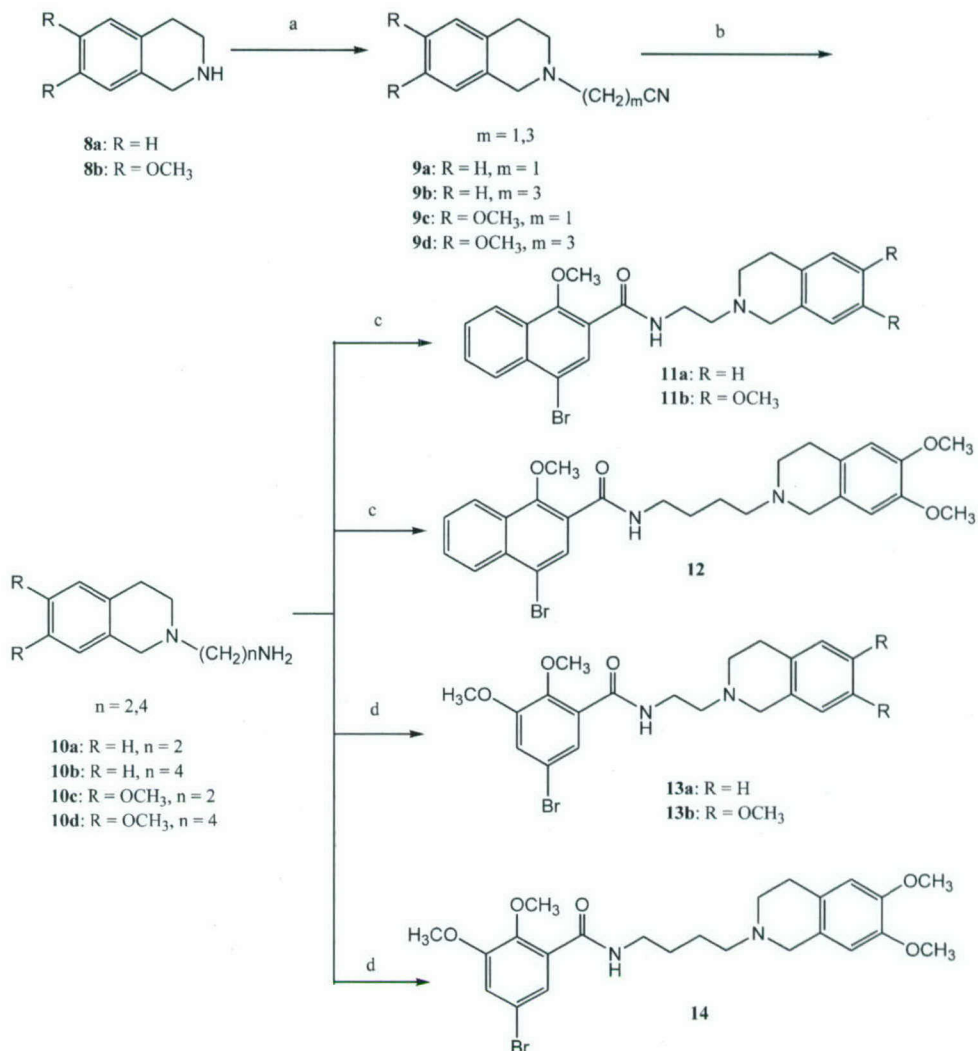
<sup>b</sup> K<sub>i</sub> values for D<sub>2</sub> receptors were measured on rat D<sub>2</sub>(long) expressed in Sf9 cells using [<sup>125</sup>I]IABN as the radioligand.<sup>18</sup>

<sup>c</sup> K<sub>i</sub> values for D<sub>3</sub> receptors were measured on rat D<sub>3</sub> expressed in Sf9 cells using [<sup>125</sup>I]IABN as the radioligand.<sup>18</sup>

<sup>d</sup> K<sub>i</sub> values for σ<sub>1</sub> receptors were measured on quinea pig brain membranes using [<sup>3</sup>H](+)-pentazocine as the radioligand.<sup>17</sup>

<sup>e</sup> K<sub>i</sub> values for σ<sub>2</sub> receptors were measured on rat liver membranes using [<sup>3</sup>H]-DTG as the radioligand in the presence of (+)-pentazocine.<sup>17</sup>

in no change in affinity for D<sub>3</sub> and σ<sub>2</sub> receptors, but a dramatic reduction in affinity for D<sub>2</sub> and σ<sub>1</sub> receptors. Replacement of the naphthamide group of **11a** with a 5-bromo-2,3-dimethoxy benzamide group (i.e., **13a**) resulted in an increase in affinity for dopamine D<sub>3</sub> receptors, and a decrease in affinity for D<sub>2</sub>, σ<sub>1</sub> and σ<sub>2</sub> receptors. Introduction of the methoxy groups into the 4- and 5-positions of the tetrahydroisoquinoline ring of **13a** to give **13b** resulted in no change in affinity for D<sub>3</sub> receptors and a reduction in affinity for D<sub>2</sub> receptors. However, this change in substitution pattern resulted in



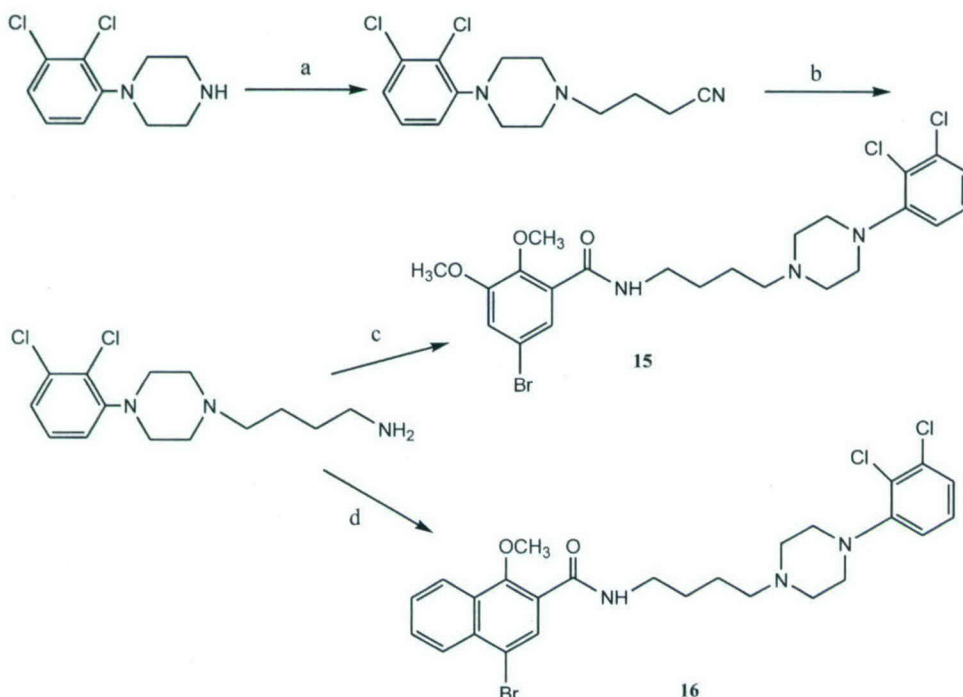
**Scheme 1.** (a) BrCH<sub>2</sub>CN or BrCH<sub>2</sub>CH<sub>2</sub>CH<sub>2</sub>CN, Et<sub>3</sub>N, CH<sub>2</sub>Cl<sub>2</sub>, rt; (b) LiAlH<sub>4</sub>, THF or H<sub>2</sub>, Pd(c), ethanol; (c) ref 10; (d) ref 12.

a dramatic decrease in affinity for  $\sigma_1$  receptors and a large increase in affinity for  $\sigma_2$  receptors. Increasing the length of the spacer group from two carbons in **13b** to four carbons in **14** resulted in large decrease in affinity for D<sub>2</sub>, D<sub>3</sub>, and  $\sigma_1$  receptors and an increase in  $\sigma_2$  receptor affinity. Compound **14** is unique in that it has over a 1500-fold higher affinity for  $\sigma_2$  versus  $\sigma_1$  receptors. Although many different classes of compounds have been shown to bind with high affinity to sigma receptors, most compounds studied to date have either (a) a higher affinity for  $\sigma_1$  versus  $\sigma_2$  receptors, or (b) equipotency with respect to binding to  $\sigma_1$  and  $\sigma_2$  receptors. Compound **14** is one of the most potent and selective  $\sigma_2$  receptor ligands reported to date.

Compound **15** was prepared to determine the effect of introducing the 5-bromo-2,3-dimethoxy benzamide moiety into NGB 2904 and its structural congeners (Fig. 1) on D<sub>2</sub> and D<sub>3</sub> receptor affinity. In addition, compound **16** was prepared to assess the effect that increasing the two-carbon spacer group of **2** (Fig. 1) to four carbons would have on dopamine receptor affinity. Compounds **15** and **16** had the highest affinity for D<sub>3</sub> receptors of the analogues prepared in this study, which further emphasizes the importance in the 2,3-dichlorophenyl-piperazine group for binding to dopamine D<sub>3</sub> receptors.

sizes the importance in the 2,3-dichlorophenyl-piperazine group for binding to dopamine D<sub>3</sub> receptors.

Compounds **17–20** were prepared with the goal of increasing the  $\sigma_2$  receptor affinity and reducing the dopamine D<sub>2</sub> and D<sub>3</sub> receptor affinity of this class of compounds (Scheme 3). The results of our previous structure–activity relationship studies indicated that both the 5-bromo and 3-methoxy groups were important for the binding the binding of pyrrole analogues shown in Figure 2 to dopamine D<sub>2</sub> and D<sub>3</sub> receptors. Therefore, removal of the 3-methoxy group, or replacement of the 5-bromo moiety with a methyl group, was expected to result in a reduction in affinity for D<sub>2</sub> and D<sub>3</sub> receptors. The results of the structure–activity relationship study are shown in Table 2. Compound **14** is included in Table 2 for comparison. Removal of the 3-methoxy group of **13a** to give **17** resulted in a large reduction in affinity for D<sub>2</sub> and D<sub>3</sub> receptors and an increase in affinity for  $\sigma_1$  and  $\sigma_2$  receptors. The same change in the structure of **13b** to give compound **18** resulted in a similar effect on dopamine receptor binding. However, there was a marked decrease in affinity of **18** for  $\sigma_1$  receptors relative to that **13b**. Compound **18** also had a

**Scheme 2.** (a)  $\text{BrCH}_2\text{CH}_2\text{CH}_2\text{CN}$ ,  $\text{Et}_3\text{N}$ ,  $\text{CH}_2\text{Cl}_2$ ; (b)  $\text{H}_2$ ,  $\text{Pd}$ ; (c) ref 12; (d) ref 10.**Table 2.** Binding affinities of **17–20** for dopamine  $\text{D}_2/\text{D}_3$  and sigma  $\sigma_1/\sigma_2$  receptors

Compd	$K_i$ (nM) <sup>a</sup>				
	$\text{D}_2$ <sup>b</sup>	$\text{D}_3$ <sup>c</sup>	$\sigma_1$ <sup>d</sup>	$\sigma_2$ <sup>e</sup>	$\sigma_1/\sigma_2$ ratio
<b>14</b>	$2200 \pm 390$	$627 \pm 244$	$12,900 \pm 111$	$8.2 \pm 1.4$	1573
<b>17</b>	$2190 \pm 351$	$310.7 \pm 54.4$	$21.8 \pm 5.6$	$89.4 \pm 13.9$	0.24
<b>18</b>	$3570 \pm 796$	$488.0 \pm 70.7$	$5484 \pm 266$	$12.4 \pm 1.8$	442
<b>19</b>	$2850 \pm 316$	$3760 \pm 618$	$10,412 \pm 462$	$13.3 \pm 0.1$	783
<b>20</b>	$642.0 \pm 141.0$	$313.0 \pm 141.0$	$3078 \pm 87$	$10.3 \pm 1.5$	300

<sup>a</sup> Mean  $\pm$  SEM,  $K_i$  values were determined by at least three experiments.<sup>b</sup>  $K_i$  values for  $\text{D}_2$  receptors were measured on rat  $\text{D}_{2(\text{long})}$  expressed in SF9 cells using [ $^{125}\text{I}$ ]IABN as the radioligand.<sup>c</sup>  $K_i$  values for  $\text{D}_3$  receptors were measured on rat  $\text{D}_3$  expressed in SF9 cells using [ $^{125}\text{I}$ ]IABN as the radioligand.<sup>d</sup>  $K_i$  values for  $\sigma_1$  receptors were measured on guinea pig brain membranes using [ $^3\text{H}$ ](+)-pentazocine as the radioligand.<sup>e</sup>  $K_i$  values for  $\sigma_2$  receptors were measured on rat liver membranes using [ $^3\text{H}$ ]-DTG as the radioligand in the presence of (+)-pentazocine.

higher affinity for  $\sigma_2$  receptors than that of **13b**. Replacement of the 5-bromo moiety of **18** with a methyl group (i.e., **19**) resulted in a further reduction in affinity for  $\text{D}_3$  and  $\sigma_1$  receptors, and no change in affinity for  $\text{D}_2$  and  $\sigma_2$  receptors. Increasing the length of the spacer group of **19** from two carbons to four carbons (i.e., **20**) resulted in an increase in affinity for  $\text{D}_2$ ,  $\text{D}_3$  and  $\sigma_1$  receptors, and no change in affinity for  $\sigma_2$  receptors. The high  $\sigma_1/\sigma_2$  selectivity ratio of compounds **14**, **18**, **19**, and **20** indicate that they have the potential to be useful lead compounds for the development of imaging agents for determining the  $\sigma_2$  receptor status of breast tumors with PET.

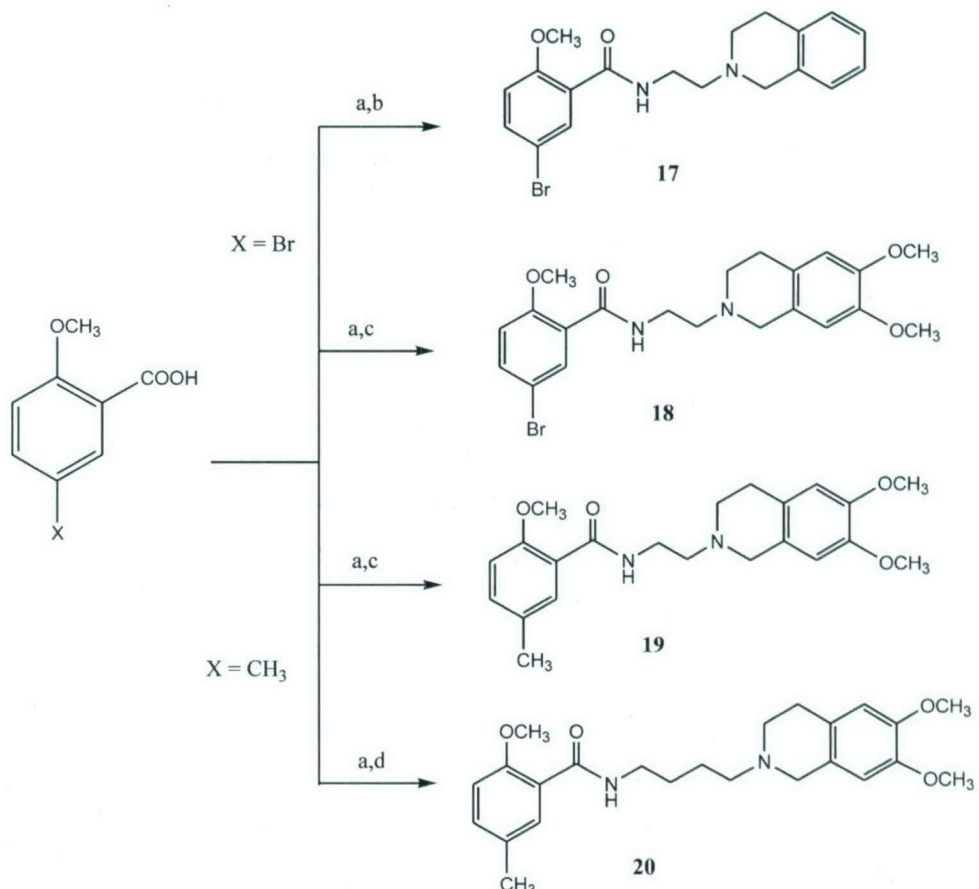
Binding assays were also conducted on compounds **13a**, **13b**, **15** and **16** to determine their affinity for dopamine  $\text{D}_{4.4}$  receptors. The results of this study are shown in Table 3. All four compounds had a lower affinity for  $\text{D}_{4.4}$  receptors relative to their binding potencies at dopamine  $\text{D}_3$  receptors. Compound **15** had the highest

**Table 3.** In vitro binding data for dopamine  $\text{D}_4$  receptors

Compd	$K_i$ (nM) <sup>a</sup>				
	$\text{D}_2$ <sup>b</sup>	$\text{D}_3$ <sup>c</sup>	$\text{D}_4$ <sup>d</sup>	$\text{D}_2/\text{D}_3$ ratio <sup>e</sup>	$\text{D}_4/\text{D}_3$ ratio <sup>f</sup>
<b>13a</b>	$429.7 \pm 76.1$	$17.8 \pm 0.5$	$47.9 \pm 11.6$	24	2.7
<b>13b</b>	$714.0 \pm 133.7$	$21.4 \pm 2.3$	$265.0 \pm 60.0$	33	12.4
<b>15</b>	$58.8 \pm 13.7$	$2.1 \pm 0.4$	$800.0 \pm 330.0$	28	381
<b>16</b>	$107.0 \pm 19.0$	$10.2 \pm 5.3$	$1345 \pm 448$	10.5	132

<sup>a</sup> Same as Table 1.<sup>b</sup> Same as Table 1.<sup>c</sup> Same as Table 1.<sup>d</sup>  $K_i$  for inhibiting the binding of [ $^{125}\text{I}$ ]IABN to human  $\text{D}_{4.4}$  receptors.<sup>e</sup>  $K_i$  for  $\text{D}_2/K_i$  for  $\text{D}_3$ .<sup>f</sup>  $K_i$  for  $\text{D}_4/K_i$  for  $\text{D}_3$ .

$\text{D}_3$  receptor affinity and highest  $\text{D}_2/\text{D}_3$  and  $\text{D}_4/\text{D}_3$  selectivity ratios of the four compounds listed in Table 3. The presence of the methoxy groups indicates that a carbon-11 labeled version of **15** can be prepared by



**Scheme 3.** (a)  $\text{SOCl}_2$ , benzene, reflux; (b) **10a**,  $\text{Et}_3\text{N}$ ,  $\text{CH}_2\text{Cl}_2$ , rt; (c) **10c**,  $\text{Et}_3\text{N}$ ,  $\text{CH}_2\text{Cl}_2$ , rt; (d) **10d**,  $\text{CH}_2\text{Cl}_2$ ,  $\text{Et}_3\text{N}$ , rt.

alkylation of the des-methyl precursor with  $^{11}\text{C}$ -methyl iodide. We are currently exploring [ $^{11}\text{C}$ ]15 as a potential radiotracer for imaging dopamine  $\text{D}_3$  receptors with PET and the relatively low affinity of 15 for  $\sigma_1$  and  $\sigma_2$  receptors indicates that there will be minimal *in vivo* binding to sigma receptors.

In conclusion, we have completed a structure–activity relationship study on a series of benzamides with the goal of identifying a potential radiotracer for imaging dopamine  $\text{D}_3$  receptors with PET. The results of this study revealed compound 15 as a candidate for labeling  $\text{D}_3$  dopamine receptors *in vivo*. The low affinity binding of 15 at sigma receptors subtypes servers to minimize sigma receptor interactions as a potential source of nonspecific/background binding. In addition, this study has lead to the identification of a number of novel,  $\sigma_2$ -receptor selective ligands. Based upon those findings we are also exploring the potential of  $^{11}\text{C}$ -labeled versions of 14, 18, 19 and 20, and  $^{76}\text{Br}$ -labeled versions of 14 and 18, as potential radiotracers for imaging the  $\sigma_2$  receptor status of breast tumors.

#### Acknowledgements

This research was funded by grants DA 12647 awarded by the National Institute on Drug Abuse and DAMD17-01-1-0446 awarded by the Department of

Defense Breast Cancer Research Program of the US Army Medical Research and Materiel Command Office.

#### References and notes

- Luedtke, R. R.; Mach, R. H. *Curr. Pharm. Des.* **2003**, 9, 643.
- Hackling, A. E.; Stark, H. *ChemBioChem*. **2002**, 3, 946.
- Morissette, M.; Goulet, M.; Grodin, R.; Blancet, P.; Bedard, P. J.; Di Paolo, T.; Levesque, D. *Eur. J. Neurosci.* **1998**, 10, 1565.
- Ryoo, H. L.; Pierotti, D.; Joyce, J. N. *Movement Disorders* **1998**, 13, 788.
- Gurevich, E. V.; Bordelon, Y.; Shapiro, R. M.; Arnold, S. E.; Gur, R. E.; Joyce, J. N. *Arch. Gen. Psych.* **1997**, 54, 225.
- Gurevich, E. V.; Joyce, J. N. *Neuropsychopharmacology* **1999**, 20, 60.
- Glase, S. A.; Akunne, H. C.; Hefner, T. G.; Johnson, S. J.; Kesten, S. R.; MacKenzie, R. G.; Manley, P. J.; Pugsley, T. A.; Wright, J. L.; Wise, L. D. *Bioorg. Med. Chem. Lett.* **1996**, 6, 1361.
- Yuan, J.; Chen, X.; Brodbeck, R.; Primus, R.; Braun, J.; Wasley, J. W. F.; Thurkauf, A. *Bioorg. Med. Chem. Lett.* **1998**, 8, 2715.
- Robarge, M. J.; Husbands, S. M.; Kielytka, A.; Brodbeck, R.; Thurkauf, A.; Newman, A. H. *J. Med. Chem.* **2001**, 44, 3175.
- Bettinetti, L.; Schlotter, K.; Hubner, H.; Gmeiner, P. *J. Med. Chem.* **2002**, 45, 4597.

11. Huang, Y.; Luedtke, R. R.; Freeman, R. A.; Wu, L.; Mach, R. H. *J. Med. Chem.* **2001**, *44*, 1815.
12. Mach, R. H.; Huang, Y.; Freeman, R. A.; Wu, L.; Blair, S.; Luedtke, R. R. *Bioorg. Med. Chem.* **2003**, *11*, 225.
13. Mach, R. H.; Smith, C. R.; Al-Nabulsi, I.; Whirrett, B. R.; Childers, S. R.; Wheeler, K. T. *Cancer Res.* **1997**, *57*, 156.
14. Al-Nabulsi, I.; Mach, R. H.; Sten, K.; Childers, S. R.; Wheeler, K. T. *Br. J. Cancer* **1999**, *81*, 925.
15. Wheeler, K. T.; Wang, L.-M.; Wallen, C. A.; Childers, S. R.; Cline, J. M.; Keng, P. C.; Mach, R. H. *Br. J. Cancer* **2000**, *82*, 1223.
16. Data for **11a**. Mp 180–182°C (oxalate salt); <sup>1</sup>H NMR (DMSO-*d*<sub>6</sub>) δ 3.02 (s, 2H), 3.19 (9s, 2H), 3.72–3.74 (m, 3H), 3.94 (s, 3H), 4.21 (s, 3H), 7.16–7.25 (m, 4H), 7.75 (t, *J*=8.1 Hz, 1H), 7.81 (t, *J*=8.1 Hz, 1H), 8.05 (s, 1H), 8.15 (d, *J*=8.3 Hz, 1H), 8.24 (d, *J*=8.3 Hz, 1H), 8.77 (t, *J*=5.4 Hz, 1H). Calcd: C: 56.72; H: 4.76; N: 5.29. Obsvd: C: 56.50; H: 4.91; N: 5.14.  
Data for **11b**. Mp 187–189°C (oxalate salt); <sup>1</sup>H NMR (DMSO-*d*<sub>6</sub>) δ 2.94 (s, 3H), 3.19 (s, 4H), 3.71 (s, 3H), 3.73 (s, 3H), 3.94 (s, 3H), 4.12 (s, 3H), 6.74 (s, 1H), 6.79 (s, 1H), 7.75 (t, *J*=7.6 Hz, 1H), 7.82 (t, *J*=7.6 Hz, 1H), 8.05 (s, 1H), 8.15 (d, *J*=8.3 Hz, 1H), 8.25 (d, *J*=8.3 Hz, 1H), 8.76 (s, 1H). Calcd: C: 55.02; H: 4.96; N: 4.75. Obsvd: C: 54.76; H: 5.04; N: 4.65.
17. Data for **12**. Mp 165–167°C (oxalate salt); <sup>1</sup>H NMR (DMSO-*d*<sub>6</sub>) δ 1.61–1.80 (m, 4H), 2.96 (s, 2H), 3.36–3.39 (m, 5H), 3.71 (s, 3H), 3.73 (s, 3H), 3.95 (s, 3H), 4.19 (s, 3H), 6.77 (s, 1H), 6.80 (s, 1H), 7.75 (t, *J*=7.4 Hz, 1H), 7.81 (t, *J*=7.4 Hz, 1H), 7.95 (s, 1H), 8.15 (d, *J*=8.3 Hz, 1H), 8.25 (d, *J*=8.3 Hz, 1H), 8.60 (t, *J*=5.6 Hz, 1H). Calcd: C: 56.41; H: 5.39; N: 4.54. Obsvd: C: 56.32; H: 5.45; N: 4.45.
18. Data for **13a**. Mp 142–144°C (oxalate salt); <sup>1</sup>H NMR (DMSO-*d*<sub>6</sub>) δ 2.99 (s, 2H), 3.10 (s, 2H), 3.61–3.63 (m, 3H), 3.73 (s, 3H), 3.85 (s, 3H), 4.15 (s, 3H), 7.13–7.23 (m, 4H), 7.34 (s, 1H), 7.36 (s, 1H), 8.59 (t, *J*=5.0 Hz, 1H). Calcd: C: 51.88; H: 4.95; N: 5.50. Obsvd: C: 51.73; H: 4.95; N: 5.51.
19. Data for **13b**. Mp 91–93°C (oxalate salt); <sup>1</sup>H NMR (DMSO-*d*<sub>6</sub>) δ 2.92 (s, 2H), 3.13 (s, 2H), 3.59–3.63 (m, 3H), 3.71 (s, 3H), 3.73 (s, 3H), 3.74 (s, 3H), 3.85 (s, 3H), 4.10 (s, 3H), 6.72 (s, 1H), 6.78 (s, 1H), 7.34 (s, 1H), 7.37 (s, 1H), 8.60 (s, 1H). Calcd: C: 50.63; H: 5.13; N: 4.92. Obsvd: C: 50.49; H: 5.30; N: 4.60.
20. Data for **14**. <sup>1</sup>H NMR (CDCl<sub>3</sub>) δ 1.70–1.79 (m, 4H), 2.59 (s, 2H), 2.73–2.76 (m, 2H), 2.81–2.84 (m, 2H), 3.51–3.52 (m, 2H), 3.58 (s, 2H), 3.85 (s, 3H), 3.86 (s, 3H), 3.88 (s, 3H), 3.90 (s, 3H), 6.52 (s, 1H), 6.60 (s, 1H), 7.12 (d, *J*=2.7 Hz, 1H), 7.78 (d, *J*=2.7 Hz, 1H), 8.05 (s, 1H). Calcd: C: 52.27; H: 5.57; N: 4.69. Obsvd: C: 52.07; H: 5.40; N: 4.64.
21. Data for **15**. <sup>1</sup>H NMR (CDCl<sub>3</sub>) δ 1.66 (s, 4H), 2.44–2.66 (m, 6H), 3.06 (s, 2H), 3.17–3.21 (m, 2H), 3.48–3.50 (m, 2H), 3.88 (s, 6H), 6.76–6.96 (m, 2H), 7.12–7.16 (m, 2H), 7.77–7.79 (m, 1H), 7.99 (s, 1H).
22. Data for **16**. <sup>1</sup>H NMR (CDCl<sub>3</sub>) δ 1.72 (s, 4H), 2.47–2.67 (m, 6H), 3.03 (s, 2H), 3.15–3.20 (m, 2H), 3.54–3.63 (m, 2H), 3.99 (s, 3H), 6.73–6.93 (m, 2H), 7.11–7.17 (m, 1H), 7.60–7.72 (m, 2H), 8.01–8.26 (m, 3H), 8.38 (s, 1H).
23. Data for **17**. Mp 166–168°C (oxalate salt); <sup>1</sup>H NMR (DMSO-*d*<sub>6</sub>) δ 3.02 (s, 3H), 3.14 (s, 2H), 3.66 (s, 2H), 3.83 (s, 3H), 4.19 (s, 3H), 7.12–7.25 (m, 5H), 7.65–7.67 (m, 1H), 7.86 (s, 1H), 8.56 (t, *J*=5.4 Hz, 1H). Calcd: C: 52.62; H: 4.84; N: 5.84. Obsvd: C: 52.38; H: 4.75; N: 5.69.
24. Data for **18**. Mp 158–160°C (oxalate salt); <sup>1</sup>H NMR (DMSO-*d*<sub>6</sub>) δ 2.93 (s, 2H), 3.16 (s, 2H), 3.60–3.66 (m, 3H), 3.71 (s, 3H), 3.73 (s, 3H), 3.84 (s, 3H), 4.14 (s, 3H), 6.73 (s, 1H), 6.78 (s, 1H), 7.13 (d, *J*=8.9 Hz, 1H), 7.66 (d, *J*=8.7 Hz, 1H), 7.86 (s, 1H), 8.57 (t, *J*=5.4 Hz, 1H). Calcd: C: 51.22; H: 5.05; N: 5.19. Obsvd: C: 51.23; H: 5.07; N: 5.04.
25. Data for **19**. Mp 160–162°C (oxalate salt); <sup>1</sup>H NMR (DMSO-*d*<sub>6</sub>) δ 2.27 (s, 3H), 2.94 (s, 2H), 3.16 (s, 2H), 3.65–3.66 (m, 3H), 3.72 (s, 3H), 3.73 (s, 3H), 3.82 (s, 3H), 4.14 (s, 3H), 6.73 (s, 1H), 6.79 (s, 1H), 7.03 (d, *J*=8.4 Hz, 1H), 7.29 (d, *J*=8.4 Hz, 1H), 7.63 (s, 1H), 8.51 (s, 1H). Calcd: C: 60.18; H: 6.42; N: 5.85. Obsvd: C: 60.32; H: 6.39; N: 5.56.
26. Data for **20**. <sup>1</sup>H NMR (CDCl<sub>3</sub>) δ 1.70–1.79 (m, 4H), 2.32 (s, 3H), 2.59 (s, 2H), 2.73–2.76 (m, 2H), 2.81–2.84 (m, 2H), 3.51–3.52 (m, 2H), 3.58 (s, 2H), 3.81 (s, 3H), 3.83 (s, 3H), 3.89 (s, 3H), 6.50 (s, 1H), 6.58 (s, 1H), 6.86–6.96 (m, 2H), 7.11 (s, 1H), 8.00 (s, 1H). Calcd: C: 62.14; H: 6.82; N: 5.57. Obsvd: C: 62.33; H: 6.60; N: 5.06.
27. **σ Receptor binding assays.** The  $\sigma_1$  receptor binding assay was conducted using guinea pig brain membrane homogenates (100 µg protein). Membrane homogenates were incubated with 3 nM [<sup>3</sup>H](+)-pentazocine (31.6 Ci/mmol) in 50 mM Tris-HCl (pH 8.0) at 25°C for either 120 or 240 min. Test compounds were dissolved in ethanol then diluted in buffer for a total incubation volume of 0.5 mL. Test compounds were added in concentrations ranging from 0.005 to 1000 nM. Assays were terminated by the addition of ice-cold 10 mM Tris-HCl (pH 8.0) followed by rapid filtration through Whatman GF/B glass fiber filters (presoaked in 0.5% polyethylenimine) using a Brandel cell harvester (Gaithersburg, MD, USA). Filters were washed twice with 5 mL of ice cold buffer. Nonspecific binding was determined in the presence of 10 µM (+)-pentazocine. Liquid scintillation counting was carried out in EcoLite(+) (ICN Radiochemicals; Costa Mesa, CA, USA) using a Beckman LS 6000IC spectrometer with a counting efficiency of 50%.  
The  $\sigma_2$  receptor binding assay was conducted using rat liver membrane homogenates (35 µg of protein). Membrane homogenates were incubated with 3 nM [<sup>3</sup>H]DTG (38.3 Ci/mmol) in the presence of 100 nM (+)-pentazocine to block  $\sigma_1$  sites. Incubations were carried out in 50 mM Tris-HCl (pH 8.0) for 120 min at 25°C in a total incubation volume of 0.5 mL. Test compounds were added in concentrations ranging from 0.005 to 1000 nM. Assays were terminated by the addition of ice-cold 10 mM Tris-HCl (pH 8.0) followed by rapid filtration through Whatman GF/B glass fiber filters (presoaked in 0.5% polyethylenimine) using a Brandel cell harvester (Gaithersburg, MD, USA). Filters were washed twice with 5 mL of ice cold buffer. Nonspecific binding was determined in the presence of 5 µM DTG. Liquid scintillation counting was carried out in EcoLite(+) (ICN Radiochemicals; Costa Mesa, CA, USA) using a Beckman LS 6000IC spectrometer with a counting efficiency of 50%.  
The IC<sub>50</sub> values at sigma sites were generally determined in triplicate from non-linear regression of binding data as analyzed by JMP (SAS Institute; Cary, NC, USA), using eight concentrations of each compound.  $K_i$  values were calculated using the method of Cheng-Prusoff<sup>19</sup> and represent mean values ± SEM. All curves were best fit to a one site fit and gave Hill coefficients of 0.8–1.0. The  $K_d$  value used for [<sup>3</sup>H]DTG in rat liver was 17.9 nM and was 4.8 nM for [<sup>3</sup>H](+)-pentazocine in guinea pig brain.<sup>11,12</sup>
28. **Dopamine receptor binding assays.** A filtration binding assay was used to characterize the binding properties of membrane-associated receptors. For rat D<sub>2</sub><sub>Long</sub>, rat D<sub>3</sub> receptors expressed in S9 cells and human D<sub>4</sub> dopamine receptors expressed in HEK 293 cells, tissue homogenates (50 µL) were suspended in 50 mM Tris-HCl/150 mM NaCl/10 mM EDTA buffer, pH 7.5 and incubated with

50  $\mu$ L of  $^{125}\text{I}$ -IABN at 37°C for 60 min. Nonspecific binding was defined using 25  $\mu\text{M}$  (+)-butaclamol. For competition experiments the radioligand concentration is generally equal to 0.5 times the  $K_d$  value and the concentration of the competitive inhibitor ranges over five orders of magnitude. Binding will be terminated by the addition of cold wash buffer (10 mM Tris-HCl/150 mM NaCl, pH 7.5) and filtration over a glass-fiber filter (Schleicher and Schuell No. 32). Filters will be washed with 10 mL of cold buffer and the radioactivity will be measured using a Packard Cobra gamma counter. Estimates of the equilibrium dissociation constant and maximum number of binding sites are obtained using unweighted nonlinear regression analysis of data modeled according to the

equation describing mass action binding.<sup>20</sup> Data from competitive inhibition experiments are modeled using nonlinear regression analysis to determine the concentration of inhibitor that inhibits 50% of the specific binding of the radioligand. Competition curves will be modeled for a single site and the  $\text{IC}_{50}$  values will be converted to equilibrium dissociation constants ( $K_i$  values) using the Cheng-Prusoff<sup>19</sup> correction. Mean  $K_i$  values  $\pm$  SEM are reported for at least three independent experiments.

19. Cheng, Y. C.; Prusoff, W. H. *Biochem. Pharmacol.* **1973**, 22, 3099.
20. McGonigle, P.; Molinoff, P. B. In *Basic Neurochemistry*, 4th ed.; Siegle Agranoff, Albers, Molinoff, Eds., Raven: 1989; Chapter 9.

## RECEPTOR-BASED RADIOTRACERS FOR IMAGING THE PROLIFERATIVE STATUS OF BREAST TUMORS

Robert H. Mach,<sup>1</sup> Clive Brown-Proctor,<sup>2</sup> Suwanna Vangveravong,<sup>2,3</sup> Joseph B. Blair,<sup>2</sup> Nancy Buchheimer,<sup>2</sup> Joey Bottoms,<sup>2</sup> and Kenneth T. Wheeler<sup>2</sup>

<sup>1</sup>Division of Radiological Sciences, Washington University School of Medicine, St. Louis, MO

<sup>2</sup>Wake Forest University School of Medicine, Winston-Salem, NC

<sup>3</sup>Anasazi BioMedical Research, Inc., Winston-Salem, NC

### INTRODUCTION

A number of studies have reported an overexpression of sigma receptors in a variety of human and murine tumors (1,2). The observation that the density of  $\sigma_2$  receptors is greater than that of  $\sigma_1$  receptors in a wide panel of tumor cells grown under cell culture conditions (3) suggests that the  $\sigma_2$  receptor is a suitable target for developing receptor-based radiotracers for noninvasive imaging procedures such as Positron Emission Tomography (PET) and Single Photon Emission Computed Tomography (SPECT). In addition, the observation that the density of  $\sigma_2$  receptors is 10-fold higher in proliferating versus quiescent mouse mammary adenocarcinoma cells both in vitro (4,5) and in vivo (6) suggests that radioligands possessing a high affinity and selectivity for  $\sigma_2$  receptors have the potential to measure the proliferative status of breast tumors using noninvasive imaging procedures such as PET and SPECT.

A number of structurally-diverse compounds have been shown to bind with high affinity to sigma receptors. However, most compounds display either a high selectivity for the  $\sigma_1$  receptor or bind with equal affinity to both  $\sigma_1$  and  $\sigma_2$  receptors. We previously reported that *N*-(9-(4-fluorobenzyl))-9-azabicyclo[3.3.1]nonan-3 $\alpha$ -yl-*N'*-(2-methoxy-4-methylphenyl)carbamate, **1** (Figure 1), has a modest affinity and moderate selectivity for  $\sigma_2$  versus  $\sigma_1$  receptors (7). The higher affinity of **1** for  $\sigma_2$  versus  $\sigma_1$  receptors, and the observation that the fluorine-18 labeled analog of **1** could be prepared via alkylation of the des-benzyl precursor with [<sup>18</sup>F]4-fluorobenzyl iodide, led us to explore the use of [<sup>18</sup>F]**1** as a potential PET radiotracer for imaging the  $\sigma_2$  receptor status of breast tumors. The goal of the current study was to synthesize [<sup>18</sup>F]**1** and conduct preliminary in vivo studies of this radiotracer in a murine model of breast cancer.

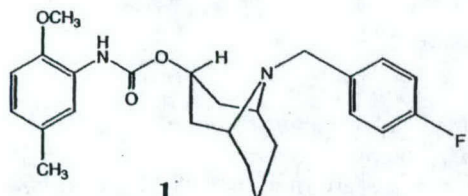
### Radiochemistry

The synthesis of [<sup>18</sup>F]**1** was accomplished via N-alkylation of the des-benzyl precursor, **2**, with [<sup>18</sup>F]4-fluorobenzyl iodide (Scheme 1). The product was obtained in an overall yield of ~10% from solubilized [<sup>18</sup>F]CsF in a specific activity of  $2320 \pm 1384$  mCi/ $\mu$ mol ( $85.1 \pm 51.2$

GBq/ $\mu$ mol). The radiotracer was of sufficient radiochemical purity (>95%) for the in vivo tumor uptake studies.

### Biodistribution Studies

Preliminary in vivo biodistribution studies were conducted in nude mice containing xenografts of the mouse mammary adenocarcinoma tumor cell line, 66. The results of this study are shown in Table I. There was a gradual increase in the uptake of [ $^{18}\text{F}$ ]1 in the tumor xenografts between 30-min and 60-min post-i.v. injection of the radiotracer. There was a slow rate of washout of radiotracer from the tumor and a progressive increase in the tumor:blood and tumor:muscle ratios over time (Table I). Blocking studies with haloperidol (50  $\mu\text{g}$ ), a known sigma ligand, resulted in a reduction in tumor uptake and tumor:background ratios. These data are consistent with the labeling of  $\sigma_2$  receptors in vivo (Figure 2).



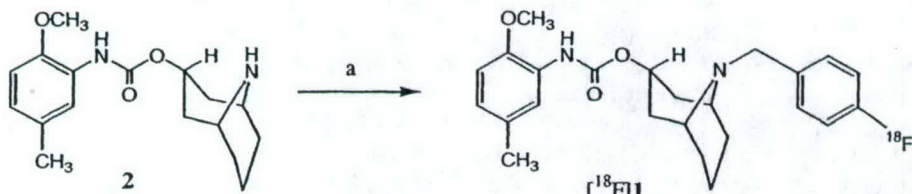
$$\sigma_1 = 202 \text{ nM}$$

$$\sigma_2 = 30 \text{ nM}$$

$$\text{Ratio} = 6.7$$

Figure 1. Structure and in vitro binding affinity of **1** for sigma receptors.

### Scheme I



Reagents: [ $^{18}\text{F}$ ]4-fluorobenzyl iodide/triethylamine/DMF/90°C.

**Discussion.** Previous studies have shown that the  $\square_2$  receptor is a useful target for developing radiotracers for imaging breast tumors. Sigma-2 receptors are expressed in high density in breast tumor cells both in vitro and in vivo, whereas surrounding normal tissue is devoid of  $\square_2$  receptors (7). Also, the density of  $\square_2$  receptors is 10-fold higher in proliferating versus nonproliferating (i.e., quiescent) mouse mammary adenocarcinoma cells growing both in vitro and in vivo (3-5).

Therefore, a  $\sigma_2$ -selective imaging agent is predicted to not only image breast tumors, but has the added feature of potentially providing information regarding the proliferative status of the tumor. Most sigma receptor-based radiotracers for imaging tumors reported to date have a higher affinity for  $\sigma_1$  versus  $\sigma_2$  receptors, or bind with equal affinity to both  $\sigma_1$  and  $\sigma_2$  receptors (8,9). Although the  $\sigma_2$  receptor affinity of 1 is somewhat lower than traditionally used for receptor-imaging studies, the relatively high selectivity of this compound for  $\sigma_2$  versus  $\sigma_1$  receptors, and the fact that the corresponding  $^{18}\text{F}$ -labeled derivative was readily accessible via alkylation of 2 with  $[^{18}\text{F}]4$ -fluorobenzyl iodide indicated that this was a radiotracer worth evaluating *in vivo*. This agent demonstrated a high tumor uptake and reasonable tumor:blood and tumor:muscle ratios, which further suggests that  $[^{18}\text{F}]1$  may be a useful agent for imaging breast tumors with PET.

**Table I.** Results of biodistribution studies of  $[^{18}\text{F}]1$  in tumor-bearing mice.

%I.D./c.c. Tissue

Tissue	30 min	60 min	120 min	240 min
Brain	1.18 ± 0.19	1.92 ± 0.24	1.18 ± 0.19	0.13 ± 0.01
Blood	1.47 ± 0.10	3.07 ± 0.45	1.90 ± 0.18	0.37 ± 0.06
Lung	6.81 ± 0.85	5.11 ± 1.36	3.77 ± 0.39	0.65 ± 0.11
Heart	2.10 ± 0.18	3.30 ± 0.54	1.80 ± 0.21	0.31 ± 0.05
Liver	7.92 ± 1.18	10.93 ± 1.00	7.36 ± 0.89	1.14 ± 0.18
Kidney	6.40 ± 0.25	14.71 ± 4.57	5.50 ± 0.76	1.08 ± 0.11
Intestine	6.49 ± 0.69	17.92 ± 3.19	9.40 ± 0.87	2.23 ± 0.21
Muscle	1.25 ± 0.23	3.43 ± 0.58	1.84 ± 0.24	0.23 ± 0.02
Spleen	4.55 ± 0.33	5.87 ± 0.71	3.45 ± 0.39	0.55 ± 0.11
Tumor	1.34 ± 0.21	5.02 ± 0.85	3.18 ± 0.12	0.89 ± 0.03
Tumor:Blood <sup>a</sup>	0.80 ± 0.08	1.66 ± 0.23	1.72 ± 0.17	2.48 ± 0.22
Tumor:Muscle <sup>b</sup>	1.13 ± 0.27	1.78 ± 0.48	1.78 ± 0.18	3.98 ± 0.30

<sup>a</sup>%I.D. tumor/%I.D. blood; <sup>b</sup>%I.D. tumor/%I.D. muscle.

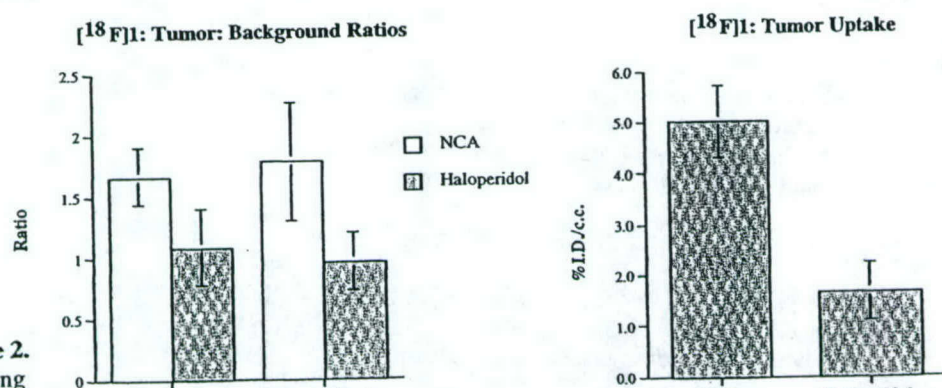


**Figure 2.** Blocking studies with  $[^{18}\text{F}]1$ : Tumor:Background Ratios and  $[^{18}\text{F}]1$ : Tumor Uptake. Co-injection of 50  $\mu\text{g}$  of haloperidol resulted in a reduction in tumor:background ratios and uptake of  $[^{18}\text{F}]1$  at 60 min post-i.v. injection of the radiotracer.

The results of the biodistribution study indicate that there is a high uptake of the radiotracer in mouse mammary adenocarcinoma xenografts (Table 1). The highest tumor:blood and tumor:muscle ratios was observed at 4 hr post-i.v. injection. In vivo blocking studies conducted with haloperidol, a known sigma receptor ligand, resulted in a dramatic reduction in the tumor uptake of [<sup>18</sup>F]1 at 60 min post-i.v. injection, which corresponds to the time of peak radiotracer accumulation in the no-carrier-added (N.C.A.) studies. Haloperidol also reduced the tumor:blood and tumor:muscle ratios to ~1.0 at this time point (Figure 2). These data are consistent with the labeling of σ<sub>2</sub> receptors in vivo.

### Conclusion

In conclusion, we report in this communication the synthesis and preliminary in vivo evaluation of an <sup>18</sup>F-labeled σ<sub>2</sub>-receptor radiotracer possessing a modest affinity and selectivity for σ<sub>2</sub> versus σ<sub>1</sub> receptors. The in vivo studies indicate that there is a high uptake of this radiotracer in mouse mammary adenocarcinoma xenografts, and that co-injecting with a known sigma ligand reduces the uptake of the radiotracer. Additional studies are currently being conducted in order to determine if this radiotracer is suitable for PET studies aimed at determining the σ<sub>2</sub> receptor status of solid tumors.

**Acknowledgements.** This research was funded by grants CA 80452 awarded by the National Cancer Institute, DE-FG02-00ER82945 awarded by the Department of Energy, and DAMD17-01-1-0446 awarded by the Department of Defense Breast Cancer Research Program of the US Army Medical Research and Materiel Command Office.

### References

1. Bem W.T., Thomas G.E., Mammone J.Y., Homan S.M., Levy B.K., Johnson, F.E., Coscia C.J. *Cancer Research* **1991**; *51*: 6558-6562.
2. Vilner B.J., John C.S., Bowen W.D. *Cancer Research* **1995**; *55*: 408-413.
3. Mach R.H., Smith C.R., Al-Nabulsi I., Whirrett B.R., Childers S.R., Wheeler KT. *Cancer Research* **1997**; *57*: 156-161.
4. Al-Nabulsi I., Mach R.H., Sten K., Childers S.R., Wheeler KT. *Brit. J. Cancer* **1999**; *81*: 925-933.
5. Wheeler K.T., Wang L.-M., Wallen C.A., Childers S.R., Cline J.M., Keng P.C., Mach R.H. *British J. Cancer* **2000**; *82*: 1223-1232.
6. Mach R.H., Vangveravong S., Huang H., Yang B., Blair J.B., Wu L. *Med. Chem. Res.* **2003**; *11*: 380-398.
7. John C.S., Vilner B.J., Schwartz A.M., Bowen W.D. *J. Nucl. Med.* **1996**; *37*: 267P.
8. John C.S., Vilner B.J., Gulden M.E., Efange S.M.N., Langason R.B., Moody T.W., Bowen W.D. *Cancer Research* **1995**; *55*: 3022-3027.
9. Caveliers V., Everaert H., John C.S., Lahoutte T. *J. Nucl. Med.* **1995**; *43*: 1647-1649.

# **Carbon-11 Labeled $\sigma_2$ Receptor Ligands for Imaging Breast Cancer**

Zhude Tu<sup>a</sup>, Carmen S. Dence,<sup>a</sup> Datta E. Ponde<sup>a</sup>, Lynne Jones,<sup>a</sup> Kenneth T. Wheeler,<sup>b</sup>  
Michael J. Welch,<sup>a</sup> and Robert H. Mach<sup>a\*</sup>

<sup>a</sup> Mallinckrodt Institute of Radiology, Washington University School of Medicine, St. Louis, MO 63110, and <sup>b</sup> Wake Forest University School of Medicine, Winston-Salem, NC 27157

**Abbreviated title:** C-11 labeled  $\sigma_2$  receptor radiotracers

**Keywords:** Sigma-2 receptors, PET, Tumor imaging agents

**Total pages:** 25

**Figures:** 3

**Tables:** 3

**Schemes:** 2

**Address correspondence to:**

Robert H. Mach, Ph.D.  
Division of Radiological Sciences  
Washington University School of Medicine  
Campus Box#: 8225  
510 South Kingshighway  
St. Louis, MO 63110  
phone: (314) 362-8538  
fax: (314) 362-0039  
email: rhmach@mir.wustl.edu

## **Abstract**

Four conformationally-flexible benzamide analogs having a high affinity and outstanding selectivity for  $\sigma_2$  versus  $\sigma_1$  receptors were synthesized and radiolabeled with carbon-11 by reaction with [ $^{11}\text{C}$ ]methyl iodide. The four  $^{11}\text{C}$ -labeled radiotracers were evaluated for their potential to image the proliferative status of breast tumors with Positron Emission Tomography (PET). In vivo studies in female Balb/C mice bearing EMT-6 breast tumors showed one radiotracer, (2-methoxy- $^{11}\text{C}$ )-N-(4-(3,4-dihydro-6,7-dimethoxy-isoquinolin-2(1H)-yl)butyl)-5-methylbenzamide ([ $^{11}\text{C}$ ]**2**) had a high tumor uptake and suitable tumor:background ratio for imaging purposes. Blocking studies were consistent with the labeling of  $\sigma_2$  receptors in vivo. A study comparing the in vivo properties of [ $^{11}\text{C}$ ]**2** and  $^{18}\text{F}$ -3'-fluoro-3'-deoxy-L-thymidine ( $[^{18}\text{F}]$ FLT) indicated that [ $^{11}\text{C}$ ]**2** had either similar (lung, fat) or better (blood, muscle) tumor:organ ratios than [ $^{18}\text{F}$ ]FLT in the tissues that are important for breast tumor imaging. Consequently, [ $^{11}\text{C}$ ]**2** is a potential radiotracer for imaging the proliferative status of breast tumors in vivo with PET.

## **1. Introduction**

Sigma ( $\sigma$ ) receptors are a distinct class of receptors that are expressed in many normal tissues, including liver, kidneys, endocrine glands and brain [1]. It has been well established that there are at least two types of  $\sigma$  receptors,  $\sigma_1$  and  $\sigma_2$ . The  $\sigma_1$  receptor has been cloned and displays a 30% sequence homology with the enzyme, yeast sterol isomerase [2]. The  $\sigma_2$  receptor has not been cloned, but evidence suggests that this receptor is linked to potassium channels and intracellular calcium release in NCB-20 cells [1,3,4].

Previous studies have reported an overexpression of sigma receptors in a variety of human and murine tumors [4-6]. The observation that the density of  $\sigma_2$  receptors is greater than that of  $\sigma_1$  receptors in a wide panel of tumor cells grown under cell culture conditions [4] suggests that the  $\sigma_2$  receptor is a suitable target for developing receptor-based radiotracers for noninvasive imaging procedures such as Positron Emission Tomography (PET) and Single Photon Emission Computed Tomography (SPECT). In addition, the recent observation that the density of  $\sigma_2$  receptors is 10-fold higher in proliferating versus quiescent mouse mammary adenocarcinoma cells both in vitro [7,8] and in vivo [9] suggests that radioligands possessing a high affinity and selectivity for  $\sigma_2$  receptors have the potential to measure the proliferative status of breast tumors using noninvasive imaging procedures such as PET and SPECT.

A number of structurally-diverse compounds have been shown to bind with high affinity to sigma receptors. However, most compounds display either a high selectivity for the  $\sigma_1$  receptor or bind with equal affinity to both  $\sigma_1$  and  $\sigma_2$  receptors [1]. We recently

reported the synthesis and in vitro binding of a number of conformationally-flexible benzamide analogs having a high affinity and outstanding selectivity for  $\sigma_2$  versus  $\sigma_1$  receptors [10]. The presence of an ortho methoxy group in each compound (Table I) indicated that it is possible to prepare the corresponding  $^{11}\text{C}$ -labeled radiotracer via O-alkylation of the corresponding phenol precursor with [ $^{11}\text{C}$ ]methyl iodide. The goals of the current study were to: a) evaluate the use of [ $^{11}\text{C}$ ]1 - 4 as PET imaging agents in a rodent model of breast cancer, and 2) compare the in vivo properties of our  $^{11}\text{C}$ -labeled  $\sigma_2$  receptor ligands with those of the radiolabeled nucleoside, [ $^{18}\text{F}$ ]FLT [11].

## 2. Methods and Materials

*2.1. General.* All chemicals were obtained from Aldrich Chemical Co. (Sigma-Aldrich, St. Louis, MO) and used without further purification unless otherwise stated.  $^1\text{H}$  NMR spectra were recorded at 300 MHz on a Varian Mercury-VX spectrometer. All chemical shift values are reported in ppm ( $\delta$ ). Elemental analyses (C, H, N) were determined by Atlantic Microlab, Inc. and the analytical results were within  $\pm 0.4\%$  of the theoretical values for the formula given unless otherwise listed. The radiolabeled nucleoside, [ $^{18}\text{F}$ ]FLT, was prepared using the procedure described by Shields et al. [11].

*2.2.2. General Procedure for the preparation of N-substituted 6,7-Dimethoxy-1,2,3,4-tetrahydroisoquinoline benzamides.*

**Method A:** A solution of substituted 2-methoxy benzoic acid (300 mmol), 1.0 equivalent of *N*-(6,7-dimethoxy-1,2,3,4-tetrahydro-1*H*-isoquinolin)-4-aminobutane or *N*-(6,7-dimethoxy-1,2,3,4-tetrahydro-1*H*-isoquinolin)-2-aminoethane in methylene chloride (30

mL) was stirred at 0°C. Then, 1.0 equivalent of benzotriazol-1-yl-oxytris(dimethylamino)phosphonium hexafluorophosphate (BOP) or 1,3-dicyclohexylcarbodiimide (DCC) and 2.5 equivalents of triethylamine were added, and the solution was allowed to warm up to ambient temperature. The reaction mixture was stirred at ambient temperature for 18 hrs. The mixture was then washed with saturated aqueous sodium bicarbonate, and the organic layer was separated and dried over anhydrous sodium sulfate. The solvent was removed under reduced pressure to provide the crude product, which was purified on a silica gel column using hexane/ethyl ether/triethylamine (50:50:1) as the eluent.

N-[4-(6,7-Dimethoxy-3,4-dihydro-1H-isoquinolin-2-yl)-butyl]-2-methoxy-5-methylbenzamide(**2**). 59.2% yield.  $^1\text{H-NMR}$  (300 MHz,  $\text{CDCl}_3$ ): 1.21-1.72 (t, 4H), 2.31 (s, 3H), 2.52-2.58 (t, 2H), 2.68-2.73 (t, 2H), 2.79-2.84 (t, 2H), 3.46-3.49 (t, 2H), 3.55(s, 2H), 3.82 (s, 3H), 3.83 (s, 3H), 3.89(s, 3H), 6.50 (s, 1H), 6.58 (s, 1H), 6.83-6.86 (d, 1H), 7.19-7.23 (d, 1H), 7.93 (s, 1H), 7.90 (s, 1H).

5-Bromo-N-[2-(6,7-dimethoxy-3,4-dihydro-1H-isoquinolin-2-yl)-ethyl]-2-methoxybenzamide (**3**). 72.0% yield.  $^1\text{H-NMR}$  (300 MHz,  $\text{CDCl}_3$ ): 2.73-2.84 (m, 4H), 3.61 (s, 3H), 3.62-3.67 (m, 4H), 3.83 (s, 3), 3.85 (s, 3H), 6.54 (s, 1H), 6.74-6.78 (d, 1H), 7.25-7.49 (d, 1H), 8.29 (s, 1H), 8.53 (s, 1H).

5-Bromo-N-[4-(6,7-dimethoxy-3,4-dihydro-1H-isoquinolin-2-yl)-butyl]-2,3-dimethoxybenzamide (**4**). 52.0% yield.  $^1\text{H-NMR}$  (300 MHz,  $\text{CDCl}_3$ ): 1.67-1.72 (m, 4H), 2.51-2.56 (t 2), 2.65-2.69 (t, 2H), 2.77-2.81 (t, 2H), 3.30-3.50 (t, 2H), 3.53 (s, 2H), 3.83 (s, 3H), 3.84 (s, 3), 3.85 (s, 3H), 3.87 (s, 3H), 6.50 (s, 1H), 6.57 (s, 1H), 7.76 (d, 1H), 8.05 (s, 1H).

**Method B:** A solution of 5-bromosalicylic acid (217 mg, 1.0 mmol) and *N*-(6,7-dimethoxy-1,2,3,4-tetrahydro-1*H*-isoquinolin)-4-aminoethane (306 mg, 1.3 mmol) in methylene chloride (30 mL) was cooled to 0°C (ice bath) and 1,3-dicyclohexylcarbodiimide (278 mg, 1.35 mmol) was added. The solution was removed from the ice bath and the reaction mixture was stirred at ambient temperature for 18 hrs. The mixture was washed with saturated aqueous sodium bicarbonate, and the organic layer was dried over anhydrous sodium sulfate. The solution was filtered, and the volatiles were removed in vacuo. The residue was purified using a silica gel column (1.0 x 20 inches) and methanol : ether (1:4) as the eluent; 74 mg of final product, **9**, was obtained. The yield was 17%.  $^1\text{H-NMR}$  (300MHz,  $\text{CDCl}_3$ ): 2.70-2.90 (m, 6H), 3.55–3.63 (m, 2H), 3.65-3.70 (s, 2H), 3.84 (s, 3H), 3.86 (s, 3H), 6.54 (s, 1H), 6.62 (s, 1H), 6.84 (d, 1H), 7.18 (s, 1H), 7.43 (d, 1H), 7.45 (s, 1H).

*N*-[2-(6,7-Dimethoxy-3,4-dihydro-1*H*-isoquinolin-2-yl)-ethyl]-2-hydroxy-5-methylbenzamide (**8**) 15% yield.  $^1\text{H-NMR}$  (300 MHz,  $\text{CDCl}_3$ ): 2.24 (s, 3H), 2.70-2.90 (m, 6H), 3.60 – 3.63 (m, 2H), 3.65 (s, 2H), 3.85 (s, 3H), 3.87 (s, 3H), 6.55 (s, 1H), 6.63 (s, 1H), 6.87 (d, 1H), 7.10 (s, 1H), 7.16 (d, 1H), 7.16 (t, 1H).

N-[2-(6,7-dimethoxy-3,4-dihydro-1H-isoquinolin-2-yl)-butyl]-2-hydroxy-5-methyl-benzamide (**10**). 60% yield. <sup>1</sup>H-NMR (300 MHz, CDCl<sub>3</sub>): 1.73-1.78 (t, 4H), 2.09 (s, 3H), 2.68 - 2.64 (t, 2H), 2.77 - 2.84 (t, 4H), 3.46-3.49 (t, 2H), 3.61(s, 2H), 3.82 (s, 3H), 3.84 (s, 3H), 6.49 (s, 1H), 6.59 (s, 1H), 6.84-6.87 (d, 1H), 7.05 (s, 1H), 7.10 - 7.16 (d, 1H), 7.26 (s, 1H).

5-Bromo-N-[4-(6,7-dimethoxy-3,4-dihydro-1H-isoquinolin-2-yl)-butyl]-2-hydroxy-3-methoxy-benzamide (**11**). 29% yield. <sup>1</sup>H-NMR (300 MHz, CDCl<sub>3</sub>): 1.16 - 1.25 (m, 2H), 1.60 - 1.80 (m, 2H), 2.54 - 2.66 (m, 4H), 2.66 - 2.90 (t, 2H), 3.43 - 3.46 (m, 2H), 3.46-3.58 (s, 2H), 3.81 (s, 3H), 3.82 (s, 3H), 3.84 (s, 3H), 5.29 (s, 1H), 6.48 (s, 1H), 6.55 (s, 1H), 6.97 (d, 1H), 7.13 (d, 1H), 7.26 (s, 1H).

### 2.2.3. Radiolabeling

Synthesis of [<sup>11</sup>C]**1**. A stream of [<sup>11</sup>C]methyliodide in helium was bubbled for 5 min. period into a solution of **8** (1.5 - 2.0 mg) in DMF (0.18 mL) and 5N NaOH (2  $\mu$ L) at 0°C (ice-water bath). The sealed reaction vessel was heated at 85°C (oil bath) for 5 min. The reaction was quenched by the addition of HPLC solvent (1.8 mL) and the residue was purified by C-18 reversed-phase semi-preparative HPLC using 17.5 % THF/82.5 % of 0.1M ammonium formate (with 0.1% formic acid) buffer at pH = 4.0 as the mobile phase (flow rate = 4.0 mL/min). Under these conditions the retention time of the [<sup>11</sup>C]**1** was 14.50 min. The product was collected into a 50 ml round bottom flask, and the volatile

components were removed in vacuo. The residue was diluted with saline (5 mL) and an aliquot (50  $\mu$ L) was taken for HPLC analysis using the same HPLC conditions described above.

The other three radiotracers ( $[^{11}\text{C}]2$ ,  $[^{11}\text{C}]3$ , and  $[^{11}\text{C}]4$ ) were synthesized with the same procedure. The radiochemical purities were greater than 95% for all four  $^{11}\text{C}$ -labeled radiotracers. The HPLC solvent, retention time, labelling yield and specific activity of each radiotracer is shown in Table II. The total radiosynthesis time, including production of  $[^{11}\text{C}]$ methyl iodide, ranged from 50 – 60 min.

### *2.3. Mouse tumor model*

All animal experiments were conducted under IACUC approved protocols in compliance with the Guidelines for the Care and Use of Research Animals established by the Washington University Medical School Animal Studies Committee. The mouse mammary carcinoma cell line EMT6 (12,13) was obtained from the laboratory of Dr. Ronald S. Pardini at the University of Nevada and maintained by serial passage in RPMI1640 containing 10% FCS in a 37°C humidified 95% air, 5% CO<sub>2</sub> incubator. Cells were harvested during exponential growth and viability of the cell suspension was greater than 90%. Female BALB/c mice, 5–6 weeks of age, were purchased from NIH-Frederick. Tumors were implanted subcutaneously in the nape of the neck using  $5 \times 10^5$  cells per 100  $\mu\text{L}$  and grown for 8-12 days prior to use. At the time of the study, mouse weight averaged 18 - 22 grams and average tumor size was between 100 - 250 mg.

#### *2.4. Biodistribution and tumor uptake studies*

A solution of [<sup>11</sup>C]1, [<sup>11</sup>C]2, [<sup>11</sup>C]3, [<sup>11</sup>C]4 (100-150 µCi) diluted in saline (100-150 µL) was injected via the tail vein into EMT6 tumor-bearing female BALB/C mice. Groups of at least four mice were used for each time point. At 5, 30 and 60 minutes after injection, the mice were euthanized. Samples of target and non-target tissue including blood, lung, liver, kidney, muscle, fat, heart, brain and tumor were removed by dissection. Activity in each sample quantified using a Beckman Gamma 8000 well counter. A dilution of the injectate was also counted with the samples from each animal. Tissues were weighed and the percentage injected dose (%I.D.) per gram tissue was calculated. The tumor:organ ratios were calculated by dividing the %I.D./gram for tumor by the %I.D./g for the tissue.

Blocking studies were conducted with [<sup>11</sup>C]2 by co-injecting the unlabeled nonselective σ<sub>1</sub>/σ<sub>2</sub> ligand, N-(4'-fluorobenzyl)piperidinyl-4-(3-bromophenyl)acetamide (2 mg/kg, i.v.). The mice were sacrificed 30 minutes after injection of the radiotracer and biodistribution studies were conducted as described above.

### **3. Results**

The results of the radiolabeling studies are shown in Table II. The labeling yield represents the %yield of the O-alkylation step and is based on the starting activity of [<sup>11</sup>C]methyl iodide. The % yield of [<sup>11</sup>C]1 and [<sup>11</sup>C]2 was quite high whereas the labeling yield of [<sup>11</sup>C]3 and [<sup>11</sup>C]4 were somewhat lower for reasons that were not clear. No attempt was made to optimize the labeling yield of [<sup>11</sup>C]3 and [<sup>11</sup>C]4. The radiochemical purity of all tracers was over 99% and all four <sup>11</sup>C-labeled radiotracers were obtained in a specific activity suitable for in vivo studies.

The tissue distribution of the radioactivity after injection of each of the four tracers into mice is summarized in Table III. Of the four <sup>11</sup>C-labeled radiotracers, [<sup>11</sup>C]2 had the highest tumor uptake at all times, with percent injected dose/g tumor (% I.D./g) values of 4.22 at 5 min, 2.35 at 30min, 1.32 at 60min, respectively. A plot of the % I.D./g tumor at 60 min versus log P for each radiotracer indicates that lipophilicity of the radiotracer may be an important property in determining tumor uptake (Figure 1). A similar relationship was demonstrated for the earlier time points (data not shown). Among the peripheral tissues, the kidney and liver showed a very high initial uptake of all four <sup>11</sup>C-labeled tracers, but the levels decreased rapidly. There was a rapid clearance of the radioactivity from blood, muscle, and fat. As shown in Table IV, [<sup>11</sup>C]2 had the highest tumor:blood and tumor:lung ratios at the 1 hr. post-i.v. injection time point. The higher tumor:organ ratios of [<sup>11</sup>C]2 indicate that this radiotracer is the best candidate for imaging breast tumors.

In order to determine that the in vivo binding of [<sup>11</sup>C]2 was specific for sigma receptors, [<sup>11</sup>C]2 was co-injected with N-(4'-fluorobenzyl)piperidinyl-4-(3-bromophenyl)acetamide (a.k.a., YUN 143), which is a sigma ligand displaying a high affinity for both  $\sigma_1$  and  $\sigma_2$  receptors [14]. Co-injection of [<sup>11</sup>C]2 with YUN 143 (2 mg/kg, i.v.) resulted in a decrease in the tumor:blood (-32%), tumor:lung (-18%), tumor:muscle (-46%) and tumor:fat (-46%) ratios at 30 min. post-i.v.-injection of the radiotracer (Figure 2). These data are consistent with the labeling of  $\sigma_2$  receptors in vivo.

A study was also conducted comparing the tumor uptake and tumor:organ ratios of [<sup>11</sup>C]2 with that of [<sup>18</sup>F]FLT, a radiolabeled nucleoside analog that is believed to measure tumor proliferation [11]. The results of this study, which are shown in Figure 3, indicate

that [<sup>18</sup>F]FLT has a higher tumor uptake than [<sup>11</sup>C]2. However, [<sup>11</sup>C]2 had either similar (lung, fat) or better (blood, muscle) tumor:organ ratios than [<sup>18</sup>F]FLT in the tissues that are important for breast tumor imaging. Consequently, [<sup>11</sup>C]2 is a potential radiotracer for imaging the proliferative status of breast tumors *in vivo* with PET.

#### 4. Discussion

Previous studies have shown that many tumors of human origin possess a high density of σ<sub>2</sub> receptors relative to that of surrounding normal tissue [4]. Although several types of human tumors possess σ<sub>1</sub> and σ<sub>2</sub> receptors, the density of σ<sub>1</sub> receptors in tumor cells is generally less than that present in normal tissues [4]. Therefore, a σ<sub>2</sub> selective imaging agent is predicted to be a better tumor imaging agent since it should have higher tumor:normal tissue ratios relative to σ<sub>1</sub> selective or σ<sub>1</sub>/σ<sub>2</sub> nonselective imaging agents. This prediction was confirmed in our earlier studies with [<sup>18</sup>F]YUN 143, which had much higher tumor:organ ratios when only σ<sub>2</sub> receptors were labeled than when both σ<sub>1</sub> and σ<sub>2</sub> receptors were labeled [14]. However, the absence of ligands displaying a higher affinity for σ<sub>2</sub> versus σ<sub>1</sub> receptors has limited the likelihood of developing σ<sub>2</sub>-selective imaging agents for PET and SPECT.

We recently reported a series of conformationally-flexible benzamide analogs having a high affinity and selectivity for σ<sub>2</sub> versus σ<sub>1</sub> receptors [10]. The presence of an ortho methoxy group in these compounds (Table I) indicated that it is possible to prepare the corresponding <sup>11</sup>C-labeled radiotracer using standard radiochemistry techniques. Therefore, the goal of the current study was to evaluate the four <sup>11</sup>C-labeled benzamide analogs shown in Table I and determine whether they would be useful imaging agents for

assessing the anatomic and/or proliferative status of breast tumors. A second goal of this study was to compare the best of the  $^{11}\text{C}$ -labeled radiotracers with  $[^{18}\text{F}]\text{FLT}$ , a nucleoside-based radiotracer that is currently being used to measure the tumor proliferation with PET [11].

Although the  $\sigma_2$  receptor affinities of  $[^{11}\text{C}]1$ ,  $[^{11}\text{C}]2$ ,  $[^{11}\text{C}]3$ ,  $[^{11}\text{C}]4$  are similar, the vivo biodistribution indicated that  $[^{11}\text{C}]2$  has the highest tumor uptake at all time points (Table III). One possible explanation for this is that  $[^{11}\text{C}]2$  may have the optimal lipophilicity since a parabolic relationship was observed between the % I.D./g tumor and the calculated log P of the radiotracer (Figure 1). These data indicate that both receptor affinity and lipophilicity are important properties that must be considered in the design of receptor-based tumor imaging agents.

In vivo blocking studies were conducted by co-injecting the nonselective sigma ligand, YUN 143 (2 mg/kg), with  $[^{11}\text{C}]2$ . This compound was chosen because our previous studies with the  $^{18}\text{F}$ -labeled version of this ligand, showed that  $[^{18}\text{F}]\text{YUN } 143$  had a high tumor uptake and efficiently labeled  $\sigma_2$  receptors in vivo [14]. In the  $\sigma_2$  blocking study, the tumor:organ ratios were reduced by 18 – 46%. Thus, these data are consistent with the labeling of  $\sigma_2$  receptors in the tumor xenograft by  $[^{11}\text{C}]2$ .

In the previous study described above, we reported that the tumor:organ ratios of  $[^{18}\text{F}]\text{YUN } 143$  under conditions favoring the labeling of  $\sigma_2$  receptors was higher than the tumor:organ ratios of the radiolabeled nucleoside,  $[^{125}\text{I}]\text{IUDR}$  [14]. Therefore, one of the goals of the current study was to compare our best  $^{11}\text{C}$ -labeled  $\sigma_2$  receptor ligand with the  $^{18}\text{F}$ -labeled DNA precursor,  $[^{18}\text{F}]\text{FLT}$ . This radiolabeled analogue of thymidine has a greater metabolic stability than  $[^{123/124}\text{I}]\text{IUDR}$  and  $[^{11}\text{C}]\text{thymidine}$ , and was introduced

recently as a radiotracer for measuring the proliferative status of solid tumors *in vivo* with PET [11]. The biodistribution data for [<sup>18</sup>F]FLT and [<sup>11</sup>C]2 in female Balb/C mice bearing EMT-6 tumors is shown in Figure 3. The top graph demonstrates that [<sup>18</sup>F]FLT has a higher uptake in the tumor xenograft relative to [<sup>11</sup>C]2 at 60 min post-i.v. injection.. However, the uptake of [<sup>18</sup>F]FLT was also higher than [<sup>11</sup>C]2 in all organs. This resulted in similar tumor:lung and tumor:fat ratios for both [<sup>11</sup>C]2 and [<sup>18</sup>F]FLT. However, [<sup>11</sup>C]2 had a higher tumor:blood and tumor:muscle ratio than [<sup>18</sup>F]FLT. We are currently conducting studies comparing [<sup>11</sup>C]2 and [<sup>18</sup>F]FLT with “gold standard” measures of proliferation.

## 5. Conclusion

In present study, we have successfully synthesized four <sup>11</sup>C-labeled conformationally-flexible benzamide analogues having a high affinity and selectivity for  $\sigma_2$  versus  $\sigma_1$  receptors. The four analogs, [<sup>11</sup>C]1, [<sup>11</sup>C]2, [<sup>11</sup>C]3, [<sup>11</sup>C]4 were evaluated as potential radiotracers for imaging  $\sigma_2$  receptors in Balb/C mice bearing EMT-6 breast tumors. Of the four <sup>11</sup>C-labeled analogues, [<sup>11</sup>C]2 showed the best tumor uptake and tumor:organ ratios. Our data also indicates that [<sup>11</sup>C]2 displays either similar or better tumor:organ ratio as that of the radiolabeled nucleoside, [<sup>18</sup>F]FLT. Additional studies are clearly needed to compare [<sup>11</sup>C]2 and [<sup>18</sup>F]FLT with “gold standard” measures of proliferation in order to determine if the  $\sigma_2$  receptor approach is appropriate for measuring the proliferative status of breast tumors with PET.

**Acknowledgments.** This work was supported by grants CA102869 awarded by the National Institutes of Health and grant DAMD17-01-1-0446 awarded by the Department of Defence Breast Cancer Research Program of the US Army Medical Research and Materiel Command Office. The authors gratefully thank Susan Adams and Pat Margenau for their excellent technical assistance.

## References

- [1] Walker JM, Bowen WD, Walker FO, Matsumoto RE, De Costa B, Rice KR. Sigma receptors: biology and function. *Pharmacol. Rev.* 1990; 42: 355-402.
- [2] Hanner M, Moebius FF, Flandorfer A, Knaus H-G, Striessnig J, Kempner E, Glossmann H. Purification, molecular cloning, and expression of the mammalian sigma<sub>1</sub>-binding site. *Proc. Natl. Acad. Sci. USA* 1996; 93: 8072-8077.
- [3] Hellewell SB, Bruce A, Feinstein G, Orringer J, Williams W, Bowen, WD. Rat liver and kidney contain high densities of σ<sub>1</sub> and σ<sub>2</sub> receptors: characterization by ligand binding and photoaffinity labeling. *Eur. J. Pharmacol. Mol. Pharmacol. Sec.* 1994; 268: 9-18.
- [4] Vilner BJ, John CS, Bowen WD. Sigma-1 and sigma-2 receptors are expressed in a wide variety of human and rodent tumor cell lines. *Cancer Res.* 1995; 55: 408-413.
- [5] Bem WT, Thomas GE, Mammone JY, Homan SM, Levy BK, Johnson FE, Coscia CJ. Overexpression of σ receptors in nonneuronal human tumors. *Cancer Res.* 1991; 51: 6558-6562.
- [6] Vilner BJ and Bowen WD. Characterization of sigma-like binding properties of NB41A3, S-20Y, and N1E-115 neuroblastomas, C6 gliomas, and NG108-15 neuroblastoma-glioma hybrid cells: further evidence for sigma-2 receptors. In: J.M. Kamenka and E.F. Domino (eds.), *Multiple sigma and PCP receptor ligands: mechanisms for neuromodulation and neuroprotection?* pp. 341-353. Ann Arbor, MI: NPP Books (1992).
- [7] Mach RH, Smith CR, Al Nabulsi I, Whirrett BR, Childers SR, Wheeler KT. Sigma-2 receptors as potential biomarkers of proliferation in breast cancer. *Cancer Res.* 1997; 57: 156-161.

- [8] Al-Nabulsi I, Mach RH, Wang L-M, Wallen CA, Keng PC, Sten K, Childers SR, Wheeler KT. Effect of ploidy, recruitment, environmental factors, and tamoxifen treatment on the expression of sigma-2 receptors in proliferating and quiescent tumor cells. *Br J Cancer* 1999; 81: 925-933.
- [9] Wheeler KT, Wang L-M, Wallen CA, Childers SR, Cline JM, Keng PC, Mach RH. Sigma-2 receptors as a biomarker of proliferation in solid tumors, *Br. J. Cancer* 2000; 82: 1223–1232.
- [10] Mach RH, Huang Y, Freeman RA, Wu L, Vangveravong S, Luedtke RR. Conformationally-flexible benzamide analogues as dopamine D<sub>3</sub> and σ<sub>2</sub> receptor ligands. *Bioorg. Med. Chem. Lett.* 2004; 14: 195-202.
- [11] Shields AF, Grierson JR, Dohmen BM, Machulla HJ, Stayanoff JC, Lawhoirn-Crews JM, Obradovich JE, Muzik O, Manger TJ. Imaging proliferation in vivo with [<sup>18</sup>F]FLT and positron emission tomography. *Nature Medicine* 1998; 4: 1334–1336.
- [12] Rockwell SC, Kallman RF, Fajardo LF. Characteristics of a serially transplanted mouse mammary tumor and its tissue-culture-adapted derivative. *J. Natl. Cancer Inst.* 1972; 49: 735–747.
- [13] Rockwell SC. In vivo-in vitro tumor systems: New models for studying the response of tumors to therapy. *Lab. Anim. Sci.* 1977; 27: 831–851.
- [14] Mach RH, Huang Y, Buchheimer N, Kuhner R, Wu L, Morton TE, Wang L-M, Ehrenkaufer RL, Wallen CA, Wheeler KT. [<sup>18</sup>F]N-4'-Fluorobenzyl-4-(3-bromophenyl) acetamide for imaging the sigma receptor status of tumors: comparison with [<sup>18</sup>F]FDG and [<sup>125</sup>I]IUDR. *Nucl Med Biology* 2001; 28: 451-458.

## **Figure Legends**

**Figure 1.** Relationship between tumor uptake and lipophilicity of the  $\sigma_2$  receptor ligands.

**Figure 2.** Comparison of the tumor:blood, tumor:lung, tumor:muscle, and tumor:fat ratios of the [ $^{11}\text{C}$ ]2 under no-carrier-added conditions and under conditions of  $\sigma_1$  and  $\sigma_2$  blockade with YUN-143 (2 mg/kg i.v.). The animals were sacrificed at 30 min post-i.v. injection.

**Figure 3.** Comparison of [ $^{18}\text{F}$ ]FLT versus [ $^{11}\text{C}$ ]2 at 30 and 60 min. post-i.v. injection of the radiotracer.

**Table I.** Structures and in vitro binding of the benzamide analogs.

#	X	R	n	Ki <sup>a</sup>			Log P <sup>e</sup>
				σ <sub>1</sub> <sup>b</sup>	σ <sub>2</sub> <sup>c</sup>	σ <sub>1</sub> : σ <sub>2</sub> <sup>d</sup> Ratio	
<b>1</b>	H	CH <sub>3</sub>	2	10,412	13.3	783	2.31
<b>2</b>	H	CH <sub>3</sub>	4	3,078	10.3	300	2.84
<b>3</b>	H	Br	2	5,484	12.2	442	3.17
<b>4</b>	OCH <sub>3</sub>	Br	4	12,900	8.2	1,573	3.33

<sup>a</sup> Mean ± SEM, K<sub>i</sub> values were determined by at least three experiments [10].

<sup>b</sup> K<sub>i</sub> values for σ<sub>1</sub> receptors were measured on guinea pig brain membranes using [<sup>3</sup>H](+)-pentazocine as the radioligand.

<sup>c</sup> K<sub>i</sub> values for σ<sub>2</sub> receptors were measured on rat liver membranes using [<sup>3</sup>H]-DTG as the radioligand in the presence of (+)-pentazocine.

<sup>d</sup> K<sub>i</sub> for σ<sub>1</sub>/K<sub>i</sub> for σ<sub>2</sub>.

<sup>e</sup> calculated value using the program Clog P.

**Table II.** The HPLC solvent, retention time, labeling yield and specific activity

#	HPLC solvent	Retention time	%Yield	Specific Activity (EOB) <sup>a</sup>
1	17.5%THF : 82.5% 0.1M buffer	14.5 min	60-75	~5000 mCi/umol
2	15%THF : 85% 0.1M buffer	12.5 min	60-75	~4000 mCi/umol
3	15%THF : 85% 0.1M buffer	17.5 min	10-15	~1000 mCi/umol
4	18.5%THF : 81.5% 0.1M buffer	15.5 min	30-40	~4000 mCi/umol

<sup>a</sup>Decay corrected to end-of-bombardment (EOB)

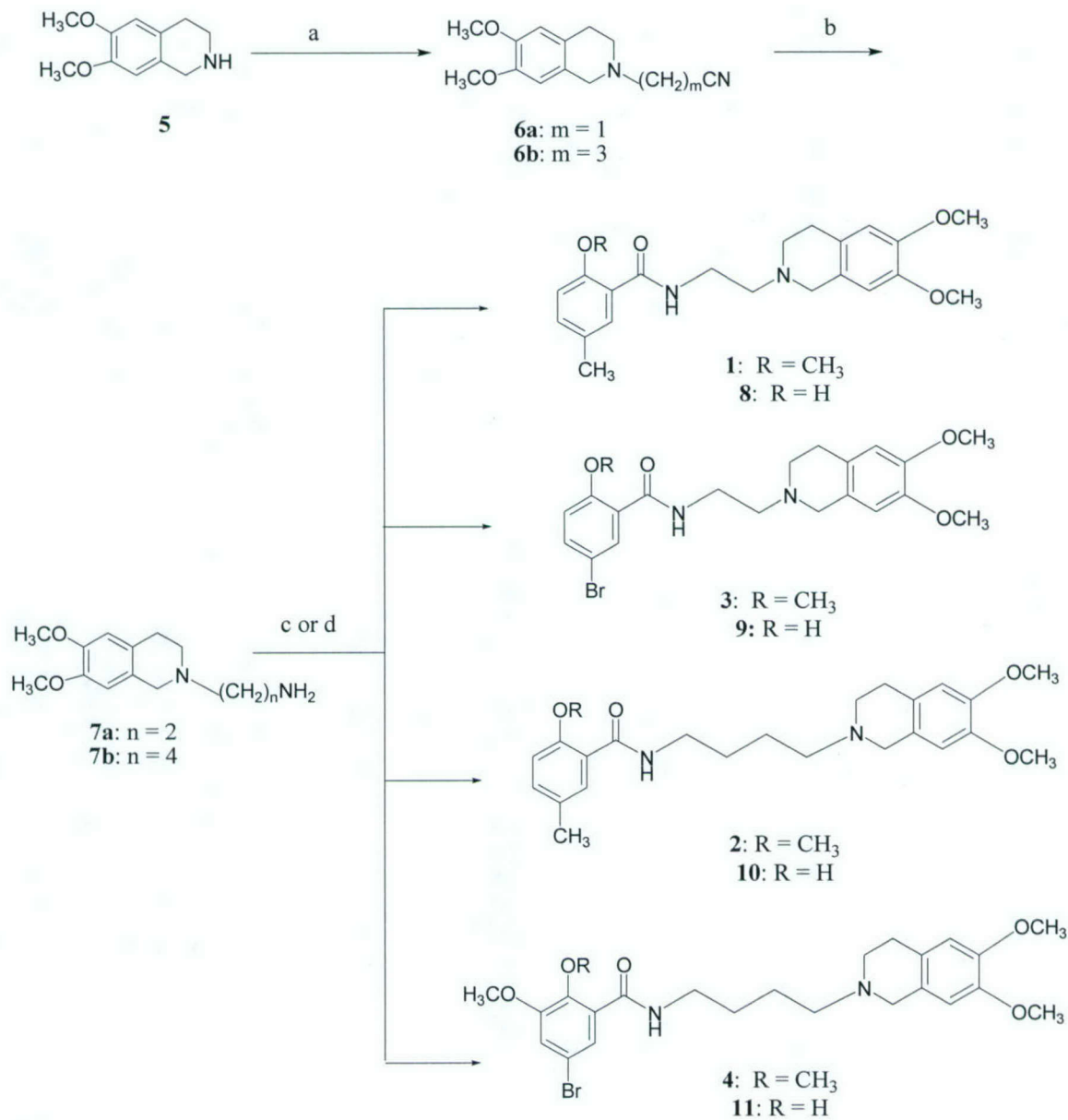
**Table III.** [<sup>11</sup>C]1 - 4 Biodistribution in female Balb/C mice bearing EMT-6 Tumors

	%I.D./g Tissue		
	5 min.	30 min.	1 hour
[ <sup>11</sup> C]1			
blood	5.89 ± 0.29	2.62 ± 0.22	1.98 ± 0.35
lung	5.69 ± 0.70	1.42 ± 0.15	1.39 ± 0.67
liver	18.49 ± 2.87	3.87 ± 0.67	1.70 ± 0.23
kidney	44.07 ± 1.67	2.77 ± 0.42	1.01 ± 0.12
muscle	1.75 ± 0.21	0.56 ± 0.19	0.41 ± 0.22
fat	3.07 ± 0.40	0.38 ± 0.12	0.26 ± 0.09
heart	2.89 ± 0.36	0.76 ± 0.06	0.76 ± 0.46
brain	1.63 ± 0.30	0.11 ± 0.01	0.10 ± 0.04
tumor	3.10 ± 0.25	1.08 ± 0.08	0.85 ± 0.14
[ <sup>11</sup> C]2			
blood	3.09 ± 0.33	1.31 ± 0.11	0.73 ± 0.05
lung	14.02 ± 1.40	2.27 ± 0.42	1.09 ± 0.26
liver	12.32 ± 1.73	9.65 ± 2.00	3.00 ± 0.21
kidney	20.50 ± 1.86	4.12 ± 0.51	2.26 ± 0.36
muscle	4.49 ± 0.45	0.75 ± 0.13	0.49 ± 0.11
fat	1.88 ± 0.50	0.68 ± 0.19	0.33 ± 0.24
heart	5.86 ± 0.47	0.95 ± 0.17	0.50 ± 0.11
brain	2.29 ± 0.28	0.28 ± 0.03	0.15 ± 0.01
tumor	4.22 ± 1.01	2.35 ± 0.27	1.32 ± 0.17
[ <sup>11</sup> C]3			
blood	5.25 ± 0.39	2.35 ± 0.16	1.88 ± 0.16
lung	5.72 ± 0.40	1.83 ± 0.13	1.32 ± 0.11
liver	19.88 ± 3.10	5.89 ± 0.82	2.65 ± 0.29
kidney	51.03 ± 7.14	34.19 ± 1.74	19.78 ± 1.99
muscle	1.73 ± 0.11	0.52 ± 0.23	0.36 ± 0.08
fat	2.05 ± 0.49	0.63 ± 0.19	0.37 ± 0.13
heart	3.18 ± 0.26	0.77 ± 0.08	0.56 ± 0.05
brain	2.52 ± 0.15	0.26 ± 0.10	0.14 ± 0.02
tumor	1.82 ± 0.39	1.06 ± 0.09	0.87 ± 0.09
[ <sup>11</sup> C]4			
blood	7.12 ± 1.01	0.99 ± 0.15	0.45 ± 0.04
lung	6.01 ± 0.77	1.34 ± 0.23	0.70 ± 0.26
liver	25.02 ± 3.70	2.48 ± 0.52	1.19 ± 0.17
kidney	19.48 ± 1.46	2.57 ± 0.78	1.34 ± 0.19
muscle	1.94 ± 0.13	2.11 ± 0.77	0.46 ± 0.40
fat	1.48 ± 0.55	0.63 ± 0.33	0.20 ± 0.08
heart	3.54 ± 0.31	0.68 ± 0.12	0.29 ± 0.10
brain	0.33 ± 0.09	0.08 ± 0.03	0.03 ± 0.00
tumor	2.82 ± 0.36	0.92 ± 0.10	0.50 ± 0.09

**Table IV.** Tumor:background ratios at 1 hr. post-i.v. injection of the radiotracer

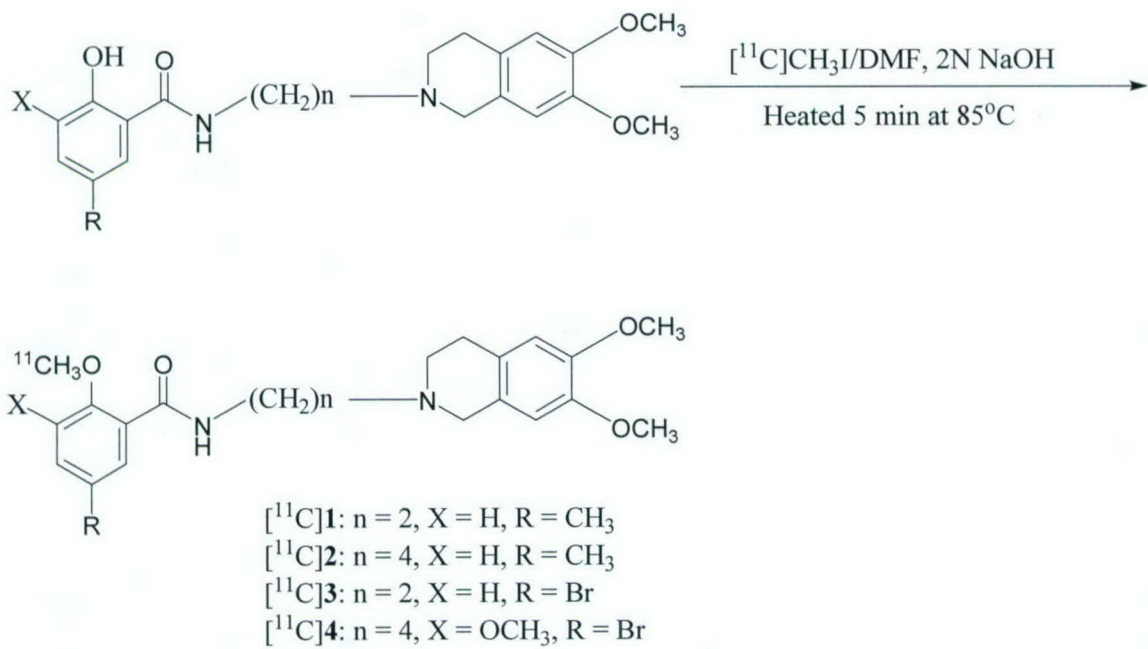
Ratio	[ <sup>11</sup> C]1	[ <sup>11</sup> C]2	[ <sup>11</sup> C]3	[ <sup>11</sup> C]4
tumor : blood	0.44 ± 0.06	1.81 ± 0.11	0.46 ± 0.02	1.10 ± 0.11
tumor : lung	0.68 ± 0.19	1.28 ± 0.41	0.66 ± 0.03	0.79 ± 0.30
tumor : muscle	2.40 ± 0.84	2.78 ± 0.62	2.52 ± 0.66	1.52 ± 0.67
tumor : fat	3.46 ± 0.91	5.36 ± 2.38	2.64 ± 1.12	2.77 ± 0.82

**Scheme I**



**Reagents:** (a) BrCH<sub>2</sub>CN or BrCH<sub>2</sub>CH<sub>2</sub>CH<sub>2</sub>CN, Et<sub>3</sub>N, CH<sub>2</sub>Cl<sub>2</sub>;  
 (b) LiAlH<sub>4</sub>, THF or H<sub>2</sub>, Pd/charcoal, ethanol; (c) BoP/C<sub>2</sub>H<sub>2</sub>Cl<sub>2</sub> or DCC / C<sub>2</sub>H<sub>2</sub>Cl<sub>2</sub>.

**Scheme II**



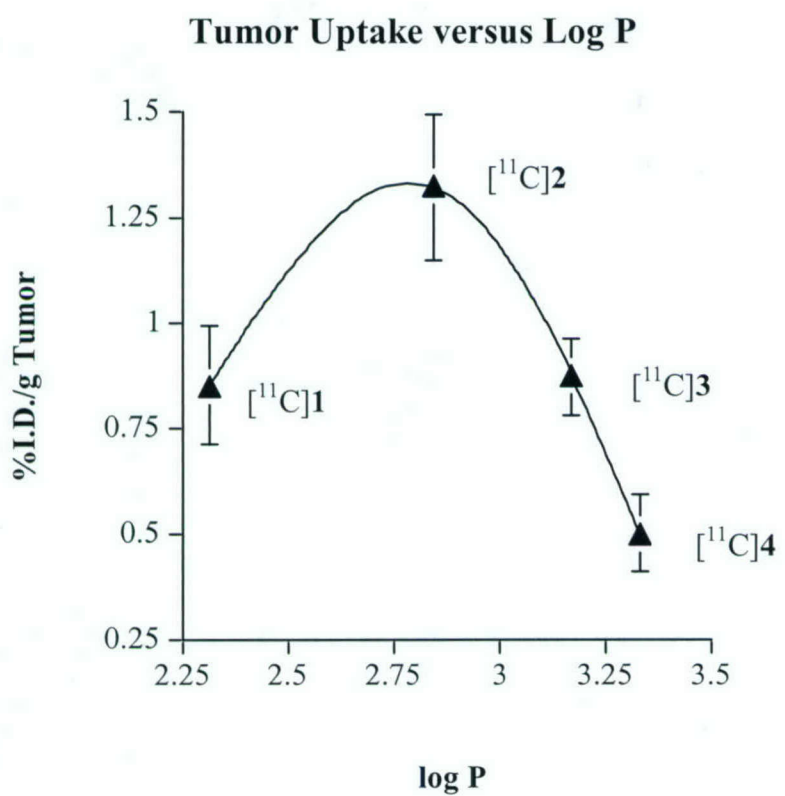


Figure 1

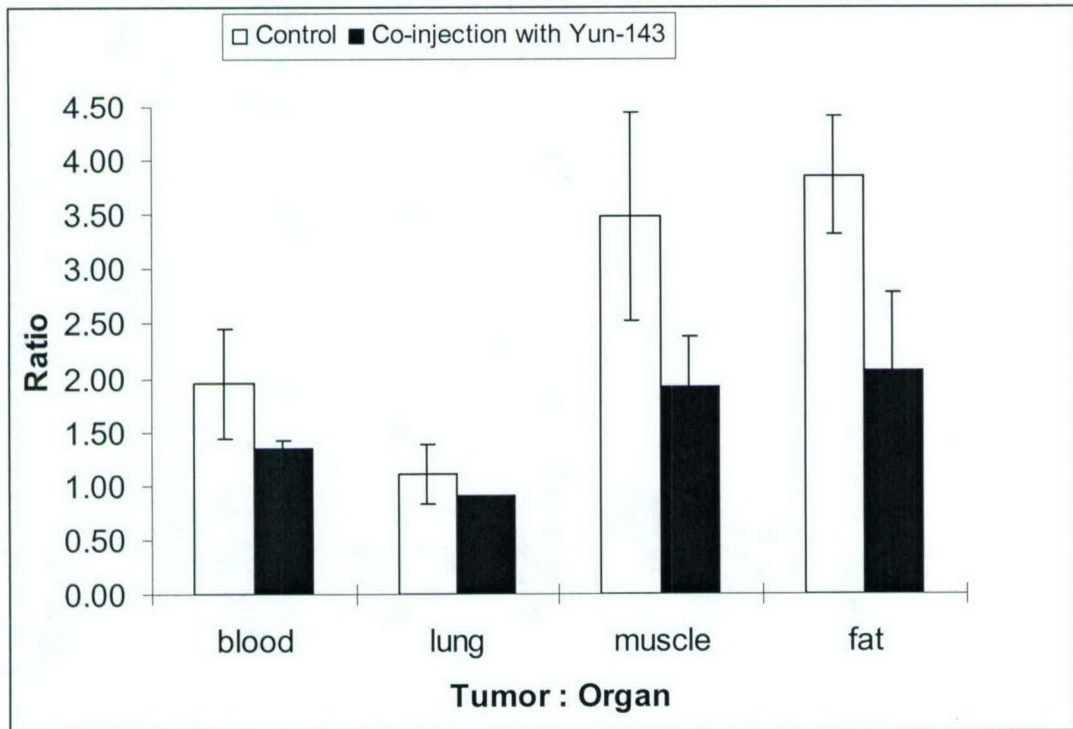
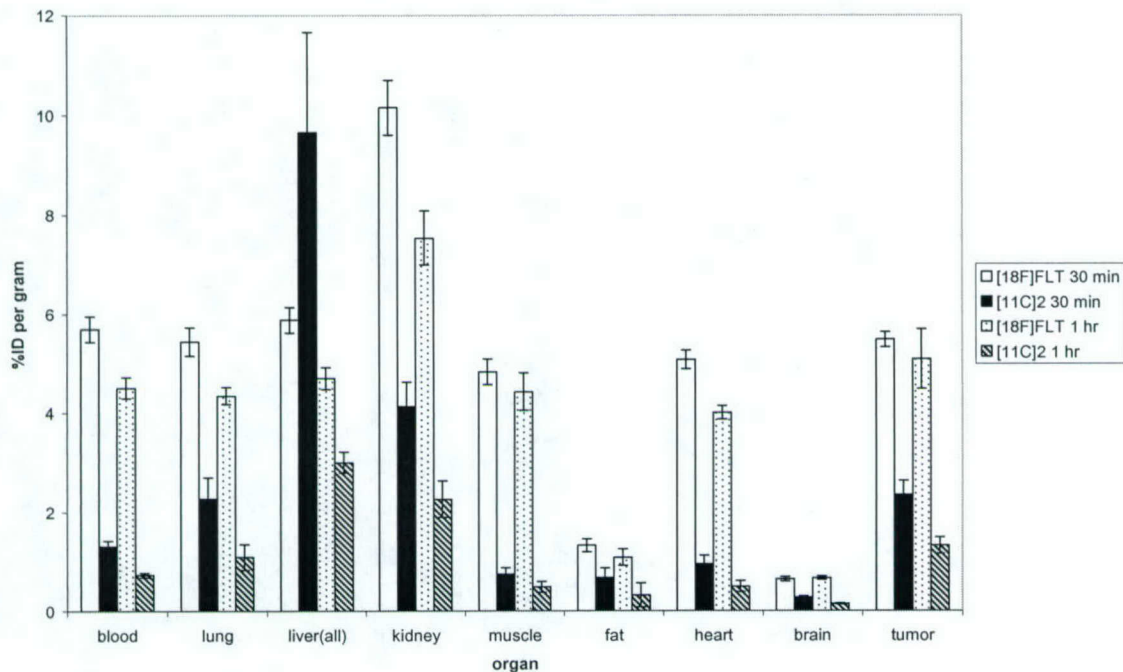


Figure 2.

[ $^{18}\text{F}$ ]FLT vs. [ $^{11}\text{C}$ ]2 Biodistribution



[ $^{18}\text{F}$ ]FLT vs. [ $^{11}\text{C}$ ]2 tumor : organ ratio

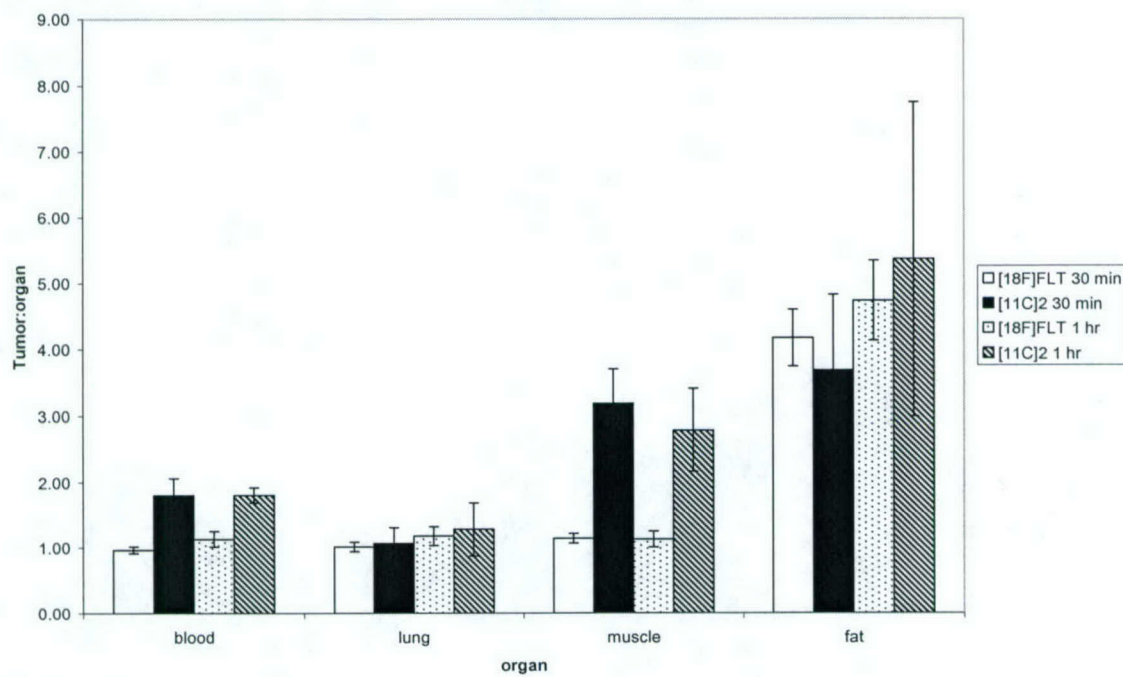


Figure 3